



Vicerrectoría de Investigación

DOCTORADO EN GENÓMICA INTEGRATIVA

“IDENTIFICATION OF GENE REGULATORY NETWORKS CONTROLLING SULFATE DEFICIENCY RESPONSE IN *SOLANUM LYCOPERSICUM.*”

Tesis entregada a la Universidad Mayor en cumplimiento parcial de los requisitos para optar al Grado de Doctor en Genómica Integrativa

JOSÉ DAVID FERNÁNDEZ PÉREZ

Directora de Tesis: Dra. Elena Alejandra Vidal Olate
Co-Directores: Dr. Javier Canales, Dr. José Álvarez.

MARZO 2025



**UNIVERSIDAD
MAYOR**

para espíritus emprendedores

Dr. Jaime Andrés Rivas

Presidente

Dr. Sebastián Reyes

Comité de evaluación

Dra. Elena Vidal

Directora de tesis

Dr. José Álvarez

Codirector de Tesis

Dra. Andrea Miyasaka

Comité de evaluación

Dr. Tomás Mátus

Comité de evaluación

Dr. Javier Canales

Codirector de Tesis

Fecha: 22 de abril de 2025

DEDICATION

*To my parents and brother, the roots of my tree. Your presence in my life
makes the fruit of my dreams the sweetest.*

I want to express my gratitude to the universe, positive energy, manifestation or God.
To my family, all over the world and in heaven. Parts of my heart stayed with you in Isnotú,
Mérida, Perú, Colombia and Spain. I always think of you.

To my chosen family, the lots of friends I have around the globe, my heart fills with joy
believing that each time we reunite it would be like time haven't passed at all. You rock!

To my friends in Chile, we will celebrate big time, you know the importance of this.
To my Chilean family, your presence makes me very happy, please know that I Love you.

And to Esteban, my partner, your company and support helps me greatly to be the better
version of me. Thank you for being my best friend. May the magic continue. Always.

ACKNOWLEDGMENTS

I express my deepest gratitude to my advisor, Dr. Elena Vidal, for her steady guidance and for continually challenging me to reach my fullest potential and fulfill timelapses. Her brilliance as a researcher, dedication as a mentor, and exemplary work ethic have been a constant source of inspiration. I hope to make her proud.

I also extend my sincere thanks to my co-advisors for their contributions to this work.

To Dr. Tomás Matus, for mentoring me during my internship in Valencia and for his valuable collaboration in the development of this research. I look forward to continuing our work together in the future.

To the members of the Plantomics and Plant Genome Regulation Labs, thank you for your support, collaboration, and insightful advice throughout this journey.

To the 2020 G.I. generation Ivania, Mafer and Miguel, so glad to have met and shared this whole experience with you, let's celebrate greatly each of our accomplishments, we deserve it!

To the Universidad Mayor Integrative Genomics Ph.D. program members and teachers for their role in my education during this pivotal stage of my career. I am especially thankful to the program for awarding me a scholarship from 2020-2023 and believing in my potential, transforming into the decision factor that allow me to go on this path.

A special thank you to the Agencia Nacional de Investigación y Desarrollo (ANID), Chile: for the doctoral scholarship (ID: 21230478) granted since 2023-2024, and by serving to funding all our research work through the projects Millennium Science Initiative Program, Millennium Institute for Integrative Biology iBio ICN17_022, ANID- FONDECYT 1211130, ANID – MILENIO – NCN2024_047, ANID-FOVI230159.

To life on planet earth, my passion.

MAIN INDEX

I. ABBREVIATIONS	9
II. RESUMEN	10
III. ABSTRACT	13
IV. INTRODUCTION	16
Sulfur is a key macronutrient for plant growth.	16
Transcriptional regulation triggered by sulfate deficiency.	20
Transcription factors controlling gene expression responses to sulfate availability.	21
Gene regulatory networks inference methods	23
Tomato lacks networks models that explain direct regulation between TFs and target genes.	26
Hypothesis	31
General Goal	31
Specific goals	31
V. MATERIALS AND METHODS	32
Aim 1	32
Tomato gene annotation update.	32
Input mRNA-seq analysis	33
Input ChIP-seq analysis	34
Input ATAC-seq and DNase-seq analysis	34
Determination of TF binding sites using FIMO	35
GENIE3 inference of regulatory interactions	35
Co-expression network generation	36
Enrichment analysis	36
Gene Set Enrichment Analysis (GSEA)	36
Network performance evaluation.	37
GRNs visualization and networks analysis	37
TF-Target pairings analysis	38
Functional validation of the GRNs.	38
Aim 2	39
Cloning vector generation	39
Protoplast extraction	39
TARGET protocol	39
TARGET RNA-Seq data analysis	40
Aim 3	41
Transgenic plants generation	41
Plant growth quantification.	41
Sulfate content analysis.	42
Quantitative real-time PCR (qPCR)	42
Transgenic plants RNA-Seq data analysis	43

VI. RESULTS	45
1. To generate organ-level reference Gene Regulatory Networks models for <i>Solanum lycopersicum</i>.	45
1.1 Updating <i>Solanum lycopersicum</i> genes and functional annotation.	45
1.2 Gene expression patterns in tomato demonstrate an organ-level component	48
1.3 Integrated tomato organ-level GRNs reveal enriched TF-Target interactions and local regulatory cascades.	51
1.4 The fruit GRN captures known regulatory interactions and identifies novel central controllers of ripening.	59
1.5 Tomato organ-level GRNs validate the role of ABF TFs on abscisic acid (ABA) regulatory cascades and identify new regulators of ABA-related genes.	62
1.6 TomViz- GRNs app: Online tool for tomato GRNs visualization.	67
2. To identify candidate TFs that are central regulators of the sulfate deficiency response in <i>S. lycopersicum</i>.	69
2.1 Context-specific GRNs of sulfate deficiency of tomato roots and leaves	69
2.2 Five candidate TFs are able to control multiple biological processes associated to sulfate deficiency treatments in tomato plants.	78
2.3 TARGET analysis supports the EIL3 role as a regulator of sulfate important genes.	81
3. To experimentally validate the function of a central TF candidate in the regulation of plant growth under sulfate deficiency.	84
3.1 OX-S/EIL3 plants reveal increased growth and enhanced S accumulation.	84
3.2 Transcriptomic changes of the OX-S/EIL3 plants are equivalent to responses to sulfate deficiency treatment.	87
3.3 The S/EIL3 controls sulfate deficiency marker genes and recapitulates tomato predicted regulatory cascades.	91
VII. DISCUSSION	98
1. To generate organ-specific reference Gene Regulatory Networks models for <i>Solanum lycopersicum</i> .	98
2. To identify candidate TFs that are central regulators of the sulfate deficiency response in <i>S. lycopersicum</i> .	106
3. To experimentally validate the function of a central TF candidate in the regulation of plant growth under sulfate deficiency.	110
VIII. CONCLUSION	115
IX. REFERENCES	116
X. APPENDIX	136

FIGURE INDEX

FIGURE N°1. Overview of plants sulfate assimilation and metabolization pathway.	18
FIGURE N°2. Comparative phenotypic effects of sulfate deficiency in <i>Arabidopsis thaliana</i> , <i>Nicotiana tabacum</i> , and <i>Solanum lycopersicum</i> .	19
FIGURE N°3. Sulfate deficiency effect in <i>Solanum lycopersicum</i> plants.	29
FIGURE N°4. Organ-level transcriptomic landscape in tomato.	50
FIGURE N°5. Multi-omic datasets used for generating organ-level GRNs in <i>Solanum lycopersicum</i> .	53
FIGURE N°6. Comparative analysis of organ-level GRNs reveals regulatory signatures and TF connectivity patterns.	58
FIGURE N°7. Identification of key transcriptional regulators of fruit ripening regulatory cascades in tomato.	61
FIGURE N°8. Tomato GRNs reveal the role of ABF TFs and identify a key regulator of ABA-related GRNs	66
FIGURE N°9. TomViz-GRNs: A web-based platform for exploring tomato organ-level GRNs.	68
FIGURE N°10. Reanalysis of RNA-seq libraries from tomato roots and leaves (Canales et al., 2020) under control and sulfate deficiency conditions at 3–4 weeks after sowing.	71
FIGURE N°11. Overview of TF analysis in context-specific and time-specific root and leaf GRNs of sulfate deficiency-responsive genes.	73
FIGURE N°12. Heatmaps of ranked scores for the top 15 potential key TFs regulating sulfate deficiency response.	75
FIGURE N°13. Context-specific GRNs display a hierarchy of TF-regulating sulfate deficiency-responsive genes.	77
FIGURE N°14. Top five TFs from organ-specific GRNs identified as candidate key regulators of the sulfate deficiency response.	79
FIGURE N°15. TARGET analysis supports EIL3 role as regulator of sulfate important genes.	83
FIGURE N°16. Overview of phenotype analysis of Col-0 and OX-S/EIL3 <i>Arabidopsis</i> plants under contrasting sulfate treatments.	86
FIGURE N°17. Transcriptome analysis of Col-0 and OX-S/EIL3 plants under contrasting sulfate treatments.	89
FIGURE N°18. Regulatory effects of SIEIL3 on <i>Arabidopsis</i> sulfate-responsive genes.	93
FIGURE N°19. Model of key TFs regulating sulfate deficiency responses in <i>Solanum lycopersicum</i>	97

TABLE INDEX

TABLE N°1. Summary of Tomato Gene Annotations	47
TABLE N°2. Summary and enrichment values of organ-level GRNs from top 2% scored GENIE3 networks	55

I. ABBREVIATIONS

APK: APS kinase

APR: APS reductase

APS: adenosine 5'-phosphosulfate

At: *Arabidopsis thaliana*

ATAC-seq: Assay for Transposase-Accessible Chromatin sequencing

AUPR: Area Under the Precision Recall

AUROC: Area Under the Receiver Operating Characteristic

ChIP-Seq: Chromatin Immunoprecipitation sequencing.

CHX: Cycloheximide

Col-0: Columbia-0 accession of *Arabidopsis thaliana*

DEG: Differentially Expressed Gene

DEX: Dexamethasone

DNase-seq: DNase I hypersensitive sites sequencing.

EIL3: Ethylene-Insensitive 3-Like

FDR: False Discovery Rate

GCN: Gene Coexpression Network

GENIE3: GENE Network Inference with Ensemble of Trees

GO: Gene Ontology

GRN: Gene Regulatory Network

GSEA: Gene Set Enrichment Analysis

IVI: Integrated Value of Influence

LSU: Response to Low Sulfur

OCS: Open Chromatin Sites

OX: Overexpression

PAPS: 3'-phosphoadenosine 5'-phosphosulfate

PP2C: *Protein phosphatase 2C*

PWMs: position weight matrices.

S: Sulfur

SAM: S-adenosyl-methionine

SDI: Sulfur Deficiency Induced

Sl: *Solanum lycopersicum*

SLIM1: Sulfur Limitation 1

TARGET: Transient Assay Reporting Genome-wide Effects of Transcription factors.

TF: Transcription Factor

WT: Wild Type

II. RESUMEN

El sulfato (forma más disponible del azufre) es un macronutriente esencial requerido para el crecimiento, desarrollo y productividad de las plantas. La deficiencia de sulfato causa reducciones significativas en la biomasa vegetal, afectando la fotosíntesis lo que conlleva a pérdidas en el rendimiento agrícola. Mientras que la mayoría de los estudios del transcriptoma enfocados en la deficiencia de sulfato se han centrado en *Arabidopsis thaliana*, el conocimiento es limitado en especies usadas como cultivos. El tomate (*Solanum lycopersicum*), es un cultivo con importancia global y un organismo modelo para el estudio del desarrollo de frutos y las respuestas de las plantas al estrés biótico y abiótico. El tomate es afectado severamente por la deficiencia de sulfato, demostrando reducción en su crecimiento, mientras que el transcriptoma de tomate demuestra que la deficiencia de azufre afecta la regulación génica en hojas y raíces de tomate, sin embargo, aún no se conocen los principales TFs que controlan estos cambios regulatorios y su efecto en el fenotipo observado durante este estrés.

Utilizando datos públicos disponibles de transcriptómica en tomate (~10,000 bibliotecas de RNA-seq), aplicamos el algoritmo GENIE3 para predecir relaciones regulatorias entre los TFs y sus genes blanco. Estas redes se refinaron integrando redes de co-expresión, predicciones de sitios de unión de TFs y datos de accesibilidad de la cromatina obtenidos de conjuntos de datos reanalizados de ATAC-seq y DNase-seq. Un análisis de enriquecimiento con datos de ChIP-seq de tomate mostró que las GRNs pueden capturar vías regulatorias relevantes biológicamente. Nuestros hallazgos muestran que, aunque los genes expresados son en su mayoría ubicuos entre órganos, las interacciones regulatorias son altamente específicas en cada órgano. Nuestra GRN de frutos detectó exitosamente los blancos de los TFs TOMATO AGAMOUS-LIKE 1 (TAGL1)

y RIPENING INHIBITOR (RIN) cuyo efecto en la maduración frutal está verificado. Además, analizando la GRN de hojas, se validó las funciones de dos TFs ABA response element binding factor (ABF), el *SlABF3* y *SlABF5* en la regulación de genes de respuesta a ABA y su correlación con la sequía. Usando las GRNs se logró encontrar dos posibles reguladores a través del análisis de redes, el Solyc03g118290 y Solyc06g063070 sugeridos como posibles reguladores centrales de la maduración frutal, y un TF de la familia bZIP Solyc01g095460, homólogo a *AtGBF3* como un nuevo regulador de las respuestas al ABA.

Utilizamos las GRNs órgano específicas para analizar las respuestas a la deficiencia de sulfato en raíces y hojas de tomate, filtrando las redes para mantener sólo los genes expresados diferencialmente (DEG) identificados previamente. Este enfoque permitió la creación de GRNs contexto-específicas, revelando que las respuestas a la deficiencia de sulfato demuestran mecanismos regulatorios órgano-específicos. Se logró detectar TFs clave asociados a la regulación de la deficiencia de sulfato, incluyendo Solyc05g009720 (HHO) y Solyc08g078340 (KUA1) en raíces, Solyc05g054650 (ZAT11) y Solyc02g071130 (WRKY71) en hojas, y reguladores compartidos como Solyc01g006650 (EIL3), Solyc04g072460 (TGA7) y Solyc10g086530 (SCL14). El *SlEIL3* surgió como el candidato más prometedor debido a su papel regulando genes de respuesta a deficiencia de sulfato en las GRNs y su homología con SLIM1, el cual es clave en la deficiencia de sulfato en *Arabidopsis*. Realizamos un análisis de perturbación denominado TARGET, que identificó los blancos de regulación directa de EIL3 en protoplastos de tomate y reveló una superposición significativa con los DEG en deficiencia de azufre y los blancos predichos de las GRNs. Más del 60% de los genes relacionados a genes de sulfato fueron validados con TARGET, demostrando a *SlEIL3* como regulador clave y dando soporte a su elección para experimentos de validación funcional.

Para validar la función del *S/EIL3*, generamos plantas de *Arabidopsis thaliana* que sobreexpresan este TF (*OX-S/EIL3*) y las estudiamos bajo tratamientos control (medio MS con todas sus sales) y de deficiencia de sulfato (-S). Las plantas *OX-S/EIL3* mostraron un mayor crecimiento, con raíces primarias más largas, áreas foliares más amplias y mayor contenido total de azufre, en ambos tratamientos. El análisis transcriptómico de las plantas *OX-S/EIL3* demostró una respuesta genotípica muy similar a tratamientos de deficiencia de sulfato en plantas WT y a plantas sobreexpresoras de *SLIM1*, también se encontró que *S/EIL3*, regula genes importantes de respuesta a deficiencia de sulfato, compartidos con *SLIM1* como 4 genes *Response to Low Sulfur (LSU)*, un *Sulfur Deficiency Induced (SDI)*, tres genes de metabolización de azufre (*APRS2*, *ATPS1*, and *APSk3*), y cinco genes transportadores *SULTRs*. Validando nuestra hipótesis debido a que el *S/EIL3* se identificó como un regulador clave del metabolismo del sulfato, sentando las bases para desarrollar estrategias que mejoren la eficiencia nutricional y la resiliencia al estrés en tomate.

Nuestros hallazgos sugieren que *S/EIL3* desempeña un papel fundamental en la regulación de los cambios en la expresión génica provocados por la deficiencia de sulfato en tomate, impulsando el desarrollo de respuestas fenotípicas como represión de crecimiento, la activación de vías de asimilación, metabolización de sulfato y catabolismo de biomoléculas. Los resultados de esta investigación proporcionan una base para estrategias de mejoramiento de cultivos y problemas de estrés en la agricultura. Adicionalmente, demostramos el potencial de las GRNs para identificar nuevos reguladores para dilucidar cascadas regulatorias en respuesta a múltiples condiciones, estadios de desarrollo y tratamientos experimentales en tomate y en otras especies de interés. Las redes regulatorias producidas en este estudio están disponibles como recurso online accesible para la comunidad científica en la plataforma TomatoViz.

III. ABSTRACT

Sulfate (the most available form of sulfur) is an essential macronutrient required for plant growth, development, and productivity. Sulfate deficiency causes significant reductions in plant biomass, affects important physiological processes such as photosynthesis, and decreases agricultural yields. While most transcriptome research on sulfate deficiency has focused on *Arabidopsis thaliana*, the knowledge is more limited in crop species. Tomato (*Solanum lycopersicum*), a globally important crop and model organism for studying fruit development and plant responses to biotic and abiotic stress, is severely impacted by sulfate deficiency. However, the regulatory mechanisms that regulate its transcriptional responses, particularly the roles of transcription factors (TFs) in controlling gene expression, are still understudied. To address this knowledge gap, we used a systems biology approach to generate tissue-specific gene regulatory networks (GRNs) for tomato roots, leaves, flowers, fruits, and seeds.

Using publicly accessible transcriptome data (~10,000 RNA-seq libraries), we used the GENIE3 algorithm to predict regulatory relationships between TFs and target genes. These networks were further refined and validated through the integration of co-expression data, TF binding site predictions, and chromatin accessibility data from reanalyzed ATAC-seq and DNase-seq datasets. Enrichment analysis with tomato ChIP-seq data showed that the GRNs can capture biologically relevant regulatory pathways.

Our findings show that, while genes expressed are mostly ubiquitous across organs, the regulatory interactions are highly organ-specific. Our fruit GRN successfully recapitulated experimentally verified ripening regulator targets from TOMATO AGAMOUS-LIKE 1

(TAGL1) and RIPENING INHIBITOR (RIN) TFs. In addition, analysis of the leaf GRN validated the functions of two ABA response element binding factor (ABF) TFs, SIABF3 and SIABF5 in regulating ABA-responsive genes and their correlation to drought. Using these two context-specific GRNs, we were able to suggest new regulators through network analysis. We identified new potential key TFs, including ERF and ARF as potential central regulators of ripening and SIGBF3 as a potential new regulator of ABA responses.

We used the organ-specific GRNs to analyze the sulfate deficiency responses in tomato roots and leaves, filtering the networks to keep only differentially expressed genes (DEGs) identified in prior studies on the tomato's sulfate deficiency transcriptome. This approach allows the creation of context-specific GRNs, revealing that sulfate deficiency responses are controlled by organ-specific regulatory mechanisms. Notably, we discovered significant TFs linked with sulfate deficiency, including Solyc05g009720 (HHO) and Solyc08g078340 (KUA1) in roots, Solyc05g054650 (ZAT11) and Solyc02g071130 (WRKY71) in leaves, and shared regulators such as Solyc01g006650 (EIL3), Solyc04g072460 (TGA7), and Solyc10g086530 (SCL14). The *S/EIL3* emerged as the most promising candidate due to its predicted key role in regulating sulfate-responsive genes and its homology with SLIM1, a key regulator of the sulfate cascade in *Arabidopsis*. We performed a perturbation analysis called TARGET and identified the EIL3 direct regulatory targets in tomato protoplasts, revealing significant overlap with the DEG under sulfate deficiency and its GRN-predicted genes. Over 60% of sulfur-related targets were validated with TARGET, highlighting the *S/EIL3* as a key regulator and supporting its selection for functional validation experiments.

To validate the *S/EIL3* function, we generated *Arabidopsis thaliana* plants that overexpress this TF (OX-*S/EIL3*). The OX plants showed enhanced growth, with longer primary

roots, broader foliar areas, and higher total sulfur content compared to wild-type (WT) plants, both under control conditions and sulfate deficiency treatments. Transcriptomic analysis of OX-*S/EIL3* plants revealed a genotypic response that resembles the transcriptomes of WT plants under sulfate deficiency and the transcriptome of SLIM1-overexpressing plants. Furthermore, *S/EIL3* was found to regulate key sulfate deficiency response genes, including shared targets with SLIM1, involved in sulfur metabolism and transport. These targets included four *Response to Low Sulfur (LSU)* genes, one *Sulfur Deficiency Induced (SDI)* gene, three sulfur metabolism cascade genes (*APRS2*, *ATPS1*, and *APSk3*), and five sulfate transporter genes (*SULTRs*). Additionally, analysis of *S/EIL3* targets indicated a broader regulatory role beyond sulfur metabolism, influencing stress response pathways, growth processes, and immune responses. In line with our hypothesis, *S/EIL3* was identified as a key regulator of sulfur metabolism and stress response pathways in tomato, including oxidative stress responses, immune activation against pathogens, and the modulation of molecule transport. These findings provide the foundation for developing strategies looking forward to enhancing plant nutrient efficiency metabolism and stress resilience in tomato plants. Our findings suggest that *S/EIL3* plays a pivotal role in regulating the gene expression changes caused by sulfate deficiency treatments in tomato, driving phenotypic responses such as growth repression and promoting processes like sulfate assimilation, sulfur compound metabolism, and biomolecule catabolism. These results provide a foundation for crop improvement strategies and to stress-related challenges in agriculture. Additionally, we proved the potential of GRNs to identify novel regulators in crops contributing to reveal regulatory cascades in response to diverse conditions, developmental stages, and experimental treatments in tomato and to other species. The networks developed in this study are available as an online resource for the scientific community on the TomatoViz platform.

IV. INTRODUCTION

Sulfur is a key macronutrient for plant growth.

Agricultural yields, crop quality, and whole plant survival depend strongly on environmental cues that extend to more than just water and sunlight availability; it is also necessary that plants grow in adequate levels of mineral nutrients (Taiz and Zeiger, 2010). Sulfur is one of these crucial mineral nutrients that is required for all living organisms' survival. Sulfur is considered a macronutrient for plants because it accounts for 0,1-0,5% of a plant's dry weight, thus crop productivity is strongly affected by sulfur availability since it directly limits plant growth (Hawkesford, 2000; Maruyama-Nakashita, 2017, Preprint; Nakai and Maruyama-Nakashita, 2020, Preprint).

The ability of plants to take up inorganic sulfur in the form of sulfate is one of their essential roles in the ecosystem dynamics since through this process plants can provide sulfur to herbivorous animals and later on to other living organisms (Takahashi *et al.*, 2011). Sulfate is necessary for plants because it is required for the synthesis of multiple essential compounds such as the amino acids cysteine and methionine. In addition, the thiol group formed during sulfur metabolization makes cysteine a crucial amino acid for protein structure, since it allows for the formation of disulfide bridges. Plants can transform sulfate into adenosine 5'-phosphosulfate (APS) using ATP, which is followed by reduction to sulfite and then to sulfide; these molecules serve as donors for other important biomolecules such as glutathione, S-adenosylmethionine (SAM), vitamins, cofactors and coenzymes (such as thiamine, biotin, and coenzyme-A), and multiple secondary metabolites (Figure 1) (Maruyama-Nakashita and Ohkama-Ohtsu, 2017; Kopriva *et al.*, 2019). These biomolecules make sulfate indispensable to sustain biological

processes related to plant growth, development, stress responses, and chemical defense metabolism (Maruyama-Nakashita, 2017, Preprint; Maruyama-Nakashita and Ohkama-Ohtsu, 2017; Henríquez-Valencia *et al.*, 2018; Nakai and Maruyama-Nakashita, 2020, Preprint).

The agronomic impacts of sulfate deficiency are well documented. Plants experiencing sulfate deficiency exhibit growth retardation, reduced photosynthetic efficiency, and decreased chlorophyll and amino acid levels, leading to an overall reduction on its development and environmental adaptability (Hawkesford, 2000; McNeill *et al.*, 2005; Zuchi *et al.*, 2009; Hubberten *et al.*, 2012, Preprint; Maruyama-Nakashita, 2017, Preprint; Zhang *et al.*, 2020a; Lyčka *et al.*, 2023) In aerial organs, sulfate deficiency primarily affects leaf development, leading to premature yellowing or chlorosis, particularly in young leaves, as sulfate is an immobile nutrient (Figure 2) (Hasan *et al.*, 2018; Lyčka *et al.*, 2023). At a physiological level, sulfur deficiency in *Arabidopsis thaliana* is related to S-storage compounds catabolism, downregulation of amino acid biosynthesis routes and an increased expression of high-affinity sulfate transporters (*SULTRI;1* and *SULTRI;2*), which increase sulfate uptake and cell transportation (Jones-Rhoades and Bartel, 2004; Maruyama-Nakashita, 2004, 2017, Preprint; Maruyama-Nakashita *et al.*, 2004; Forieri *et al.*, 2017; Siddiqui *et al.*, 2020) In crops plants, the effects of sulfur deficiency translates into stunted growth and reduced photosynthetic rates which adds up in poor quality fruits or seeds and overall reduced yields (Narayan *et al.*, 2022; Fernández *et al.*, 2024) .

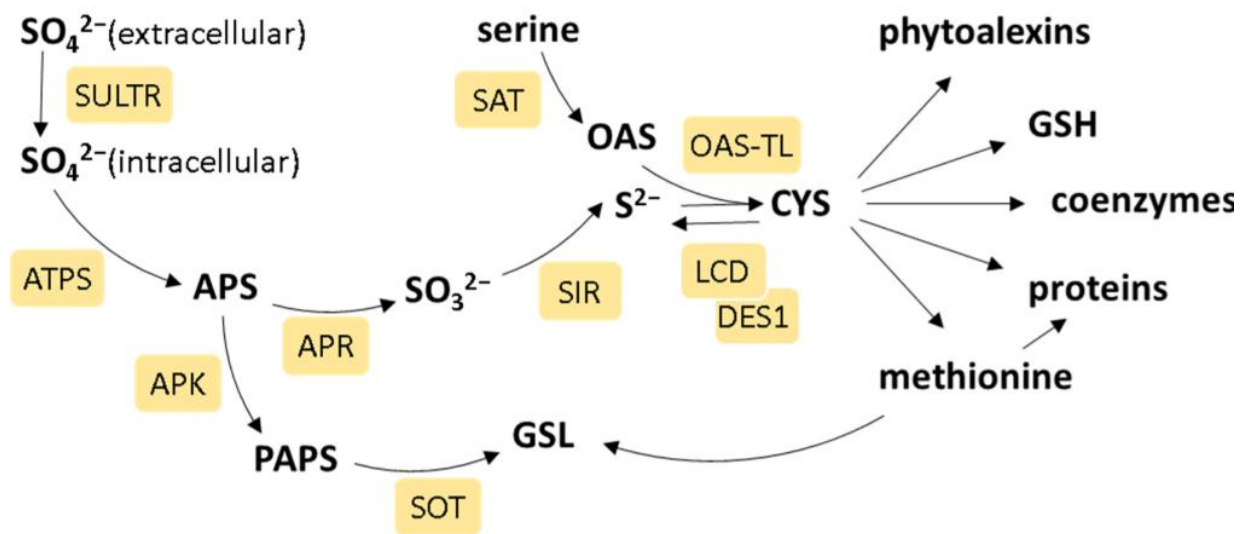


FIGURE N°1. Overview of plants sulfate assimilation and metabolization pathway. Enzymes are highlighted in yellow. Legend: sulfate transporter (*SULTR*), ATP sulfurylase (*ATPS*), adenosine 5'-phosphosulfate reductase (*APR*), sulfite reductase (*SIR*), serine acetyltransferase (*SAT*), O-acetyl-thiol-lyase (*OAS-TL*), cysteine desulphydrase (*LCD*, *DES*), APS kinase (*APK*), and sulfotransferase (*SOT*). The metabolites in the scheme are as follows: 5'-phosphosulfate (APS), 3'-phosphoadenylylsulfate (PAPS), O-acetylserine (OAS), cysteine (CYS), glutathione (GSH), and glucosinolates (GSLs). Image from (Wawrzynska & Sirko, 2024).

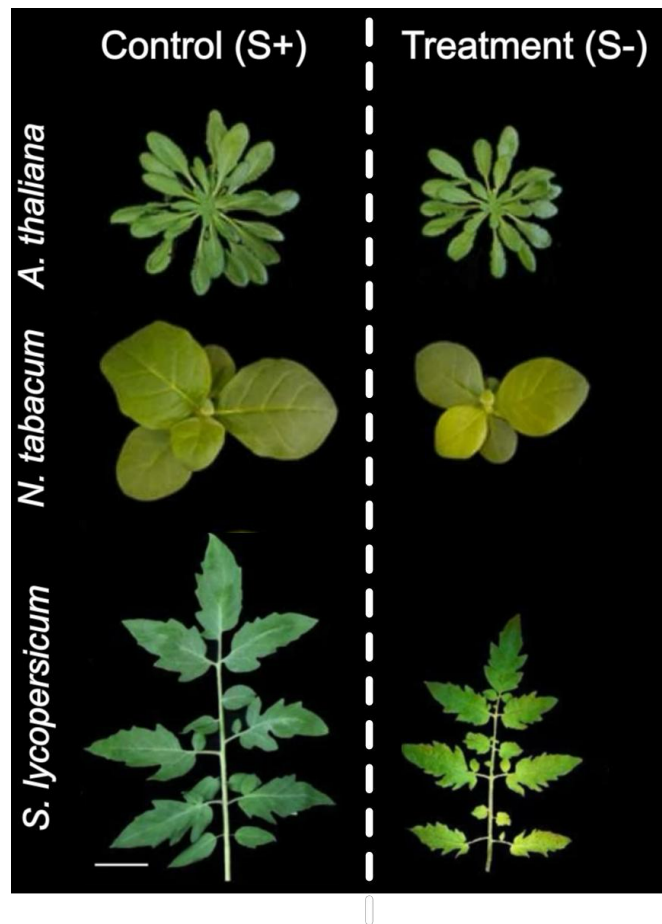


FIGURE N°2. Comparative phenotypic effects of sulfate deficiency in *Arabidopsis thaliana*, *Nicotiana tabacum*, and *Solanum lycopersicum*. Representative images illustrate the morphological differences between sulfate-sufficient (Control S+) and sulfate-deficient (Treatment S-) conditions for each species. *A. thaliana* shows a reduction in rosette size and chlorosis under S- conditions. *N. tabacum* exhibits stunted growth and yellowing of leaves, while *S. lycopersicum* demonstrates impaired leaf development and chlorosis. Images adapted from (Hasan *et al.*, 2018; Lyčka *et al.*, 2023).

Transcriptional regulation triggered by sulfate deficiency.

From past decades, numerous studies have explored the transcriptomic effects of sulfate deficiency, particularly in the model plant *Arabidopsis thaliana*. These analyses have identified a wide array of genes whose expression depends on sulfate availability (Aarabi et al., 2016; Bielecka et al., 2015; Dietzen et al., 2020; Forieri et al., 2017; Henríquez-Valencia et al., 2018; Iyer-Pascuzzi et al., 2011; Maruyama-Nakashita et al., 2004, 2006; Ristova & Kopriva, 2022; Zhang et al., 2020; Zuchi et al., 2009). Henríquez-Valencia et al. (2018) identified 27 sulfate-responsive genes, including those critical for sulfate acquisition, remobilization, and assimilation, such as the sulfate transporters *SULTR1;1*, *SULTR2;1*, and *SULTR4;2*, *APS reductase 3 (APS3)*, and genes involved in glucosinolate metabolism, such as *BCAT4* and *CYP79B3*. Additionally, genes related to glutathione metabolism, such as *GSTU20*, and established sulfate deficiency markers, including *Sulfur deficiency induced genes (SDIs)* and *response to low sulfur genes (LSUs)*, were consistently affected (Bonnot et al., 2020; Wawrzyńska and Sirko, 2020). Sulfate deficiency in crops commonly leads to growth retardation and reduced productivity, often linked to the downregulation of amino acid biosynthesis pathways and the depletion of sulfur-containing metabolites, such as glucosinolates, glutathione, S-adenosylmethionine and O-acetylserine (Courbet et al., 2019; Watanabe and Hoefgen, 2019, Preprint).

We performed a review of the transcriptomic studies in crop plants under sulfate deficiency and found a significant gap in available datasets addressing gene expression changes under this stress (Fernández et al., 2024). In wheat (*Triticum aestivum*), sulfate starvation induces the expression of genes involved in sulfur and nitrogen transport, carbon metabolism,

and sulfur-containing metabolites, including glutathione and glucosinolates, along with canonical markers like *SDI1*, *SDI2*, and *LSU* orthologs (Bonnot *et al.*, 2020). Comparable transcriptomic responses have been observed in *Brassica* spp., *Pisum sativum*, *Medicago truncatula*, *Solanum lycopersicum*, and *Oryza sativa*, characterized by the upregulation of *SULTRs*, *ATP-sulfurylases*, *glycosyl-transferases*, and *APS reductases* (Canales *et al.*, 2020; Courbet *et al.*, 2021; Fernández *et al.*, 2024). This limited data availability underscores the need for further research in this area to better understand the molecular responses to sulfate limitation.

Transcription factors controlling gene expression responses to sulfate availability.

Most of our understanding of TFs involved in the sulfate deficiency response comes from studies on *Arabidopsis thaliana*. Among these, SLIM1/EIL3, a member of the plant-specific EIL TF family, has emerged as a key regulator (Maruyama-Nakashita *et al.*, 2006; Wawrzyńska and Sirko, 2014). While other EIL family members, such as EIN3, EIL1, and EIL2, are associated with ethylene signaling, the roles of EIL4 and EIL5 remain poorly defined (Dolgikh *et al.*, 2019). In contrast, the SLIM1 TF does not respond to ethylene but instead binds directly to sulfur response elements in the promoters of sulfur deficiency-responsive genes, including *SULTR* genes. It also plays a critical role in reprogramming secondary sulfur compound biosynthesis pathways during sulfate deficiency (Maruyama-Nakashita *et al.*, 2004, 2006; Kawashima *et al.*, 2011; Maruyama-Nakashita, 2017, Preprint).

Interestingly, SLIM1's transcript levels and subcellular localization are unaffected by sulfate availability, suggesting a post-transcriptional regulation mechanism (Maruyama-Nakashita *et al.*, 2006). Phylogenetic analysis performed in our recent review article (Fernández *et al.*, 2024),

places Arabidopsis SLIM1/EIL3 in a specific clade with 286 other taxa, including rice homologs OsEIL3;1 (Os08g0508700) and OsEIL3;2 (Os09g0490200) reported to be involved in *SULTR* genes regulation, and the tomato homolog SLIM1/EIL3 (Solyc01g006650) which has been identified as a potential key regulator of sulfur transport and metabolism in tomato leaves and roots (Canales *et al.*, 2020). Beyond SLIM1, other TFs have been implicated in the regulation of the sulfate deficiency response, since over 50% of the responsive genes found in Arabidopsis shoots can't be explained by the effect of SLIM1 (Dietzen *et al.*, 2020). EIL1 has been shown to act as a supportive regulator in the control of sulfate deficiency responses, complementing SLIM1/EIL3 (Kawashima *et al.*, 2011; Dietzen *et al.*, 2020). Multiple TFs from the MYB family, including MYB28 and MYB29, have been found to positively regulate sulfur-containing secondary metabolites (glucosinolates) biosynthesis (Hirai *et al.*, 2007; Frerigmann, 2016; Mitreiter and Gigolashvili, 2021). Integrated meta-analyses of transcriptome data in Arabidopsis suggest that other TFs, such as the bZIP1, RVE2, and NF-YA2, may play a role in regulating sulfate deficiency response (Henríquez-Valencia *et al.*, 2018; Watanabe and Hoefgen, 2019, Preprint). A recent review conducted by our laboratory identified over 25 TFs primarily from the EIN/EIL, MYB, bZIP and GBF TF families with a potential role as regulators of the sulfate deficiency response (Fernández *et al.*, 2024). Most of them were identified through TF binding site prediction, yeast one-hybrid (Y1H), ChIP-seq, and electrophoretic mobility shift assays (Fernández *et al.*, 2024). However, the direct role of these TFs in the regulation of sulfate deficiency response has not been experimentally validated yet in Arabidopsis nor any other species.

Gene regulatory networks inference methods

In systems biology, researchers look forward to accurately reconstructing a panoramic view of the regulatory cascades occurring inside the cell, particularly to find the effect of TFs on their target genes. A strategy to represent these regulatory pathways is through the generation of genome-wide Gene Regulatory Networks (GRNs). These networks show TFs and targets as nodes connected by edges pinpointing a regulatory directed interaction, therefore GRNs can be interpreted as blueprints to detect the hierarchical relations of gene regulation (Chai *et al.*, 2014; Swift and Coruzzi, 2017). GRN models have allowed for the identification of important TFs as key hubs controlling regulatory cascades in multiple organisms (Alvarez *et al.*, 2014; Doidy *et al.*, 2016; Swift *et al.*, 2020; Vidal *et al.*, 2020).

Various approaches exist to help in the identification of TF-target interactions and generate gene networks. TF binding sites can be predicted by the analysis of DNA-binding motifs and identifying the matching binding sites within gene promoters (Mercatelli *et al.*, 2020). If it includes open chromatin sites (OCS) sequences, obtained using methods such as DNase-seq (Zhang *et al.*, 2012) or ATAC-seq (Li *et al.*, 2007), it allows accurate predictions of TF binding on a genome-wide scale under cellular context. Alternatively, Chromatin immunoprecipitation followed by sequencing (ChIP-seq) and DNA affinity purification sequencing (DAP-seq) can directly assess events of TF binding in genomic regions; however, these methods are technically challenging, particularly in non-model organisms (P. J. Park, 2009).

An alternative method to ChIP-Seq that integrates information about direct regulation and changes in gene expression has arisen in the last years, Transient Assay Reporting Genome-wide Effects of Transcription factors (TARGET), is a cell-based TF perturbation assay (Bargmann *et al.*, 2013, Preprint). This method allows for rapid identification of genome-wide targets of a TF on cells. The TARGET assay in plants uses protoplasts that are transformed with a vector that expresses a TF fused to a glucocorticoid receptor sequence. The chimeric GR-TF protein can be induced to relocate to the nucleus by the addition of the glucocorticoid–ligand dexamethasone (DEX), where it can bind to its target genes and activate gene expression. Cells can also be treated with the translation inhibitor cycloheximide (CHX), which blocks the synthesis of secondary TFs allowing the distinction of direct target genes regulated by the TF under study (Bargmann *et al.*, 2013, Preprint). TARGET has been successfully used to study the effect of different TFs in gene expression control and epigenetic regulation in *A. thaliana* and few other plants (Doidy *et al.*, 2016; Brooks *et al.*, 2019; Alvarez *et al.*, 2020; Li *et al.*, 2020; Swift *et al.*, 2020; Shanks *et al.*, 2022), moreover TARGET has been used to obtain the direct target genes involved in nutrient deficiency regulatory cascades and, more importantly, interactions identified by this assay have also been shown to have *in planta* relevance for TFs involved in nitrate regulation (TGA1, NAP, bZIP3, RAV1, etc) (Brooks *et al.*, 2019; Alvarez *et al.*, 2020; Li *et al.*, 2020; Safi *et al.*, 2021; Shanks *et al.*, 2022).

GRNs models can be obtained by using machine learning algorithms that take advantage of omic information and infer regulatory relationships, a standout method is GENIE3 (Gene Network Inference with Ensemble of Trees), which uses high-throughput gene expression data with iterative random forests to infer TF-target regulatory pairs (Huynh-Thu *et al.*, 2010; Huynh-Thu and Geurts, 2019). GENIE3 has demonstrated superior performance in the DREAM4

Multifactorial Network challenge and the DREAM5 Network Inference challenge (Huynh-Thu *et al.*, 2010; Huynh-Thu and Geurts, 2019); additionally, GENIE3 has demonstrated its accuracy on predicting accurate *in vivo* regulation through GRNs on multiple plant species (Huang *et al.*, 2018; Harrington *et al.*, 2020; Tu *et al.*, 2020; De Clercq *et al.*, 2021; Shanks *et al.*, 2022; Chen *et al.*, 2023; Ranjan *et al.*, 2024). Furthermore, the integration of high throughput omic information, like gene expression data with TF binding predictions, might improve GRN accuracy and reduce the existence of false positives (Haque *et al.*, 2019). Thus, integrative strategies that combine computational predictions of TF binding sites in various genomic regions, predicted GRNs, and validations with experimental data are powerful approaches that have been successfully applied in model organisms such as *Arabidopsis* and wheat, resulting in comprehensive and reliable GRNs (Chen *et al.*, 2023; De Clercq *et al.*, 2021). Such approaches provide useful insights into TF regulatory potential and provide a solid foundation for future research in other organisms.

In a recent review article, our research team used GRN modeling to address the knowledge gap regarding potential regulatory TFs involved in the sulfate deficiency response. We integrated available GRNs from *Arabidopsis thaliana* and predictive information from two relevant crops, tomato and rice, to generate predictive GRNs in an effort to elucidate the molecular mechanisms driving phenotypic changes and regulatory cascades associated with sulfate deficiency (Fernández *et al.*, 2024). However, we faced significant limitations because crop plants often lack comprehensive GRN data, and in many cases, sufficient data on TF-target interactions are unavailable, particularly for stress responses like sulfate deficiency.

Tomato lacks networks models that explain direct regulation between TFs and target genes.

Tomato (*Solanum lycopersicum* L.) is a plant of the Solanaceae family and one of the most widely consumed crops globally, according to the FAOstat website (<http://www.fao.org/faostat>). The tomato plant grows as a medium-sized herb and produces a fleshy fruit enriched with nutrients considered essential for the human diet (Shi and Le Maguer, 2000; Canene-Adams *et al.*, 2005). Tomato is considered a model organism (Kimura and Sinha, 2008; The Tomato Genome Consortium, 2012), primarily for the study of fleshy fruit development and ripening, plant responses to pathogens (Kimura and Sinha, 2008; Gascuel *et al.*, 2017, Preprint). In molecular biology, multiple resources for genomic analysis in tomato have been produced (The Tomato Genome Consortium, 2012); nevertheless, despite its importance, tomato regulatory cascades in response to external or internal cues are poorly understood.

In tomato, the discovery of *in vivo* interactions between TFs and target genes is an area still in development. In *Solanum lycopersicum*, only a limited number of TFs have been studied using ChIP-seq (Fujisawa *et al.*, 2011; Ricardi *et al.*, 2014; Du *et al.*, 2017; Lü *et al.*, 2018; Gao *et al.*, 2019; Lira *et al.*, 2020; Liu *et al.*, 2020; Ding *et al.*, 2022; Tu *et al.*, 2022; Yang *et al.*, 2022; Jiang *et al.*, 2023). Similarly, few TFs have been studied using DAPseq (López-Vidriero *et al.*, 2021; Chong *et al.*, 2022; Huang *et al.*, 2023; Zhu *et al.*, 2023). While these approaches have identified TF binding sites and regulatory targets of TFs, they are typically limited to individual TFs. Alternatively, a limited number of studies have addressed accessible chromatin sites in *S. lycopersicum* particularly to analyze responses to abiotic stress mostly in fruits using ATAC-seq (Maher *et al.*, 2018; Reynoso *et al.*, 2019; Hendelman *et al.*, 2021; Kajala *et al.*, 2021) and DNAase-seq (Qiu *et al.*, 2016; Lü *et al.*, 2018).

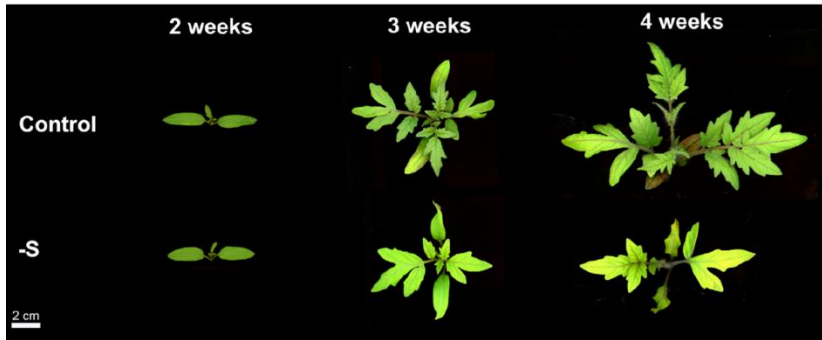
Biological network models for tomato are limited, with most studies focused on protein-protein interactions or GCNs derived from single experiments or small datasets integrating fewer than 10 studies (Arhondakis *et al.*, 2016; Bizouerne *et al.*, 2021; Ichihashi *et al.*, 2014; Pirona *et al.*, 2023; Wang *et al.*, 2023; Yue *et al.*, 2016). Comprehensive GCNs that integrate data from multiple experiments are scarce; for example, (Fukushima *et al.*, 2012; Kim *et al.*, 2017) combined transcriptomic data from microarrays and a limited number of RNA-seq experiments, whereas (Zouine *et al.*, 2017) integrated data from 29 RNA-seq studies to generate a global GCN. However, these networks are organ-independent or exclusively focused on fruits and were generated using limited gene lists based on outdated tomato annotations (ITAG2.3 or ITAG3.0) (Fukushima *et al.*, 2012; Kim *et al.*, 2017; Zouine *et al.*, 2017). In this context, developing GRN models that include a more complete set of annotated genes based on newer reference genome assemblies, from wider universe of high-throughput omics data and that can represent organ-specific regulation is imperative to uncover regulatory mechanisms in tomato.

Sulfate deficiency affects tomato plant growth, resulting in reduced plant size accompanied with reduced shoot and root fresh weight, chlorosis in younger leaves (due to decreased chlorophyll content), impaired CO₂ assimilation and photosynthesis, lower protein levels, and decreased yield (weight and number of fruits). It also alters other nutrients homeostasis, affecting nitrate, phosphate, calcium, magnesium, molybdenum, potassium, and iron levels. Sulfate deficiency affects the levels of metabolites like sulfides, cysteine, γ -glutamyl-cysteine, GSH, and SAM but increases serine and OAS levels in shoots and roots (Lopez *et al.*, 1996; Alhendawi *et al.*, 2005; Zuchi *et al.*, 2009; Zhao *et al.*, 2014; Hasan *et al.*, 2018; Canales *et al.*, 2020; Siddiqui *et al.*, 2020; Cao *et al.*, 2023; Coppa *et al.*, 2023)

To characterize the molecular response of tomato plants to sulfate deficiency, Canales et al. (Canales et al., 2020) conducted a detailed transcriptomic analysis with temporal and organ-specific resolution. Their findings showed a significant effect of growth reduction in roots and aerial organs, as shown by decreased total dry weight (Figure 3). Significant transcriptome changes were found in both leaves and roots after three weeks of sulfate deficiency, with the majority of DEGs responding to organ-specific conditions. Only 10% of the upregulated and 20% of the downregulated DEGs were shared between the two organs, with downregulated genes prevailing in abundance overall (Figure 3b).

Upregulated root genes were enriched for plant defense and phosphate metabolism, while those in leaves were associated with hormone signaling (e.g., salicylic acid and abscisic acid pathways) and senescence. Shared upregulated processes included cellular responses to sulfur starvation and cell transport. In contrast, downregulated root genes were enriched for metal ion responses and oxidative stress, whereas downregulated leaf genes were linked to photosynthesis and light responses. Both organs showed decreased expression of cytokinin and auxin signaling pathways, as well as cell wall regulation. This study also identified potential TFs involved in sulfate transport, assimilation, and metabolism routes using co-expression networks and TF-target interaction data from PlantRegMap (Tian *et al.*, 2020). However, TF selection relied on outdated *S. lycopersicum* annotations (ITAG 2.4) and a limited TF set, and their regulatory roles in sulfate deficiency responses remain to be experimentally validated.

a



b

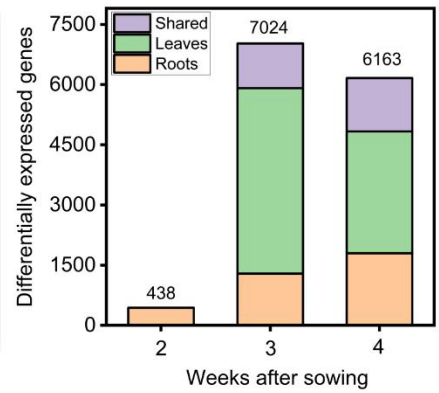


FIGURE N°3. Sulfate deficiency effect in *Solanum lycopersicum* plants. a. Images of tomato plants grown under full nutrient or S-limiting conditions for 2,3 and 4 weeks after sowing. **b.** Transcriptome effect of sulfate deficiency on tomato roots and leaves 3-4 weeks after sowing. Images from Canales, et al. (2020).

In this study, we integrated a large-scale of tomato genomic datasets to generate, validate, and refine organ-specific Gene Regulatory Networks (GRNs) in *Solanum lycopersicum*. We then applied these networks to investigate the roots and leaves responses to sulfate deficiency, identifying key regulatory genes through their influentiality within the networks. Among these, we identified *S/EIL3* as a promising candidate and performed a perturbation analysis followed by functional validation through the generation of overexpressing plants. Our results demonstrate that *S/EIL3* acts as a central regulator of sulfate deficiency-responsive genes, controlling multiple biological processes contributing to the observed phenotypic growth changes in tomato plants under stress. The organ-specific GRNs produced in this work provide a valuable foundation for exploring a range of experimental conditions, from developmental processes to stress responses, offering a robust framework to address open questions in tomato biology. The organ-level GRNs are available at (<https://plantaeviz.tomsbiolab.com/tomviz>).

Hypothesis

The growth limitation of *S. lycopersicum* exposed to sulfate deficiency is caused by a reprogramming of the roots and leaves transcriptome evoked by one or more central TFs commanding sulfate-responsive genes.

General Goal

To identify central Transcription factors (TFs) controlling global gene expression reprogramming in *Solanum lycopersicum* during sulfate deficiency.

Specific goals

Aim 1. To generate organ-specific reference Gene Regulatory Network models for *Solanum lycopersicum*.

Aim 2. To identify candidate TFs that are central regulators of the sulfate deficiency response in *S. lycopersicum*.

Aim 3. To experimentally validate the function of a central TF candidate in the regulation of plant growth under sulfate deficiency.

V. MATERIALS AND METHODS

Aim 1

Tomato gene annotation update.

To track the gene models added in ITAG 4.1 and those removed compared to ITAG 4.0, a new version, ITAG 4.1c, was generated through a conditional merge. Gene models from ITAG 4.1 were integrated into the 4.0 annotation file (.gff3) when their genome coordinates did not overlap with existing entries, resulting in the final ITAG4.1c annotation file. To expand the functional annotations for tomato, ITAG 4.1c protein sequences were analyzed using eggNOG-mapper to predict Gene Ontology (GO) terms, functional categories, and orthology relationships based on evolutionary genealogy (Cantalapiedra *et al.*, 2021). Additionally, functional annotations for all genes in ITAG 4.1c were generated using InterProScan v5.57-90 (Jones *et al.*, 2014) under default parameters. The resulting GO annotations for molecular functions and biological processes were consolidated, and the unique annotations for each gene were used to create an updated GO set.

To update the list of TFs in ITAG 4.1c, we integrated evidence from multiple sources. The selection criteria included annotated TFs from ITAG 4.0 and ITAG 4.1 (Fernandez-Pozo *et al.*, 2015), the TF catalogs from PlantTFDB (Jin *et al.*, 2017) and ITAK (Zheng *et al.*, 2016). In addition, a keyword search within ITAG 4.1c GO annotations, an ortholog analysis using default parameters in Orthofinder v.3.0 (Emms & Kelly, 2019) with the Arabidopsis TF list from TAIR (Rhee *et al.*, 2003), and results from the InterProScan proteome analysis (Jones *et al.*, 2014), was carried out. Genes supported by at least three independent sources of evidence were classified as TFs. We generated an updated set of tomato Position Weight Matrices (PWMs) of DNA-binding motifs by combining previously identified PWMs from CisBP (Weirauch *et al.*, 2014)

with *in silico* predictions for the final TF list. The PWMs were inferred using the JASPAR “infer_profile.py” script (Castro-Mondragon *et al.*, 2022). This tool uses sequence similarity search algorithms to link a TF proteome to reference PWMs from Arabidopsis and Maize, thus providing a new set of DNA-binding motifs for tomato TFs based on the best sequence-similarity hits (associated to p-values).

Input mRNA-seq analysis

To obtain tomato RNA-seq datasets, we queried the NCBI SRA database using (“*Solanum lycopersicum*”[Organism] AND ILLUMINA[Platform]) NOT (RIP-Seq[Strategy] OR OTHER[Strategy] OR ChIP-Seq[Source] OR METATRANSCRIPTOMIC[Source] OR Bisulfite-Seq[Strategy] OR GENOMIC[Source] OR METAGENOMIC[Source] OR DNase-Hypersensitivity[Strategy] OR WGS[Strategy] OR ncRNA-Seq[Strategy] OR WCS[Strategy] OR degradome OR miRNA-Seq[Strategy] OR small RNA[Title] OR sRNA[Title]) (Leinonen *et al.*, 2011). The metadata was classified by organ of origin following Santiago *et al.* (2024) protocol. The libraries were downloaded using SRAtools (Kans, 2010). Adapters were trimmed, and low-quality reads (reads with average quality inferior to $q < 30$ and shorter than 20 bases) were filtered out using fastp v.0.20.0 (Chen *et al.*, 2018). Reads were aligned to the SL4.0 *S. lycopersicum* genome assembly (Hosmani *et al.*, 2019) using STAR v.2.7.3 (Dobin *et al.*, 2013). After mapping, a total of 10,618 mRNA-seq libraries were retained. Gene counts were obtained with FeatureCounts v.2.0.0 (Liao *et al.*, 2014) using the ITAG4.1c annotation. Total counts were normalized to transcripts per million (TPM); Finally, the genes with ≥ 5 TPM in at least 10% of the total libraries for each organ were classified as specifically expressed, following Huang *et al.*, (2018) protocol.

Input ChIP-seq analysis

The following query (("Solanum lycopersicum"[Organism] AND ILLUMINA[Platform]) AND ChIP-Seq[Source]) was used to obtain tomato TF-binding (ChIP-seq) datasets from the NCBI SRA website (Leinonen *et al.*, 2011). ChIP-seq libraries were processed using the methods available on ENCODE pipelines (Hitz *et al.*, 2023). Briefly, the libraries were downloaded from the NCBI SRA using SRAtools (Kans, 2010). Adapters were trimmed, and low-quality reads (reads with average quality inferior to $q < 30$ and shorter than 20 bases) were dismissed using Cutadapt v.4.9 (Martin, 2011). Each file was mapped with Bowtie2 v.2.54 (Langmead and Salzberg, 2012) to the SL4.0 assembly (Hosmani *et al.*, 2019). Alignment files were sorted and filtered with Samtools v.1.21 (Li *et al.*, 2009) and peaks were identified with MACS2 v.2.2.9.1 (Zhang *et al.*, 2008). Only libraries with $\geq 80\%$ mapping efficiency and over 1,000 peaks assigned to annotated genes were retained as high-quality datasets for downstream analysis.

Input ATAC-seq and DNase-seq analysis

The following query (("Solanum lycopersicum"[Organism] AND ILLUMINA[Platform]) AND ATAC-Seq[Source] AND DNase-Seq[Source]) was used to obtain tomato open chromatin sites (OCS) approximations datasets from the NCBI SRA website (Leinonen *et al.*, 2011) A total of 183 open chromatin experiments (DNase-seq, ATAC-seq libraries) were downloaded using SRAtools (Kans, 2010). Reads were trimmed for adapters, and low-quality reads (reads with average quality inferior to $q < 30$ and shorter than 20 bases) were dismissed using Cutadapt v.4.9 (Martin, 2011). The ATAC-seq libraries were processed following Reynoso *et al.*, (2019) pipeline, while the DNase-seq libraries were processed following Moyano *et al.*, (2021) protocol. Briefly, both groups of reads were mapped to the SL4.0 genome assembly (Hosmani *et al.*, 2019) using Bowtie2 v.2.54 (Langmead and Salzberg, 2012). The ATAC-seq alignments were sorted

and filtered with Samtools v.1.21 (Li *et al.*, 2009) and peaks were identified with HOMER v.4.11 (Heinz *et al.*, 2010). The DNase-seq regions were mapped into DNase hypersensitive sites using HOTSPOT (Meuleman *et al.*, 2020). OCS peak files were then merged by experiment and converted into FASTA sequences with BedTools v.2.31.1 (Quinlan and Hall, 2010).

Determination of TF binding sites using FIMO

Two TF-binding networks were generated by mapping all tomato TF DNA binding motifs, represented as Position Weight Matrices (PWMs) to genomic regions of the *Solanum lycopersicum* SL4.0 genome assembly using the Find Individual Motif Occurrences (FIMO) search tool (Grant *et al.*, 2011). FIMO calculates the probability of a motif binding to a specific DNA sequence. The DNA fasta sequences used as queries differed between the networks: one network included all promoter sequences collected from two kilobases upstream of each gene's transcription start site (TSS), whereas the second network used the organ-specific OCS sequences. The results were assigned to genes using BedTools v.2.31.1 ClosestGene (Quinlan and Hall, 2010).

GENIE3 inference of regulatory interactions

The processed transcriptomes represented as count tables for each organ, were given as input to the GENIE3 algorithm, as well as the updated list of ITAG4.1C annotated TFs. The GENIE3 tool was run in an R environment with standard parameters, using 2,000 decision trees and a seed of 122 for reproducibility. The output scores were used to create subnetworks based on the top 1%, 2%, 5%, 8%, and 10% scores of TF-target pairings. These thresholds were used in previously published GENIE3 networks (Huang *et al.*, 2018; Cuesta-Astroz *et al.*, 2021; Olivares-Yañez *et al.*, 2021).

Co-expression network generation

To generate co-expression networks for tomato organs, we used the pipeline described in Orduña, et al. (Orduña *et al.*, 2023). Briefly, the gene counts tables from the transcriptome of each organ were used to calculate the Pearson correlation indices for each gene. The results were ordered by gene rank in descending order and computed in a highest reciprocal ranking (HRR) matrix per organ following the formula: $HRR(A,B) = \max(\text{rank}(A,B), \text{rank}(B,A))$. Finally, to avoid noise and low confidence pairings, the top 1% (3500 genes) of the highest frequency HRR per gene were chosen to make the tomato organ-specific GCNs.

Enrichment analysis

In order to evaluate the significance of the intersection between gene lists, we used the R package GeneSectR (<https://github.com/NateyJay/genesectR>). The GeneSectR utilizes the Fisher exact test to evaluate whether the observed overlap between gene sets is greater than what would be expected by chance, calculating a p-value that indicates the likelihood of the overlap occurring randomly.

Gene Set Enrichment Analysis (GSEA)

Gene Set Enrichment Analysis (GSEA) was conducted to identify overrepresented biological process GO terms using a hypergeometric test with Benjamini and Hochberg false discovery rate (FDR) correction (threshold p-value < 0.05). The analysis was performed using the BinGO v.3.0.5 tool (Maere *et al.*, 2005) within Cytoscape, with input from the updated tomato 4.1c GO terms catalog. The REVIGO v. 1.8.1 (Supek *et al.*, 2011) web application was used to improve and narrow down the grouping of GO terms, and a focus on GO terms within levels 5–7 was to focus on more specific biological processes.

Network performance evaluation.

To evaluate the accuracy of the predicted GRNs in capturing true regulatory interactions, we employed the Contreras-López et al., (2022) pipeline to compute the area under the receiver operating characteristic (AUROC) and precision-recall (AUPR) curves. Briefly, these analyses were performed using organ-level GRNs and tested against validated regulatory interactions derived from reanalyzed tomato ChIP-seq datasets. True and false positive rates were calculated using the *precrec* v.0.14.4 package in R (Saito and Rehmsmeier, 2017). Gene interactions were filtered to retain only regulatory genes present in both the GENIE3-inferred and ChIP-seq networks, with edges assigned as binary labels indicating the validation status. To assess statistical significance, the AUROC and AUPR values were compared against 1,000 randomized networks generated by shuffling edge weights. Percentile-based confidence intervals (2.5–97.5%) were used to benchmark the GENIE3 network's performance, and significance was determined via a permutation test.

GRNs visualization and networks analysis

Network visualizations were generated using Cytoscape v.3.10.1 (Shannon *et al.*, 2003) and network topology analyses were conducted using the Cytoscape *NetworkAnalyzer* tool. The R package *Influential* v.2.2.9 (Salavaty *et al.*, 2020) was used to identify the TF hubs with the highest connectivity and integrated centrality (IVI) of network nodes. IVI is a comprehensive measure of node influence that integrates topological features to identify hub nodes within gene networks (Salavaty *et al.*, 2020).

TF-Target pairings analysis

The outdegree of each transcription factor (TF) was used to estimate node connectivity within the GRNs. The frequency of TF-target pairs across all network interactions was quantified and categorized based on the degree of overlap among different TFs. The percentage of conserved targets for each TF was calculated by dividing the number of shared pairs by the total number of target genes associated with that TF. This percentage of conserved targets, combined with TF connectivity metrics, was used to visualize the distribution of TF connectivity within all networks.

Functional validation of the GRNs.

To functionally validate the organ specific GRNs, multiple transcriptomic datasets were reanalyzed. RNA sequencing libraries from the NCBI SRA repository were downloaded and processed, with adapters trimmed and quality filtered ($q > 30$) Cutadapt v.49 (Martin, 2011). The reads from each library were pseudo-aligned to tomato transcript annotations (ITAG4.1c) using *kallisto* v0.44, and the resulting counts were normalized to Transcripts Per Million (TPM). Differentially expressed genes (DEGs) between different genotypes (knockouts/RNAi) or treatments compared to control conditions were identified using the *DESeq2* package (Love *et al.*, 2014), with an adjusted p-value threshold of < 0.05 (Benjamini-Hochberg correction). DEGs and binding targets from ChIP-seq experiments were analyzed to assess their overlap with predicted TF-target interactions in the GRNs.

Aim 2

Cloning vector generation

The TF *S/EIL3* coding sequence was initially cloned into the pENTR vector (Invitrogen) and transferred into the pBOB11_GFP vector (TARGET protocol) and into the pEarleyGate101 vector (transgenic plants generation) following the manufacturer's protocol of LR recombination (Gateway cloning system) (Earley *et al.*, 2006). The final vectors, from different colonies, were sequenced.

Protoplast extraction

Seeds of *S. lycopersicum* cv. Moneymaker were grown for four weeks in sterile culture vessels containing, consisting of half-strength Murashige & Skoog medium (MS) (Murashige & Skoog, 1962). Leaf protoplasts were isolated following an optimized version of the (Yoo *et al.*, (2007) protocol. Briefly, leaf explants were cut into small pieces and incubated in the dark in an enzyme solution containing cellulase (Ozonuka R-10, Duchefa) and macerozyme (R-10, Duchefa) at a ratio of 1:0.27% for four hours, the cell suspension was filtered sequentially through 70 μm and 40 μm cell strainers (BD Falcon), pelleted and washed with W5 buffer (154 mM NaCl, 125 mM CaCl_2 , 5 mM KCl, 5 mM MES, 5 mM glucose, pH 5.7). Cells were stored in MMg solution (400 mM mannitol, 10 mM MgCl_2 , 4 mM MES, pH 5.7). Protoplast integrity and viability were assessed using a hemocytometer after staining with 1 mM Evans blue (Sigma-Aldrich).

TARGET protocol

TARGET protocol was performed following Brooks *et al.*, (2019) protocol. Briefly, 100 μL of protoplast suspension (~ 1 million protoplasts/ μL), 20 μg of plasmid DNA (pBOB11-GFP containing the *S/EIL3* or empty vectors), and 100 μL of PEG solution (40% polyethylene glycol

4000, 200 mM mannitol, 100 mM CaCl₂) were mixed up gently in falcon 15ml tubes, cells were washed three times with W5 buffer and incubated overnight. The following day, the cell solution was aliquoted into 3 replicates in different wells of a 24-well plate and washed with W5 buffer, each well was treated with 35 μM cycloheximide solution for 20 minutes, and then with 10 μM dexamethasone. Transfected cells were quantified using a cytometer (e.g., Accuri™) and sorted by fluorescence-assisted cell sorting (FACS) to isolate GFP-expressing cells. The total mRNA was obtained using the PureLink RNA kit (Thermofisher) and following manufacturer instructions.

Genomic DNA contamination was eliminated by on-column DNase I treatment following the TURBO DNase (Invitrogen) protocol. RNA integrity and concentration were assessed using a NanoDrop spectrophotometer (Thermo Fisher), and RNA quality was further verified by agarose gel electrophoresis. One microgram of DNase I-treated RNA was used to generate poly-A-enriched sequencing libraries using the Tru-Seq Stranded mRNA Library Prep kit (Illumina). Libraries were sequenced as 150 paired end reads on a NextSeq500 system (Illumina).

TARGET RNA-Seq data analysis

Raw reads for each library were preprocessed, adapters sequences were trimmed, and low-quality reads (reads with average quality inferior to $q < 30$ and shorter than 20 bases) were dismissed using Cutadapt v.4.9 (Martin, 2011). Each library was pseudo-aligned to *Solanum lycopersicum* annotations (ITAG4.1c) using kallisto v0.44 (Bray *et al.*, 2016), and the resulting counts were normalized to Transcripts Per Million (TPM). The DEGs between different empty vector and transfected cells (EIL3) were identified using the DESeq2 package (Love *et al.*, 2014), with an adjusted p-value threshold of $p < 0.05$.

Aim 3

Transgenic plants generation

A laboratory strain of *A. tumefaciens* was transformed following Wise et al. (Wise *et al.*, 2006) protocol. Briefly, *A. tumefaciens* strain GV3101 competent cells were inoculated with 0.5-1 µg of plasmid DNA (pEarleyGate101-S/EIL3), and incubated for 5 minutes on ice, 5 minutes in liquid nitrogen and 10 minutes at room temperature, cells were transferred into a growth medium (LB + 0.2 g/l $MgSO_4$) and incubated at 28°C at 200 rpm. Following the incubation the cells were plated on LB with ampicillin and stored as liquid cell suspensions.

Seeds of *A. thaliana* ecotype Col-0 (Wild type or WT) were grown in soil for 6 weeks. Plant transformation was performed using *A. tumefaciens*-mediated floral dip protocol modified from Clough & Bent (Clough and Bent, 1998). Briefly, *A. tumefaciens* recombinant cell suspension (with the destination OX vector) pre-culture was prepared in 250 ml LB liquid medium at 30 °C at 225 rpm for 24 hours. The culture was pelleted and resuspended in 100 ml of infiltration media (5% sucrose, 0.5% of Silwet L-77). *A. thaliana* inflorescences were submerged into the infiltration media to incorporate the expression vector, transformed plants were grown in sterile conditions chambers at 25°C in 16/8 light and dark cycle until the completion of the life cycle. Harvested seeds were selected for glufosinate ammonium (herbicide) resistance. Overexpression (OX) lines were grown from resistant seeds, until the completion of 3 generations (T3).

Plant growth quantification.

Arabidopsis thaliana seeds of wild-type (WT) and transcription factor overexpression (OX) genotypes were sown on agar plates containing five WT and five OX seeds per plate under two treatment conditions: control (sulfur sufficient, S+), which consisted of half-strength Murashige

& Skoog medium (MS) (Murashige and Skoog, 1962) and sulfate-deficient (S-), in which sulfate salts in the MS medium were replaced with equivalent chloride salts. The plants were grown vertically in a sterile growth chamber for two weeks at 25 °C with a 16/8 light-dark cycle. We used fifteen replicates per growth condition, since the seedlings from these treatments were used for qPCR quantification, RNA-seq analysis, sulfur content and phenotype quantifications. Phenotypic measurements, such as root length and total aerial organs area, were taken under control and sulfate deficit treatments. Plant images were captured using an EPSON Perfection V700 scanner and analyzed in ImageJ v.52 (Abramoff *et al.*, 2004).

Sulfate content analysis.

Using *Arabidopsis* seedlings from the phenotype analysis, total sulfur concentration was calculated using the turbidimetric method described by Tabatabai and Bremne (Tabatabai and Bremner, 1970). Briefly, three biological replicates with 700-1000mg of fresh tissue were frozen and pulverized with liquid nitrogen. Ground samples were incubated in 0.1M HCl solution for 2 hours, then 1 ml of the supernatant was divided into glass tubes with 200 ul of Gelatin-BaCl solution and incubated for an additional hour. Next, 200 µl of each sample was placed into a 96-well microplate in triplicate. The absorbance at 452 nm was measured using a plate reader (Infinite® M200 pro-i-control), the calculation of total sulfur content was obtained by regression curves with known standards.

Quantitative real-time PCR (qPCR)

Total RNA was extracted from whole seedlings of two *Arabidopsis thaliana* genotypes: wild type (WT) and overexpressing (OX) the *S/EIL3* TF. Seedlings were grown under two treatment conditions: sulfur sufficient (control, S⁺), consisting of half-strength Murashige & Skoog (MS) medium (Murashige and Skoog, 1962), and sulfate-deficient (S-), in which sulfate salts in the

MS medium were replaced with equivalent chloride salts. Two weeks after sowing, seedlings were harvested, flash-frozen in liquid nitrogen, and stored at -80°C until RNA extraction. Total RNA was isolated using the mirVana miRNA Isolation Kit (Invitrogen) according to the manufacturer's protocol for total RNA isolation. Genomic DNA contamination was eliminated by on-column DNase I treatment following the TURBO DNase (Invitrogen) protocol. RNA integrity and concentration were assessed using a NanoDrop spectrophotometer (Thermo Fisher), and RNA quality was further verified by agarose gel electrophoresis. For cDNA synthesis, 500 ng of total RNA was reverse transcribed using the 5X All-In-One RT MasterMix (Applied Biological Materials, Canada) according to the manufacturer's instructions. The resulting cDNA was diluted 1:5 in nuclease-free water before use in qPCR reactions. qPCR was performed using PowerUp SYBR Green Master Mix (Applied Biosystems™) with 25 ng of cDNA per reaction in a QuantStudio 1 Real-Time PCR System (Thermo Fisher).

Raw fluorescence data were processed using Real-Time PCR Miner 4.0 (Zhao and Fernald, 2005) to calculate cycle thresholds (Ct values) and gene-specific amplification efficiencies. Gene expression levels were normalized to the reference gene *Ubiquitin 1 (UBQ1, AT3G52590)* using the $\Delta\Delta C_t$ method (Livak and Schmittgen, 2001). Three biological replicates, each with three technical replicates, were analyzed per condition. Statistical significance of differential expression between conditions was determined using a student's t-test with post hoc Tukey's test, depending on the number of comparisons. Graphical representation of relative gene expression was performed using R (*ggplot2* package).

Transgenic plants RNA-Seq data analysis

We used the RNA-seq extracted from *Arabidopsis thaliana* genotypes: wild type (WT) and overexpressing (OX) the *S/EIL3* from previous section. Genomic DNA contamination was

eliminated by on-column DNase I treatment following the TURBO DNase (Invitrogen) protocol. RNA integrity and concentration were assessed using a NanoDrop spectrophotometer (Thermo Fisher), and RNA quality was further verified by agarose gel electrophoresis. One microgram of DNase I-treated RNA was used to generate poly-A-enriched sequencing libraries using the TruSeq Stranded mRNA Library Prep kit (Illumina). Libraries were sequenced as 150 paired end reads on a NextSeq500 system (Illumina).

Raw reads for each library was preprocessed, adapters sequences were trimmed, and low-quality reads (reads with average quality inferior to $q < 30$ and shorter than 20 bases) were dismissed using Cutadapt v.4.9 (Martin, 2011). Each library was pseudo-aligned to *Arabidopsis thaliana* transcript annotations (TAIR10) (adding the cDNA sequence of *SIEIL3* to be mapped onto) using kallisto v0.44 (Bray *et al.*, 2016), and the resulting counts were normalized to Transcripts Per Million (TPM). differentially expressed genes (DEGs) between different genotypes, treatments and the interaction of both factors were identified using the *DESeq2* package (Love *et al.*, 2014), with an adjusted p-value threshold of $p < 0.05$. The z-score normalized expression values of DEGs were subjected to k-means clustering to identify distinct expression patterns. The analysis was conducted in an R environment, using the *kmeans* clustering function. Z-score normalization was applied to the expression matrix prior to clustering to ensure comparability across genes.

VI. RESULTS

1. To generate organ-level reference Gene Regulatory Networks models for *Solanum lycopersicum*.

Rationale: Generation of GRNs that integrate different lines of evidence of TF-target regulation at a global scale is a common approach to identify central regulators of cellular processes. These GRNs are available for model organisms, such as human, mouse, fly, or plants like Arabidopsis (Ravasi *et al.*, 2010; Ramírez-González *et al.*, 2018; Harrington *et al.*, 2020; De Clercq *et al.*, 2021; Shanks *et al.*, 2022). However, in the case of tomato, no GRN models are currently available, making the identification of these central TFs a challenging task. In our work, we aim to identify GRNs and central TFs controlling the sulfate deficiency response, comparing these networks in tomato roots and leaves. Thus, as a first aim in our work, we developed reference GRN models at an organ level in roots and leaves and extended our work generating similar GRNs for fruits, flowers and seeds, for the use of the plant community.

1.1 Updating *Solanum lycopersicum* genes and functional annotation.

The most recent genome data available in the SolGenomics Network database (Fernandez-Pozo *et al.*, 2015) is the SL4.0 genome assembly (Hosmani *et al.*, 2019), together with the ITAG4.1 annotation released in January 2020. While we initially aimed to use ITAG4.1, an RNA-seq alignment revealed the loss of 3,393 gene models compared to the previous ITAG4.0 version, including key functional genes like *RIPENING-INSENSITIVE* (*RIN*). To prevent the omission

of relevant genes, we developed a new annotation by integrating ITAG4.0 and ITAG4.1 gene models, resulting in a total of 37,467 genes. Based on this gene list and given that only 15.53% of tomato genes had a functional annotation in ITAG4.0, we performed a functional annotation by dataset integration. These included assigning GO terms from a mapping analysis using EggNOG-mapper(Cantalapiedra *et al.*, 2021), obtaining the tomato annotations compiled in PLAZA 5.0 (Van Bel *et al.*, 2022), as well as retrieving GO annotations from an Interproscan analysis (Jones *et al.*, 2014) of predicted tomato proteins. We achieved a 65% functional annotation coverage, with 25,689 genes assigned to at least one GO term, for a total of 509,559 annotations (Table 1; Supplementary Table 1).

The tomato transcription factor (TF) list was updated by integrating evidence from multiple sources. This involved reviewing annotations and GO terms, retrieving TF catalogs from various repositories, and conducting orthologous TF analyses using *Arabidopsis thaliana* TF lists. Only TFs supported by at least three lines of evidence were selected, resulting in a curated set of 1,840 TFs for further analyses (Table 1, Supplementary Table 2). DNA-binding preferences were determined by retrieving position weight matrices (PWMs) from CisBP (Weirauch *et al.*, 2014) or assigning PWMs from Arabidopsis and Maize orthologs in CisBP and JASPAR (Castro-Mondragon *et al.*, 2022), yielding 846 TFs with assigned PWMs (Supplementary Table 2).

TABLE N°1. Summary of Tomato Gene Annotations. Overview of total gene counts, transcription factors (TFs), and Gene Ontology (GO) annotations for each tomato genome assembly.

Source	Genome assembly	Total genes	Total TFs	Genes with GO annotations
ITAG2.4	SI2.0	30130	1847	19663
ITAG3.0	SI3.0	34658	1500	-
ITAG4.0	SI4.0	34075	1781	5845
ITAG4.1	SI4.0	34688	2486	13142
ITAG4.1c	SI4.0	37468	1840	25689

1.2 Gene expression patterns in tomato demonstrate an organ-level component

As a first step to generate organ-level GRNs for tomato, we performed a search for available *Solanum lycopersicum* RNA-seq datasets in the Sequence Read Archive (SRA) database of the National Center for Biotechnology Information (NCBI) (<https://www.ncbi.nlm.nih.gov/sra/>). The transcriptomic libraries (SRA runs) were categorized into five main organs: roots (1,840 runs from 124 studies), leaves (3778 runs from 279 studies), flowers (568 runs from 55 studies), fruits (4149 runs from 147 studies), and seeds (270 runs from 13 studies). These libraries encompass diverse tomato genotypes and growth conditions, providing a robust dataset for generating reference GRNs that can be applicable to address different research questions. After applying quality filters, 10,510 libraries were retained for further analysis (Supplementary Table 3).

Reads were mapped to gene models using the ITAG4.1c annotation, and genes with expression levels above 5 TPM in more than 10% of the total libraries for a given organ were considered as expressed in that organ. We found that 26,922 genes (71.85%) are expressed in at least one of the organs, with most genes found expressed across all organs. Smaller subsets are shared between multiple organs, while a minor fraction exhibit organ-level expression (Figure 4a). Similar expression patterns have been reported in maize, flaxseed and wheat (Huang *et al.*, 2018; Ramírez-González *et al.*, 2018; Qi *et al.*, 2023). Examples of specific genes include *Solyc06g051770* and *Solyc10g047720* in seeds, whose Arabidopsis homologs, *Oleosin 1* and *2* (*AT4G25140*, *AT5G40420*) (*OLEO1-2*), are involved in seed oil body formation (Siloto *et al.*, 2006). In roots, we identified *SULTRI;1* (*Solyc10g047170*), which encodes a sulfate transporter associated with external sulfate uptake (Takahashi *et al.*, 2000). In flowers, *Tapetum Determinant 1-like* (*TPD1-like*) paralogs such as *Solyc11g005500*, *Solyc12g009850*,

Solyc05g010190 and *Solyc04g071640* were specifically expressed, consistent with their role in tapetal cell development and gametogenesis (Ezura *et al.*, 2017). In leaves, we found *Longifolia 1* (*SILNG1*, *Solyc02g089030*), whose Arabidopsis homolog *LNG1* (*AT5G15580*) influences leaf morphology (Lee *et al.*, 2006) (Figure 4a).

Concerning TFs, 1609 (87.6%) were expressed in at least one organ. Among them, 1016 (63.2%) were expressed across all organs, while a smaller subset of 232 TFs exhibited organ-level expression (Figure 4b). This latter group includes *SIBRC1a* and *SIBRC1b* (*Solyc03g119770* and *Solyc06g069240*), paralogs of Arabidopsis *BRANCHED1*, involved in leaf and axillary bud development (Martín-Trillo *et al.*, 2011), *SIFER* (*Solyc06g051550*) a key regulator of root iron uptake (Aviña-Padilla *et al.*, 2023), *SIWUSCHEL* (*WUS*, *Solyc02g083950*), which controls floral meristem identity and development (Hawar *et al.*, 2022), *SISHINE2* (*SHN2*, *Solyc12g009490*), encoding a TF that controls epidermal growth in developing fruits (Bres *et al.*, 2022), and two Arabidopsis *ABI4* paralogs (*Solyc03g095977* and *Solyc03g095973*) that exclusively expressed in seeds, consistent with their role in seed vigor (Bizouerne *et al.*, 2021). While most TFs and genes were expressed across all organs, their expression levels varied substantially depending on the organ analyzed (Figure 4c-d). These quantitative differences suggest organ-level regulatory mechanisms, where distinct expression patterns contribute to the specialized functions and characteristics of each organ.

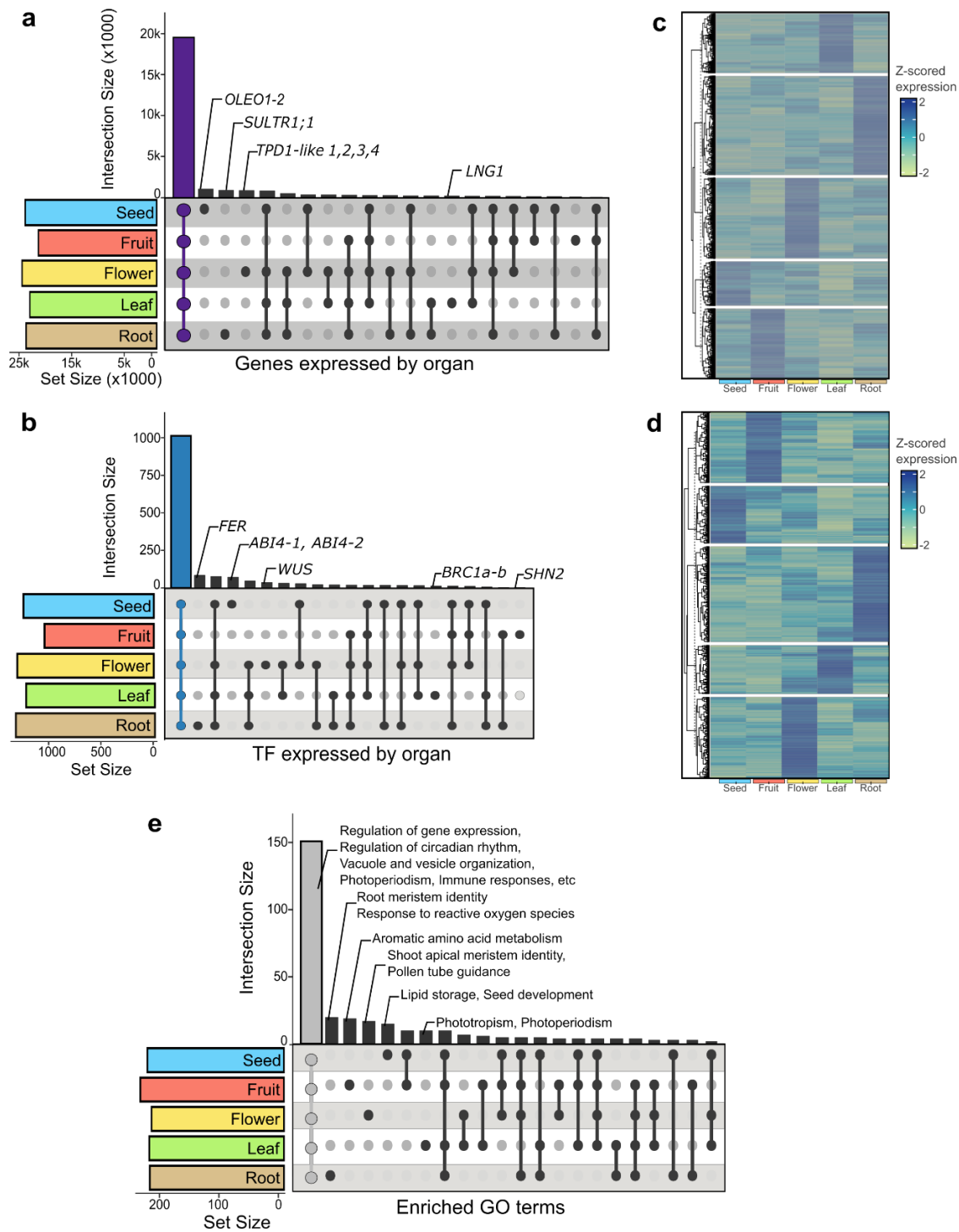


FIGURE N°4. Organ-level transcriptomic landscape in tomato. (a) Distribution of expressed genes across organs. (b) Distribution of expressed transcription factors (TFs) across organs. (c) Heatmap of normalized (Z-scored) gene expression levels across organs. (d) Heatmap of normalized (Z-scored) TF expression levels across organs. (e) Enriched biological process Gene Ontology (GO) terms associated with expressed genes across organs (adjusted p-value < 0.05).

To assess how gene expression in tomato organs relates to possible biological processes, we performed a Gene Set Enrichment Analysis (GSEA) for each organ. The analysis revealed that most enriched biological processes (151 GO terms) were common across all organs (adjusted p-value < 0.05) (Figure 4e), including terms such as gene expression regulation, circadian rhythm, vacuole and vesicle organization, immune responses, mRNA methylation and response to abscisic acid (Supplementary Figure 1). In contrast, only 22 enriched GO terms were identified as unique for each organ. These include processes related to fruit ripening in fruits, root meristem identity and response to reactive oxygen species in roots, phototropism and photoperiodism in leaves, shoot apical meristem identity, brassinosteroid signaling, and pollen tube guidance in flowers as well as lipid storage and seed development in seeds (Supplementary Table 4). These findings demonstrate that, while important vital biological processes are conserved across all tomato organs, a subset of organ-level processes support their unique functions, emphasizing the specialized regulatory frameworks that govern organ identity and development in tomato.

1.3 Integrated tomato organ-level GRNs reveal enriched TF-Target interactions and local regulatory cascades.

We compiled a comprehensive dataset of tomato omics data for the GRNs generation, encompassing over 10,000 transcriptomes, nearly 100 chromatin accessibility experiments, and 16 ChIP-seq libraries (Figure 5). To generate organ-level GRNs, we utilized the GENIE3 algorithm using the processed mRNA-seq count tables categorized by organ and the updated TFs list as input. GENIE3 generated a ranked list of putative TF-target interactions, from which we selected the top 1%, 2%, 5%, 8% and 10% of the highest-scoring interactions to evaluate the networks accuracy. The inferred organ-level networks were benchmarked against high-quality

in vivo ChIP-seq datasets that met ENCODE standards for tomato TFs, only 8 ChIP-seq experiments surpassed the quality filters of non-redundant Fraction and PCR Bottlenecking Coefficients (Hitz *et al.*, 2023), the TFs: GLK1-2 (Solyc07g053630, Solyc10g008160) (Tu *et al.*, 2022), MYC2 (Solyc08g076930) (Du *et al.*, 2017), JMJ4 (Solyc08g076390) (Ding *et al.*, 2022), WOX13 (Solyc02g082670) (Jiang *et al.*, 2023), EIL4 (Solyc06g073730), TAGL1 (Solyc07g055920) and RIN (Solyc05g012020) (Fujisawa *et al.*, 2011; Gao *et al.*, 2019) (Supplementary Table 5). Each GENIE3 network was compared against a ChIP-seq derived network through enrichment tests, based on the expression levels of the TFs in each organ. GLK1-2, MYC2, EIL4, JMJ4, and WOX13 binding targets were used across all organ networks, while RIN and TAGL1 were not used on the root and leaf networks, given their specific reproductive organ-level expression pattern.

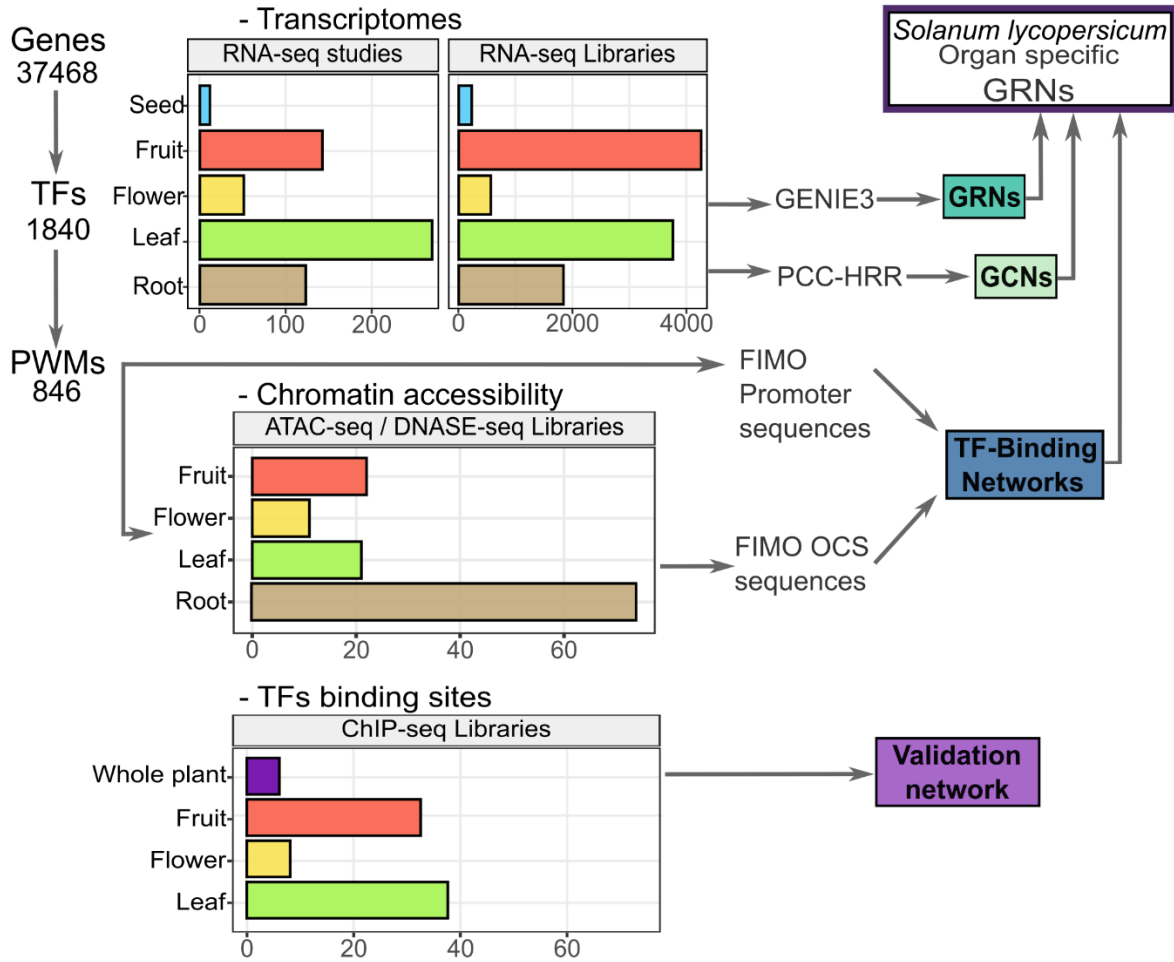


FIGURE N°5. Multi-omics data used for generating organ-level GRNs in tomato. Overview of datasets used to generate organ-specific gene regulatory networks (GRNs) in *Solanum lycopersicum*. Bar plots indicate the number of available datasets per organ for transcriptomics (RNA-seq), chromatin accessibility (ATAC-seq/DNase-seq), and transcription factor binding sites (ChIP-seq). Arrows illustrate data flow into regulatory network construction, including GRNs, co-expression networks (GCNs), TF-binding networks, and validation datasets.

The top 2% networks showed the highest enrichment (indicated by higher \log_2 -transformed Fisher odds ratios) and statistical significance (lower \log_{10} -transformed adjusted p-values) in the overlap between GENIE3-identified TF-target pairs and the ChIP-seq validation dataset (Table 2, Supplementary Table 6). The distribution of node degree values also shows a scale-free topology with a power-law distribution, frequently exhibited by real-world networks including biological networks (Albert, 2005; Khanin and Wit, 2006) (Supplementary Figure 2). Furthermore, comparison with existing tomato gene networks from PlantRegmap (Tian *et al.*, 2020) and TomatoNet (Kim *et al.*, 2017) demonstrated that the GENIE3-derived GRNs exhibited greater enrichment and overlap with the gold-standard dataset, indicating a better performance in predicting TF-target interactions obtained experimentally (Supplementary Table 7).

To further evaluate the performance of the top 2% GRNs, we calculated the AUROC (Area under the receiver Operating Characteristic) and AUPR (Area under the precision-recall curve) for each organ-level network and compared these values against a network consisting of TF-target interactions obtained from the ChIP-seq validation dataset. The GRNs derived from tomato roots, leaves, flowers, fruits and seeds libraries showed statistically higher AUROC and AUPR values than randomly generated TF-target pairs (Table 2, Supplementary Figure 3). These results confirm that the GRNs successfully recapitulate experimentally validated TF-target interactions, underscoring their utility in predicting regulatory interactions for TFs lacking experimental validation.

TABLE N°2. Enrichment metrics for organ-level GRNs. Summary of enrichment metrics for organ-specific GRNs, considering the top 2% of interactions identified by the GENIE3 algorithm. Enrichment results obtained from a Fisher's exact test that assessed gene set overlap significance, reporting log₂ fold change, p-value, and intersection size to the validation network (ChIp-seq). -inf represents log₁₀ adjusted p-values < -400.

	Root	Leaf	Flower	Fruit	Seed
Total TFs	1,297	1,216	1,300	1,058	1,241
Total Genes	23,226	22,511	23,988	20,888	23,124
Total edges	797,120	743,902	798,851	665,116	817,504
log ₂ Fisher odd ratio	1.89	2.66	2.01	3.01	2.22
log ₁₀ adj p-value	-156.72	-inf	-196.33	-305.17	-inf
Genes in Overlap	1714	2967	1912	2226	4204
AUROC	0.72	0.65	0.65	0.72	0.53
AUPR	0.51	0.45	0.46	0.52	0.32

To further strengthen the robustness of our GRNs, we incorporated additional layers of regulatory evidence into the TF-target interactions identified by GENIE3. Gene co-expression is widely used to infer biologically relevant relationships between genes (Wolfe *et al.*, 2005; Yin *et al.*, 2021). Using the same RNA-seq datasets, we generated aggregated gene co-expression networks (GCNs) following Orduña *et al.*, (2023) protocol. Then, we extracted the TF-target pairs from each GCN as supporting evidence for the GENIE3-predicted interactions. Notably, organ-level TF-target interactions identified through co-expression analysis showed significant correlation with those inferred by GENIE3 (Supplementary Figure 4). While the GENIE3 algorithm predicts regulatory interactions based on expression patterns, additional evidence is necessary to determine whether these interactions occur via direct TF binding to regulatory sequences, leading to the generation of two TF-binding networks. To integrate TF-binding information into the GENIE3 networks, we extracted upstream sequences (2 Kb from the transcription start site) for each annotated gene on ITAG4.1c and performed TF-binding motif prediction using the FIMO tool part of the MEME suite (Grant *et al.*, 2011). Additionally, we conducted the same analysis on sequences within open chromatin sites (OCSs) identified in tomato fruit, flower, leaf, and root organs, using data from reanalyzed DNase-seq and ATAC-seq experiments (Supplementary Table 8).

The results from all evidence layers were compiled, ensuring that our analysis remained strictly constrained to TF-target pairs identified by GENIE3. This approach maintained the predefined network structure, with additional regulatory evidence mapped onto it rather than introducing new interactions. We found that between 51% and 61% of GENIE3-predicted interactions were supported by at least one independent source, with most edges validated by one or two complementary approaches. Specifically, co-expression analysis confirmed

approximately 20% of the GENIE3-predicted interactions (Figure 6a). Furthermore, a substantial portion of GRN edges was validated by the presence of cis-binding motifs detected by FIMO within promoter sequences or OCSs.

As previously mentioned, most genes and TFs were expressed across all tomato organs, although differences exist between gene expression levels. To assess how these patterns influence regulatory interactions, we examined the distribution of TF-target gene pairs across the five organ-level GRNs. Over 75% of these pairs were unique to a single organ (Figure 6b), indicating that while TFs and targets are broadly expressed, the GENIE3 algorithm assigns regulatory relationships based on expression levels differences, leading to organ-level regulatory pairings. This distinction arises from the algorithm's scoring, where only the top 2% of interactions were retained per network. These findings suggest that organ-level regulatory pairings are dictated by expression-dependent scoring, with most TFs exhibiting distinct regulatory interactions across organs. To further evaluate how specific TF-target pairs distribute across organs and how target conservation correlates with TF connectivity, we calculated the percentage of conserved targets for each TF across all organs. As expected, most TFs showed low target conservation due to the organ-level nature of TF-target interactions (Figure 6c). A GSEA of the targets of these highly connected-highly conserved TFs across organ-specific networks revealed a significant enrichment for GO terms associated with essential cellular processes, such as nucleic acid metabolism, vesicle transport, and RNA metabolism (FDR $\text{adj.p.val} < 0.05$). These findings indicate that TFs with high connectivity and target conservation may act as whole-plant regulators of fundamental cellular functions; in contrast, the organ-specific TFs with fewer targets are likely to control tissue-specific processes.

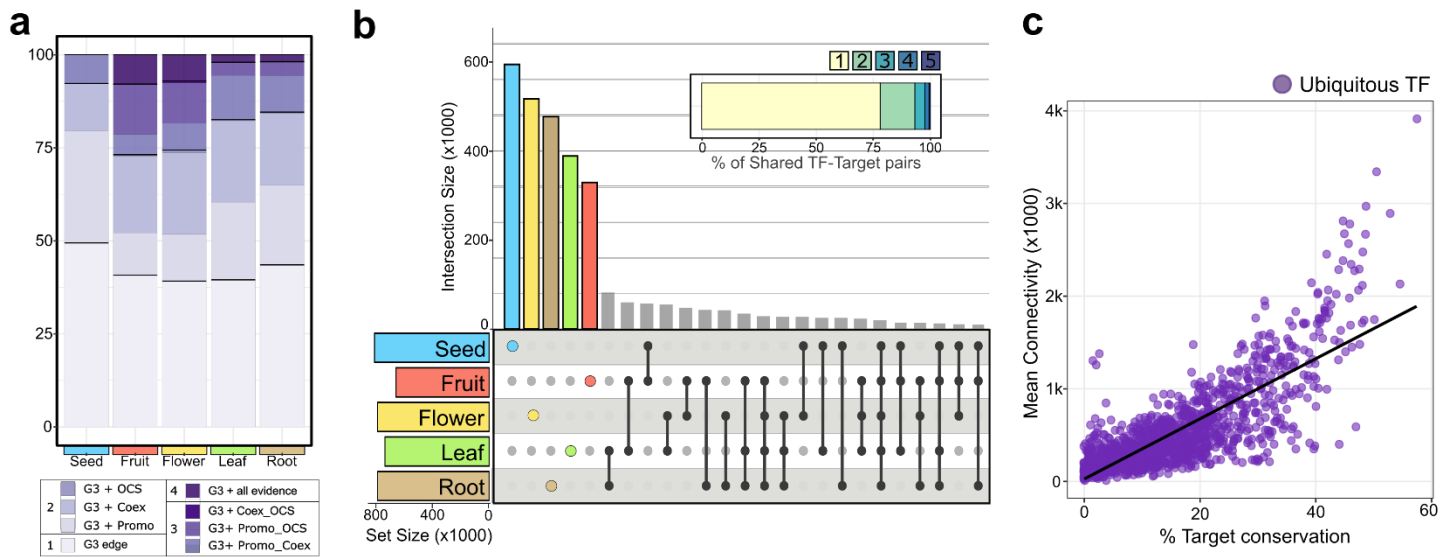


FIGURE N°6. Comparative analysis of organ-level GRNs reveals regulatory signatures and TF connectivity patterns. (a) Stacked bar plot of the proportion of supporting evidence for TF-target pairs of the GENIE3-inferred GRN. Evidence categories include GENIE3 predictions (G3), open chromatin site binding (OCS), GCNs (Coex), and promoter binding predictions (Promo). Darker shades indicate interactions supported by multiple evidence sources. (b) UpSet plot displaying the overlap of TF-target interactions across organ-specific GRNs, with an inset showing the distribution of shared versus unique interactions. (c) Relationship between TF mean connectivity (average number of target genes across organs) and target conservation (proportion of shared targets across organs). A black trend line highlights the general pattern in the data.

1.4 The fruit GRN captures known regulatory interactions and identifies novel central controllers of ripening.

To evaluate the ability of the organ-level GRNs to capture biologically relevant regulatory interactions, we focused on ripening, one of the most extensively studied processes in tomato, linked to hormonal signaling pathways such as ethylene and abscisic acid (ABA), cell wall remodeling and other processes (Karlova *et al.*, 2014; Kou *et al.*, 2021). Tomato fruit ripening is governed by a complex regulatory cascade, involving epistatic interactions between well-characterized TFs, including APETALA2a (AP2a), NON-RIPENING (NOR), FRUITFULL (FUL1/TDR4 and FUL2/MBP7), TOMATO AGAMOUS-LIKE 1 (TAGL1), RIPENING INHIBITOR (RIN) and COLORLESS NON-RIPENING (CNR) (Kou *et al.*, 2021; Li *et al.*, 2021). Among these, TAGL1 and RIN are recognized as central regulators of ripening, with their roles supported by multiple ChIP-seq studies (Kou *et al.* 2021; Li *et al.* 2021).

To determine whether the fruit GRN reproduced regulatory interactions of known TFs, we compared the targets of TAGL1 and RIN (TFs exclusively expressed in fruits) from the GRN with gene lists compiled from previous omics studies. These included differentially expressed genes (DEGs) identified in TAGL1 and RIN knockout and RNAi plants (Li *et al.*, 2018; Gao *et al.*, 2019; Ito *et al.*, 2020), as well as direct binding targets identified via RIN ChIP-chip and ChIP-seq (Fujisawa *et al.*, 2013; Zhong *et al.*, 2013; Gao *et al.*, 2019), and TAGL1 ChIP-seq (Gao *et al.*, 2019) experiments. For RIN, we observed a statistically significant overlap of the targets determined in our fruit GRN with targets obtained in all the experiments, including ChIP-binding targets and regulatory targets identified in RIN-deficient plants (Figure 7a). This finding highlights the potential of the GENIE3 GRN to capture experimentally validated regulatory interactions, with many of these corresponding to direct binding of a TF to a target promoter

(45% of RIN GRN targets (411/857) and 89% of TAGL1 GRN targets (740/827) are validated by ChIP binding evidence (Figure 7b).

To further investigate the regulatory roles of RIN and TAGL1 in fruit ripening, we generated two subnetworks focusing on the target genes from the 98 ripening-associated genes identified by Kou et al., (2021). Furthermore, most of the GENIE3 edges connecting RIN and TAGL1 to these target genes (90% for RIN and 100% for TAGL1) are supported by ChIP evidence (Figure 7c-d). Additionally, the subnetworks highlight the broad regulatory influence of RIN and TAGL1 across diverse biological processes and their interactions with key TFs such as CNR, NOR, and AP2.

To identify potential novel ripening regulators, we analyzed the TFs connected to the 98 ripening-associated genes and their functions (Kou et al., 2021). We applied the Integrated Value of Influence (IVI) (Salavaty *et al.*, 2020), a metric centrality measures such as degree centrality, neighborhood connectivity, betweenness centrality, and collective influence into value that quantify hub influence (Salavaty *et al.*, 2020). The analysis confirmed that recognized TFs such as CNR, NOR, FUL1, FUL2, AP2a, RIN, and TAGL1 are central regulators of fruit ripening genes. Notably, two additional TFs, *SIARF2A* (Soly03g118290) and *SIERF.E2* (Soly06g063070), emerged as major hubs with high IVI, thus as potential regulatory role controlling ripening-related genes (Supplementary Table 9). The *SIARF2A* has been identified as a regulator of axillary shoot development (Xu *et al.*, 2016) and is expressed in the late stages of ripening. RNAi lines targeting *SIARF2A* exhibit ripening defects and ethylene insensitivity, while overexpression (OX) lines show accelerated and uneven ripening (Hao *et al.*, 2015; Breitel *et al.*, 2016). In contrast, *SIERF.E2* is linked to key ripening regulators and ripening-associated

genes, as its expression is downregulated in *cnr*, *nor*, and *rin* mutants. However, its function remains unknown (Liu *et al.*, 2016).

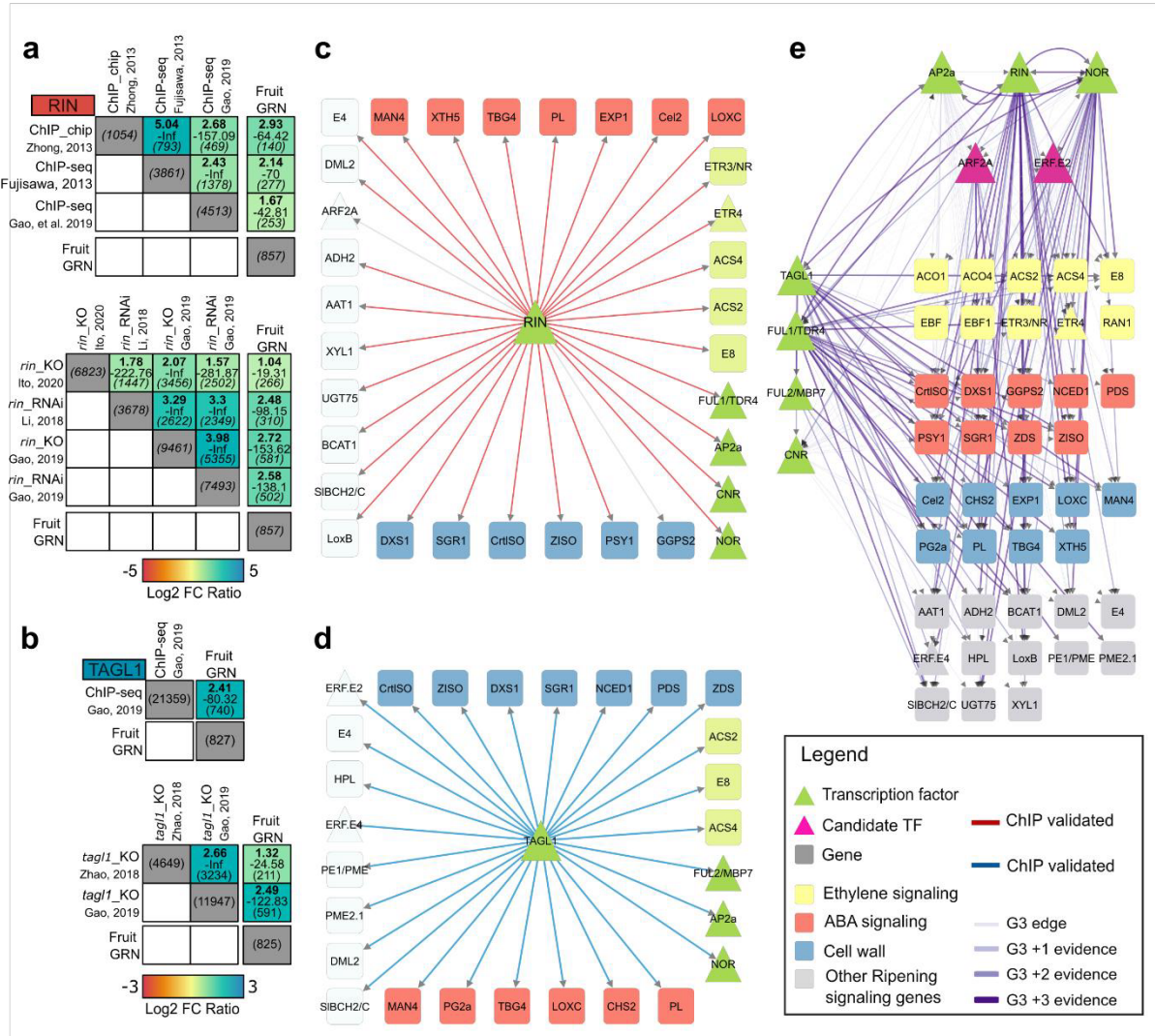


FIGURE N°7. Identification of key transcriptional regulators of fruit ripening regulatory cascades in tomato. (a–b) Enrichment and validation of fruit GRNs for *RIN* (a) and *TAGL1* (b) using knockout mutant data and ChIP-seq analyses. Box heatmaps display enrichment obtained from a Fisher’s exact test (log₂ fold change, p-value, and intersection size) to the validation network (ChIP-binding). (c–d) Network representation of ripening-associated TF-target interactions for *RIN* (c) and *TAGL1* (d) derived from the fruit GRN. Triangles represent TFs, squares represent target genes. Node colors indicate function. Borders and edges are colored in red (*RIN*) or blue (*TAGL1*) when interactions are validated by ChIP-seq evidence. (e) Network of key regulators of ripening-associated genes (adapted from Kou *et al.*, 2021), applying the same node and edge color scheme as in (c–d). Edge darker shades indicate accumulated regulatory evidence.

A GSEA of the target genes for the two TF candidates revealed a significant enrichment in the fruit ripening process (adjusted p-value < 0.05) (Supplementary Figure 5). Using both established and newly uncovered TFs, along with ripening-relevant target genes, we developed a fruit ripening GRN to provide a comprehensive view of the impact of key TFs on the expression of ripening associated genes (Figure 7e). Our network analysis reveals that *SlARF2A* and *SlERF.E2* may act upstream on important TFs such as AP2, NOR, and CNR, providing a novel perspective on the fruit ripening regulation cascade. These findings show the potential of GRNs to recapitulate transcriptional hierarchies driving complex biological processes, as well as new insights into the regulatory mechanisms that control fruit ripening.

1.5 Tomato organ-level GRNs validate the role of ABF TFs on abscisic acid (ABA) regulatory cascades and identify new regulators of ABA-related genes.

Abscisic acid (ABA) is a key plant hormone involved in the regulation of seed dormancy, germination, seedling development, root growth, flowering, and responses to abiotic and biotic stresses (Vishwakarma *et al.*, 2017; Krukowski *et al.*, 2023). Notably, the GO term “response to ABA” was consistently enriched across all organ-level GRNs (Supplementary Figure 6), highlighting its central role in plant growth and development. This category includes 730 genes, 91.3% of which are ubiquitously expressed in tomato organs (Supplementary Table S10, hereafter referred as “ABA-related genes”). The AREB/ABF (ABA response element binding/ABA response element binding factor) family of bZIP TFs mediates ABA signaling (Uno *et al.*, 2000; Krukowski *et al.*, 2023); however, their role in organ-level regulation remains

unclear. To address this, we generated organ-level GRNs for the ten ABF TFs identified in tomato (Pan *et al.*, 2023), focusing specifically on their regulation of ABA-related genes. While most ABF family members are expressed at similar levels across organs, except for *SlABF6* (not expressed in flowers) and *SlABF7* (not expressed in fruits and leaves), their regulatory potential differs. Specifically, *SlABF1* and *SlABF4* appear to play key roles in regulating ABA-related genes in fruits, whereas *SlABF2*, *SlABF3*, *SlABF5*, and *SlABF10* regulate more genes in the leaf GRN. *SlABF5*, *SlABF9*, and *SlABF10* are involved in ABA regulation in roots, while *SlABF2* seems to play a substantial role in the flower GRN. For seeds, *SlABF6* and *SlABF7* exhibit the most regulatory activity on ABA-related genes (Figure 8a). These findings point out that the ABF TFs have specific patterns of regulation of ABA-related genes.

Plant drought regulation is closely linked to ABA (Kang *et al.*, 2002; Krukowski *et al.*, 2023). To validate the regulatory predictions from our GRNs, we focused on two TFs, *SlABF3* and *SlABF5*, which have been identified as relevant regulators of drought responses (Kang *et al.*, 2002; Hsieh *et al.*, 2010). Using the leaf GRN, we extracted the predicted targets of both TFs and compared them to the DEGs found in a transcriptome analysis of leaves from drought-exposed plants (Wang *et al.*, 2023b). Our analysis revealed a significant enrichment of drought-responsive genes among the targets of both TFs (Figure 8b). Next, we generated two GRNs by focusing on ABA-related genes. Our analysis revealed a significant enrichment of drought-responsive genes among the targets of both TFs (Fig. 5B, Supplementary Table S16). We found that 284 out of 410 (~69%) ABF5 targets and 63 out of 168 (~38%) ABF3 targets overlapped with drought-responsive DEGs. Additionally, 14 out of 22 (~64%) ABF3 targets and 35 out of 45 (~78%) ABA-relevant genes were also present among the drought DEGs. The GRN also indicated that both TFs regulate multiple ABA signaling genes encoded by *protein phosphatase*

class 2 C (PP2C) genes (Kang *et al.*, 2002; Fujii *et al.*, 2009; Krukowski *et al.*, 2023), including *Solyc03g121880* and *Solyc05g052980* (regulated by both TFs), and *Solyc03g096670* and *Solyc06g076400* (regulated specifically by SIABF5). Furthermore, we observed a potential feedback regulatory mechanism between *SIABF3* and *SIABF5* (Figure 8B). These findings highlight the key roles of *SIABF3* and *SIABF5* in the ABA-related drought regulatory cascades (Hsieh *et al.*, 2010; Kang *et al.*, 2002; Pan *et al.*, 2023) and demonstrate how the GRNs can recapitulate known important regulatory pathways in hormone responsive regulatory cascades.

To identify novel regulators of ABA-related genes beyond the ABF family across all organs, we filtered the five organ-level GRNs to retain TFs with regulatory connections to ABA-related genes. A network analysis calculating the Integrated Value of Influence (IVI) (Salavaty *et al.*, 2020) of the network hubs identified *SIGBF3* (Solyc01g095460) as one of the top 10 most influential TFs in the ABA-related networks across all organs (Supplementary Table 11). The *SIGBF3* has recently been found to be co-expressed with drought-responsive genes in tomato leaves (Bortolami *et al.*, 2024), but its direct regulatory effect in tomato regulatory cascades remains unexplored. Notably, *SIGBF3* is an ortholog of the Arabidopsis gene *AtGBF3* (AT2G46270), a TF associated with drought tolerance and ABA insensitivity in Arabidopsis (Ramegowda *et al.*, 2017; Dixit *et al.*, 2019). To further explore the role of *SIGBF3*, we performed a GSEA on its target genes in each organ-level GRN. We found a significant enrichment of genes belonging to the “response to abscisic acid stimulus” shared across all organ networks, indicating a potential conserved role in the regulation of ABA-related genes (adjusted $p\text{-value} < 0.05$) (Figure 8c). In the leaf GRN, over 60% of the targets of *SIGBF3* were identified as drought stress-responsive genes, including *PP2C* genes (*Solyc03g121880*, *Solyc03g096670*, *Solyc05g052980*, *Solyc06g076400*), two *SNF1-related protein kinases 2 (SnRK2)* genes

(*Solyc08g077780*, *Solyc04g012160*). Additionally, this TF may act upstream of key TFs such as *SIABF2*, *SIABF3*, and *SIABF5* (Figure 8d). In other organ-level networks, *SIGBF3* targets smaller subsets of *PP2C* genes, and other TFs, such as MYB1 (*Solyc12g099120*), a TF implicated in pathogen susceptibility (Abuqamar *et al.*, 2009) (Supplementary Figure 6). This result suggests a conserved regulatory role of *SIGBF3* across different organs, reinforcing its significance in ABA-mediated stress responses.

Our findings confirm the GRNs potential to recapitulate important ABA transcriptional regulators and its capacity to discover new potential key regulators; the *SIGBF3* can be considered a promising candidate for further studies.

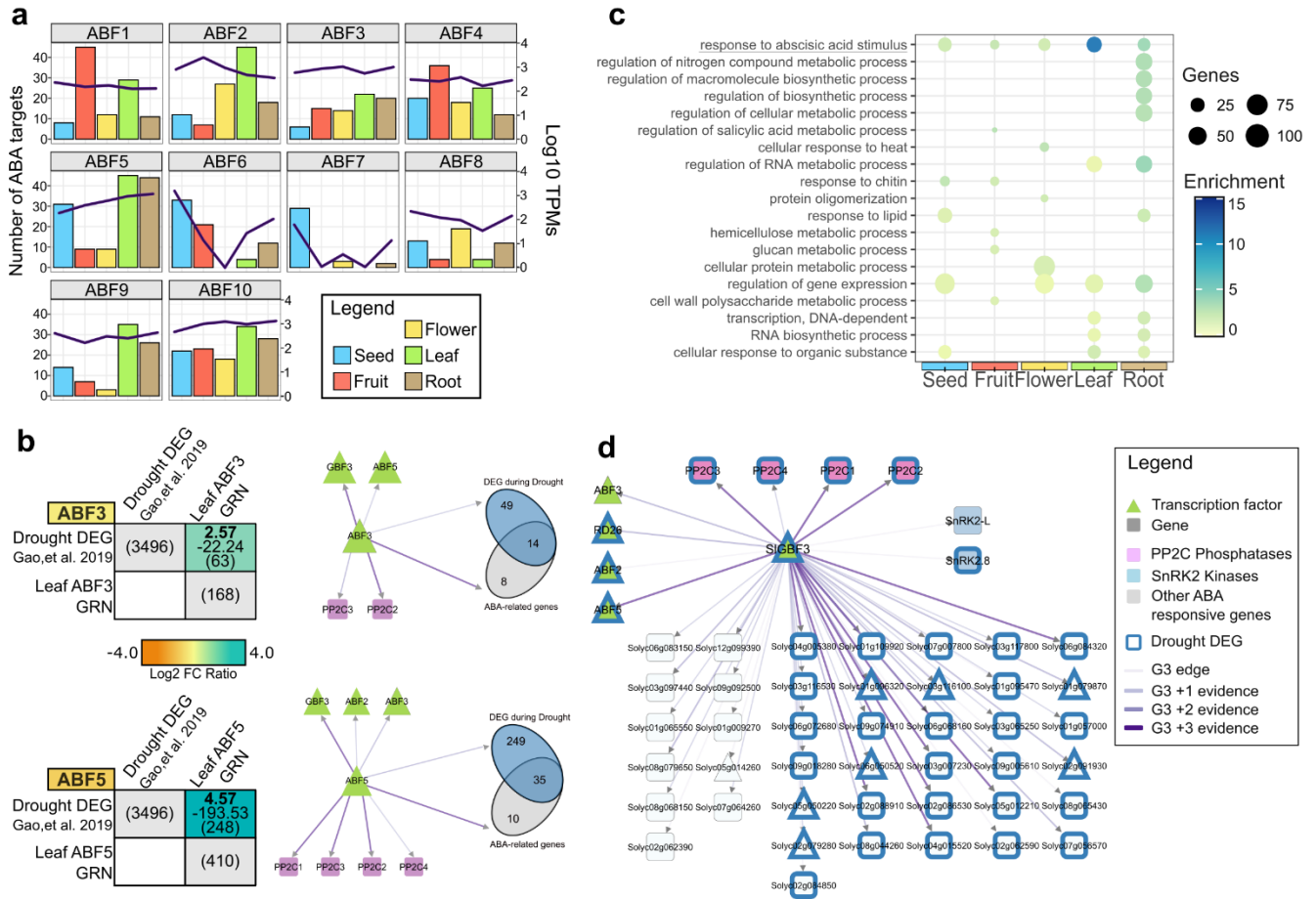


FIGURE N°8. Tomato GRNs reveal the role of ABF TFs and identify a key regulator of ABA-related GRNs. (a) Bar plots showing organ-specific expression levels and the number of ABA-related target genes regulated by ABF TF. Bars indicate target counts, while black lines represent log₁₀ TPM expression values. (b) Enrichment and validation of leaf GRNs for *ABF3* and *ABF5* using differentially expressed genes (DEGs) from drought-stressed leaves (Gao et al., 2019). Box heatmaps (left) display enrichment results from a Fisher's exact test (log₂ fold change, p-value, and intersection size). The networks (right) show distribution of ABA-related and drought regulated targets of these TFs. (c) Gene Set Enrichment Analysis (GSEA, FDR-adjusted p-value < 0.05) of *SIGBF3* target genes in organ-specific GRNs. Dot size represents gene number, while color intensity reflects enrichment values. (d) Network visualization of *SIGBF3*-regulated ABA-related genes in the leaf GRN. Triangles represent TFs, rectangles represent target genes. Node colors indicate function. Blue-bordered nodes indicate DEGs from drought-stressed leaves (Gao et al., 2019). Edge darker shades indicate accumulated regulatory evidence.

1.6 TomViz- GRNs app: Online tool for tomato GRNs visualization.

To provide the scientific community with a comprehensive framework of tomato organ-level GRNs and a user-friendly resource, we have developed a public web platform featuring an interactive interface that allows users to explore the results of this study. Our GRN apps within the TomViz module of the PlantaeViz platform (<https://plantaeviz.tomsbiolab.com/tomviz>) adhere to the Findability, Accessibility, Interoperability, and Reusability (FAIR) principles (Santiago *et al.*, 2024). Through the website app, users can interact with organ-level GRNs, select and subset network data for download (Figure 9a-c). The TomViz-GRNs app provides various features for data analysis. In the Regulatory Targets Tab, users can query individual TFs or genes to explore central regulatory TFs and their validation layers (Figure 9b). The D3 Subnetwork Tab allows users to upload gene lists and generate GRNs based on specific queries. It categorizes data and enables an organ-level study of stress responses, helping to detect novel regulatory pathways and TFs involved in multiple regulatory cascades (Figure 9c). The TomViz-GRNs app thus provides an intuitive platform for studying tomato gene regulation and investigating stress responses across different organs.

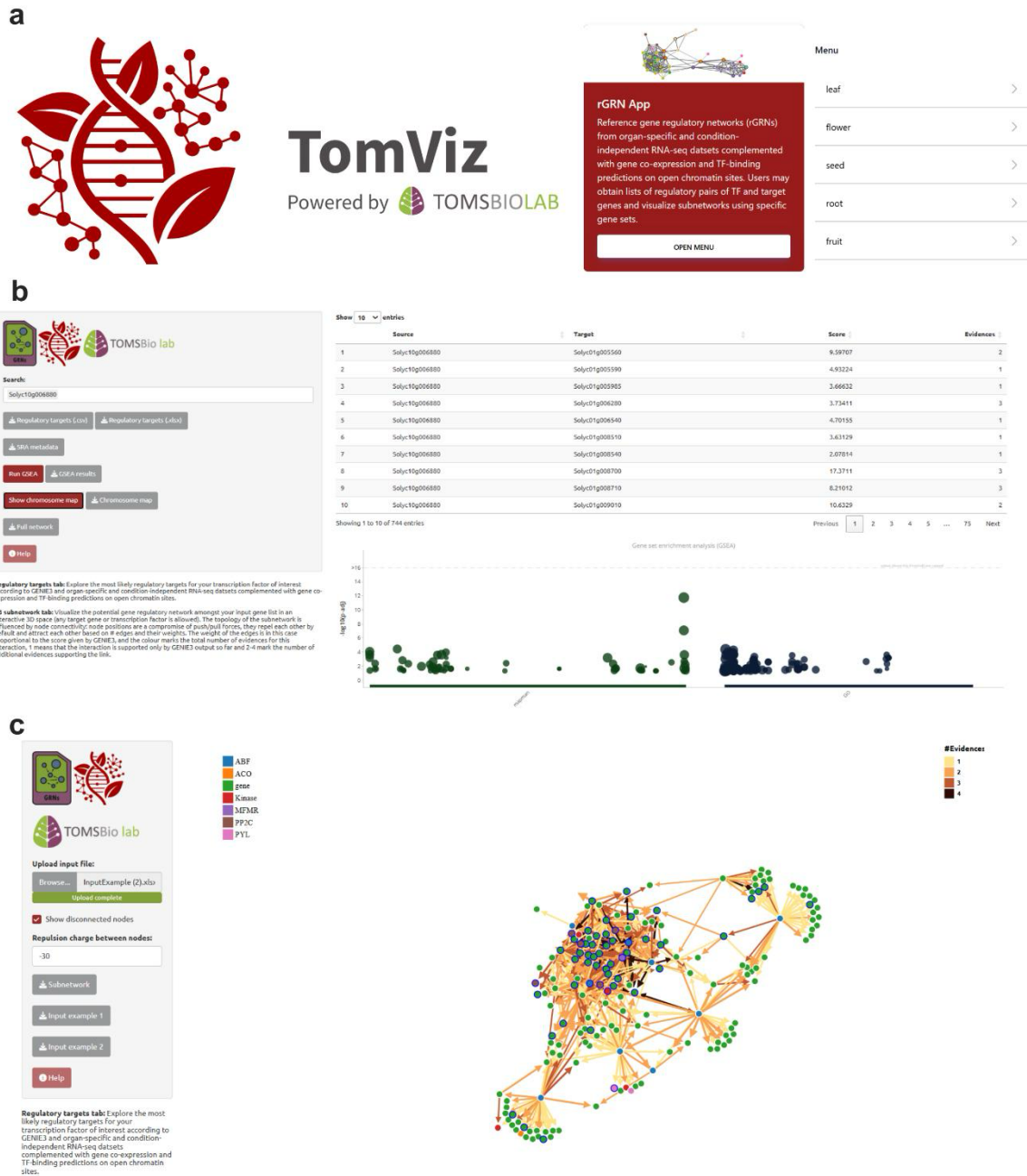


FIGURE N°9. TomViz-GRNs: A web-based platform for exploring tomato organ-level GRNs. (a) TomViz interface within the PlantaeViz platform (Santiago et al., 2024), providing access to GRN exploration tools. (b) Regulatory Targets Tab: Users can query TFs or genes to explore regulatory interactions and validation layers. The interface includes options to download TF target lists, perform GSEA, and visualize target distributions on a chromosome map. (c) D3 Subnetwork Tab: Users can upload gene lists, visualize GRNs, and analyze regulatory pathways at the organ level. The visualization includes directional edges representing regulatory interactions from TFs to targets, with edge colors indicating the level of supporting evidence. Additional options allow customization of network layout and node separation.

2. To identify candidate TFs that are central regulators of the sulfate deficiency response in *S. lycopersicum*.

Rationale: Identifying TFs that act as key regulators of specific biological processes is critical for understanding gene regulatory mechanisms. The purpose of this study is to identify candidate TFs that regulate the sulfate deficiency response in *Solanum lycopersicum*. Using the organ-specific GRNs as foundational frameworks, as second aim of our thesis we analyzed the sulfate deficiency transcriptome at both time and organ-specific scales to create context-specific GRNs for tomato roots and leaves. By comparing root and leaf sulfate-responsive GRNs main hubs, we are able to identify TFs that control the regulatory cascades underlying the sulfate deficiency response.

2.1 Context-specific GRNs of sulfate deficiency of tomato roots and leaves

Primarily, to identify the GRNs underlying gene expression changes and the key regulators involved in the sulfate deficiency response in tomato plants. We reanalyzed the RNA-seq libraries from Canales et al., (2020), we obtained new results from the transcriptomes of tomato roots and leaves at 3 and 4 weeks after sowing under control and sulfate-deficient treatments, using the ITAG4.1C annotations. The analysis found 5,920 and 3,386 DEGs in roots and 5,847 and 4,522 DEGs in leaves at 3 and 4 weeks, respectively. The results demonstrate that the majority of DEGs were downregulated after sulfate deficiency, with little overlap of genes between the different time points, thus transcriptome of tomato roots and leaves is affected in a time-specific and organ-specific manner as mentioned in Canales, et al. (2020) (Figure 10a). A

GSEA of the DEG lists revealed upregulated processes associated with molecular transport, sulfur deprivation responses, and amino acid metabolism that are shared across the organs. Sulfur amino acid metabolism and immunological responses were among the upregulated processes in the roots, while senescence was found exclusively enriched in the leaves (Figure 10b). In contrast, the downregulated biological processes included phytohormone responses (auxin and cytokinin), cell wall metabolism, and biomolecule catabolism, including amino acid catabolism. Additionally, processes involved in reactive oxygen species regulation were significantly downregulated in roots, whereas photosynthesis-related processes were enriched in the leaves DEG (Figure 10c).

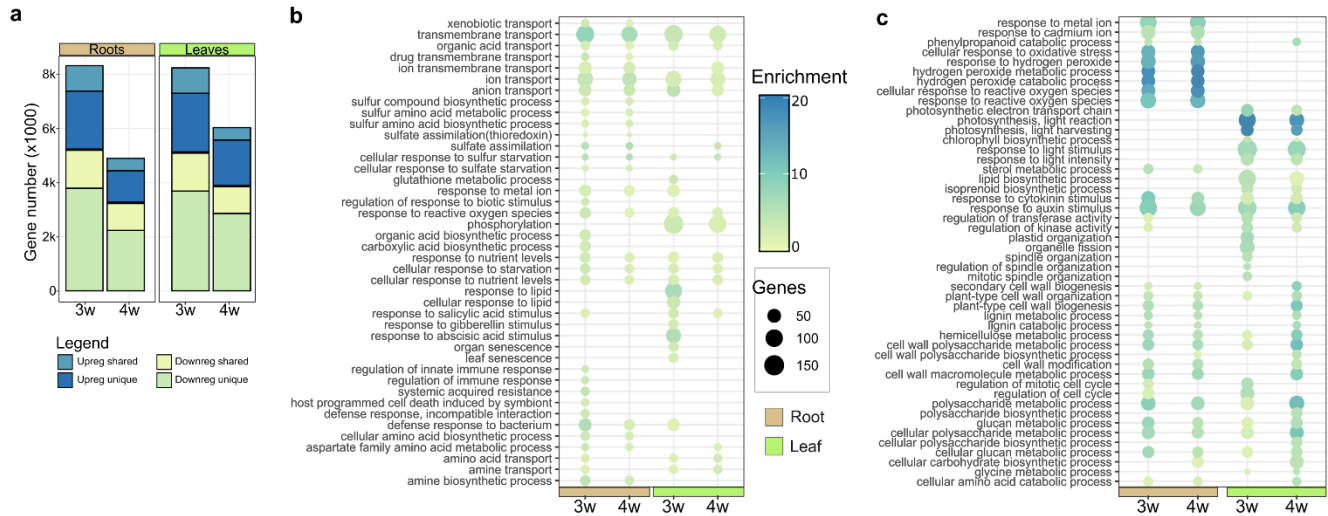


FIGURE N°10. Reanalysis of RNA-seq libraries from tomato roots and leaves (Canales et al., 2020) under control and sulfate-deficient conditions at 3–4 weeks after sowing. (a) Bar plots illustrating shared and unique DEGs between time points (3w: three-week-old plants; 4w: four-week-old plants). (b) Gene set enrichment analysis (GSEA) results (FDR-adjusted p-value < 0.05) showing enriched GO terms for upregulated DEGs in response to sulfate deficiency. (c) GSEA results (FDR-adjusted p-value < 0.05) for downregulated DEGs in response to sulfate deficiency.

To determine if the time-specific DEG may involve specific regulatory cascades or specific central TFs as key regulators during sulfate deficiency treatments, we filtered the root and leaf GRNs using the DEGs from tomato plants treated with sulfate deficiency 3–4 weeks after sowing. The networks were analyzed to determine centrality measures of the TFs. The distribution of clustering coefficients and outdegrees of the TFs show similar patterns, suggesting the networks have a similar topology, independent of the time point or organ of origin (Figure 11a-b). Interestingly, although the lists of DEGs differ between different time points and organs, we found that most TFs (1133 out of 1381 TFs) controlling these DEGs are shared, suggesting a common set of regulators in roots and leaves control sulfate-dependent gene expression, and that the rest TFs are only shared between organs (Figure 11c).

As shown in Aim 1, most TF-target pairs in tomato are organ-specific. We looked forward to determining whether this observation was also true for the subset of sulfate deficiency-responsive genes, and whether time of treatment had an impact on the distribution of TF-target pairs. To address this, we performed an analysis of the distribution of specific TF-target pairs within sulfate context-specific networks, we found that, as previously shown, most pairings are dependent on the organ of origin (Figure 11d). Although we found some differences on TF-target pairs that were dependent on time, especially on the leaves network, most connections were shared between time points. Based on these findings, we decided to focus our analysis exclusively into the generation of two context-specific GRNs for roots and leaves, in order to search for key regulators of the sulfate deficiency response: a root network, consisting of all sulfate-deficiency DEGs occurring in roots at both time points, and a leaves network, consisting of all sulfate-deficiency DEGs occurring in leaves at both time points.

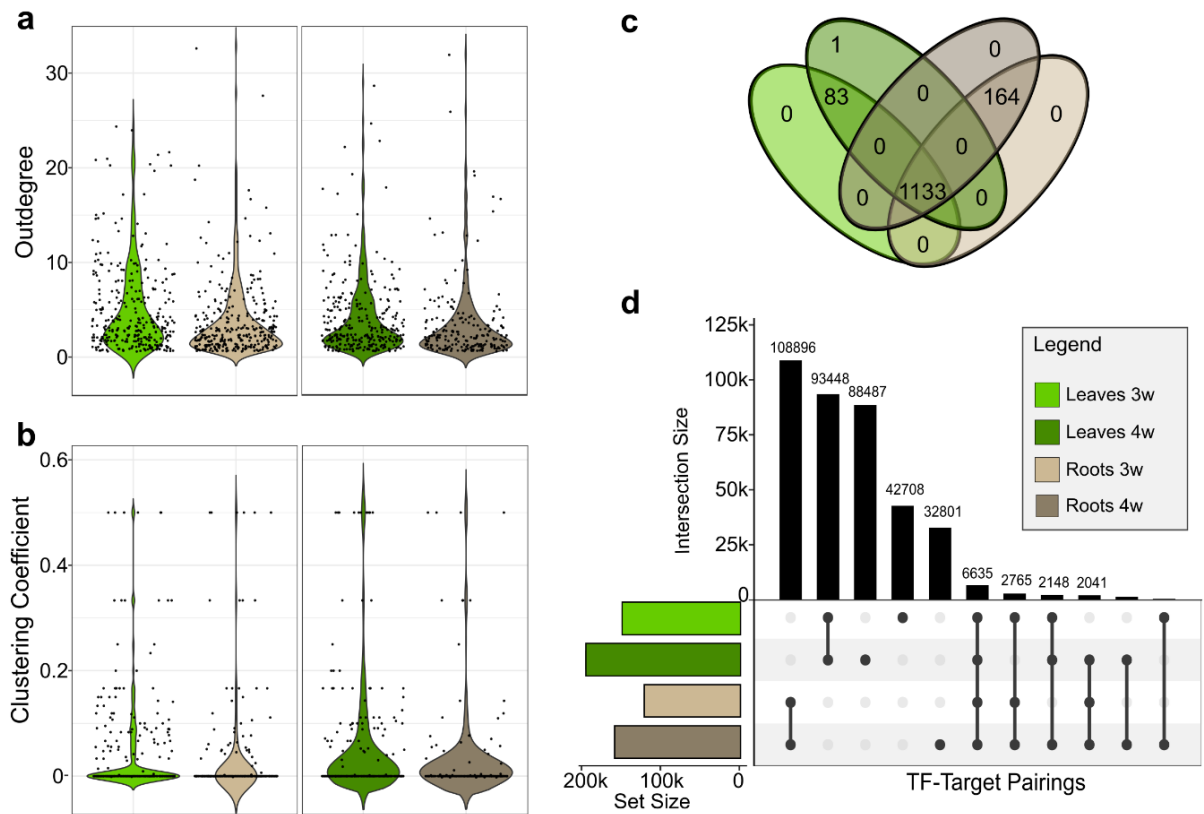


FIGURE N°11. TF analysis in context- and time-specific root and GRNs of sulfate deficiency-responsive genes. (a) Violin plot showing the outdegree distribution of TFs, highlighting connectivity differences across GRNs. (b) Violin plot showing the clustering coefficient distribution of TFs, emphasizing network modularity variations. (c) Venn diagram of overlaps among differentially expressed TFs in the specific GRNs. (d) Upset plot illustrating TF-target distributions across GRNs, integrating shared and unique regulatory interactions.

In order to identify candidate TFs that may act as key regulators of the sulfate deficiency response in tomato roots and leaves, we ranked the TFs based on different criteria: node centrality, based on the influential analysis performed with IVI (Salavaty *et al.*, 2020); the percentage for sulfate-responsive target genes; the log₂ fold of change of the TF in response to sulfate deficiency (only positive values were included); the proportion of targets categorized as sulfate-related based on GO annotations (Genes extracted from the GO terms: GO:0000096, GO:0000101, GO:0000103, GO:0006790, GO:0008272, GO:0009970, GO:0010438, GO:0019379, GO:0019419, GO:0031335, GO:0042762, GO:0044272, GO:0044273, GO:0055063, GO:0072348, GO:1900058, GO:1902358). For each TF, we considered the top 500 values per criterion and ranked them from highest to lowest and assigned scores depending on the position of each TF across the roots and leaves networks (Supplementary Tables 12-13). The top 15 TFs were put into a final matrix to produce a combined score that indicates the TF possible role as a key regulator of the sulfate deficiency responsive genes on tomato roots and leaves (Figure 12).

As the final aim of our work is to find key TFs involved in the regulation of the phenotypical changes associated with sulfate deficiency response treatments, we searched if the top ranked TFs had a known function or possible role involved in growth-related processes according to literature, if functionality is not documented, we extracted functional information available for their *Arabidopsis thaliana* orthologs, after an Orthofinder (Emms and Kelly, 2019) analysis and evaluate the functionality of the corresponding Arabidopsis TFs using data from the Arabidopsis information resource website (TAIR) (Berardini *et al.*, 2015) (Supplementary Table 14). Candidate TFs associated with growth regulation, stress responses, and sulfate deficiency were prioritized for further study (Figure 12).

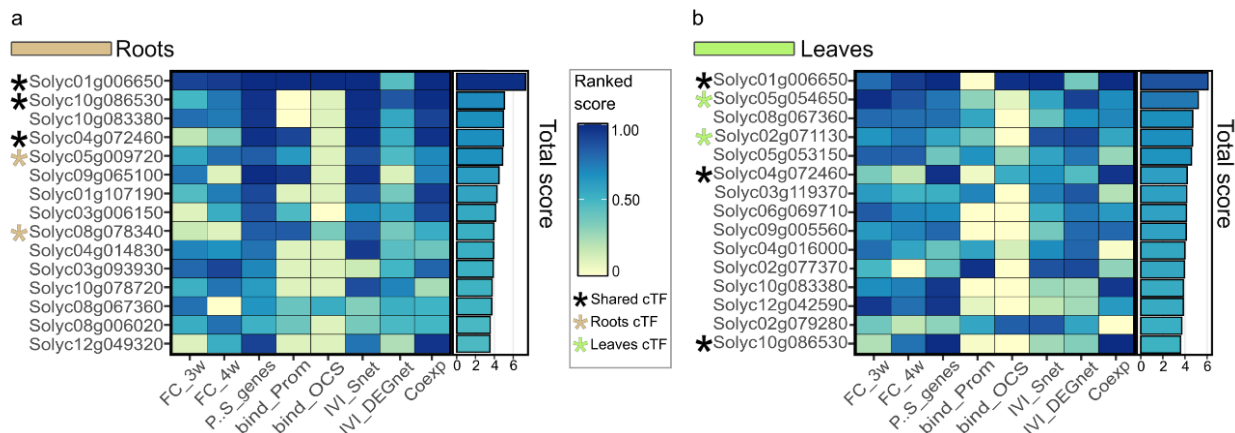


FIGURE N°12. Heatmaps of ranked scores for the top 15 potential key TFs regulating sulfate deficiency responses. (a) Top 15 TFs in roots. (b) Top 15 TFs in leaves. Heatmaps display ranked scores based on selected criteria, with darker colors indicating higher scores. Adjacent bars represent total TF scores. Candidate TFs are marked with asterisks: green for leaf-specific, brown for root-specific, and black for shared candidates. Criteria legend: FC_3w (log₂ fold change at 3 weeks), FC_4w (log₂ fold change at 4 weeks), P.S_genes (proportion of sulfate-important target genes), FIMO_Prom (predicted promoter-binding targets), FIMO_OCS (predicted OCS-binding targets), IVI_Snet (influentiality on sulfate-important genes), IVI_DEGnet (influentiality on DEG network), Coexp (proportion of coexpressed targets).

We generated two sulfate deficiency context-specific GRNs to identify the most relevant regulators involved in sulfate deficiency responses, from these networks we isolated the edges representing the target genes involved in sulfur transport, metabolism and signaling cascade according to their GO annotations (sulfate-related GOs) and organized them into a TFs hierarchy based on nodes outdegree. The root-specific GRN included 4,088 nodes and 46,179 edges, while the leaf-specific GRN comprised 7,973 nodes and 137,988 edges. Of these edges, 82.14% of the root network and 42.12% of the leaf network were shared between organs. Additionally, 25,321 (54.83%) of the root GRN edges, and 75,443 (54.67%) of the leaf GRN edges had one or more edges with validation evidence from the GCNs and TF-binding predictions. Furthermore, 20.73% of the root network and 21.33% of the leaf network showed evidence of potential direct TF binding. The main hubs consisted of 73 TFs in top-tier regulatory positions, 10 of which were shared between organs, including all top TFs from the root network (Figure 13a-b). The selected TFs in the ranked list (Figure 12) appear in the top tiers of hierarchy in the networks (Figure 13a-b), we found that Solyc01g006650 (EIL3), Solyc04g072460 (TGA7), and Solyc10g086530 (SCL14) were found as central TFs in both organ networks, while Solyc05g009720 (HHO) and Solyc08g078340 (KUA1) emerged as central controllers in roots and Solyc05g054650 (ZAT11) and Solyc02g071130 (WRKY71) were identified for leaves.

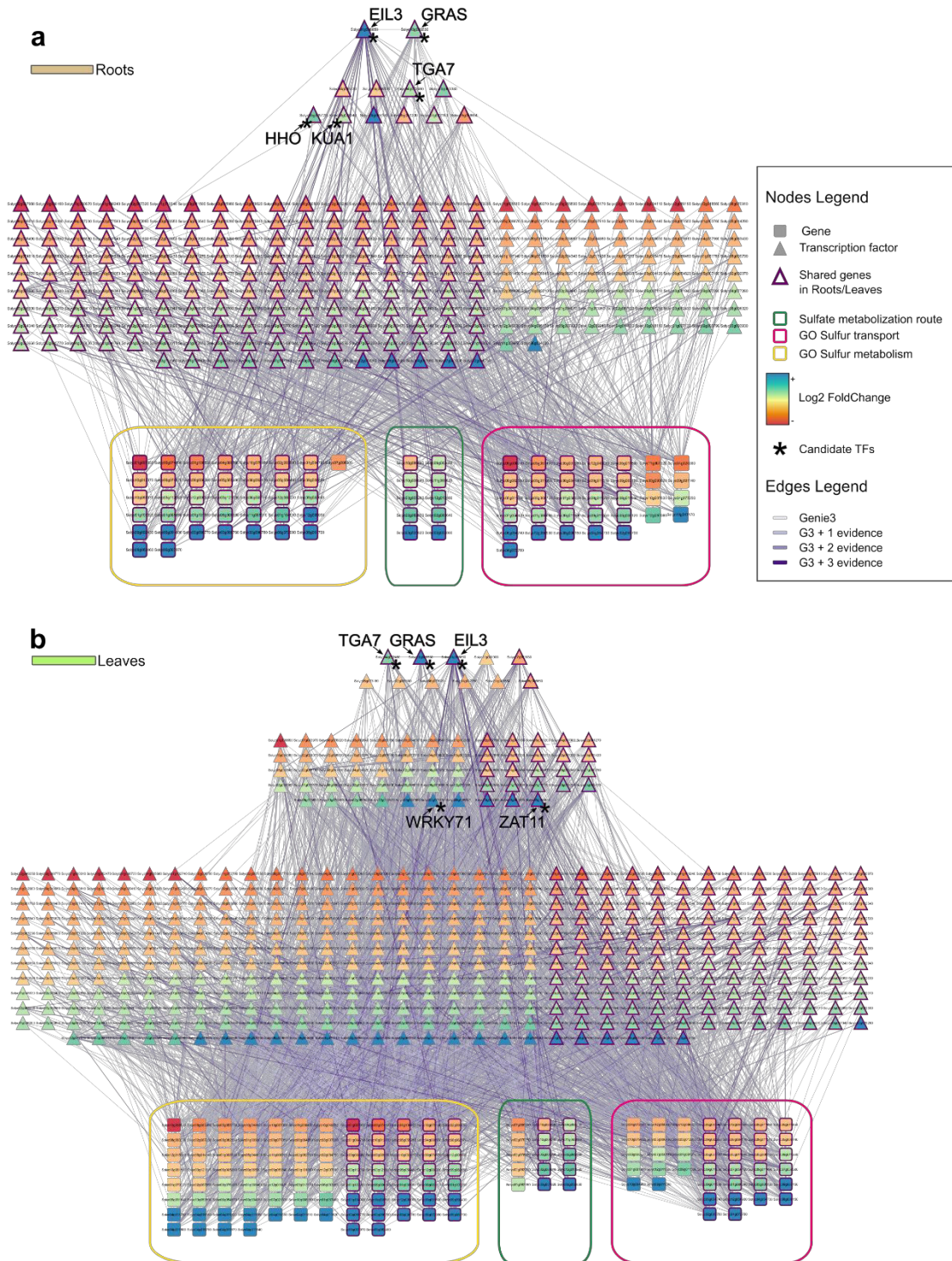


FIGURE N°13. Context-specific GRNs revealing TF hierarchy in sulfate deficiency responses. (a) Root GRN. (b) Leaf GRN. Highlighted groups: sulfate metabolization routes (green), sulfate metabolism (yellow), and sulfate transport (pink). Node color scale indicates mean log₂ fold change value. Violet-bordered nodes indicate shared genes between networks. Black asterisks mark selected candidate TFs. Edge darker shades indicate accumulated regulatory evidence.

2.2 Five candidate TFs are able to control multiple biological processes associated to sulfate deficiency treatments in tomato plants.

We conducted a GSEA analysis on the candidate key TFs by selecting their target genes identified in the sulfate-responsive GRNs to determine their enriched biological processes (adj.p.val < 0.05) (Figure 14 a-b). The shared key regulators EIL3, TGA, and SCL14 common to both root and leaf networks, showed the highest enrichment in biological processes such as “cellular response to sulfate starvation,” “sulfate assimilation,” and “response to nutrient levels” (adj.p.val < 0.005), indicating a possible important role regulating sulfate metabolism during sulfate deficiency. In contrast, organ-specific TFs exhibited enrichment in distinct biological processes. In roots, terms related to molecule transport are enriched for multiple TFs. Consistent with the role of its Arabidopsis homolog (Wang *et al.*, 2020), the HHO TF appears to be involved in phosphate deficiency regulation (Figure 14a). In leaves, the WRKY and ZAT TFs appear to regulate targets enriched on functions related to glutathione metabolism and multiple terms associated with defense responses including salicylic, jasmonic and abscisic acid signaling (Figure 14b). The analysis of the top five candidate TFs and their target genes obtained from the context-specific GRNs revealed that they collectively regulate more than 20% of the DEGs in response to sulfate deficiency in both roots and leaves. The root-specific networks showed a high enrichment in phosphate starvation regulation, a process that has been linked to sulfate deficiency responses as previously reported (Canales *et al.*, 2020; Fernández *et al.*, 2024).

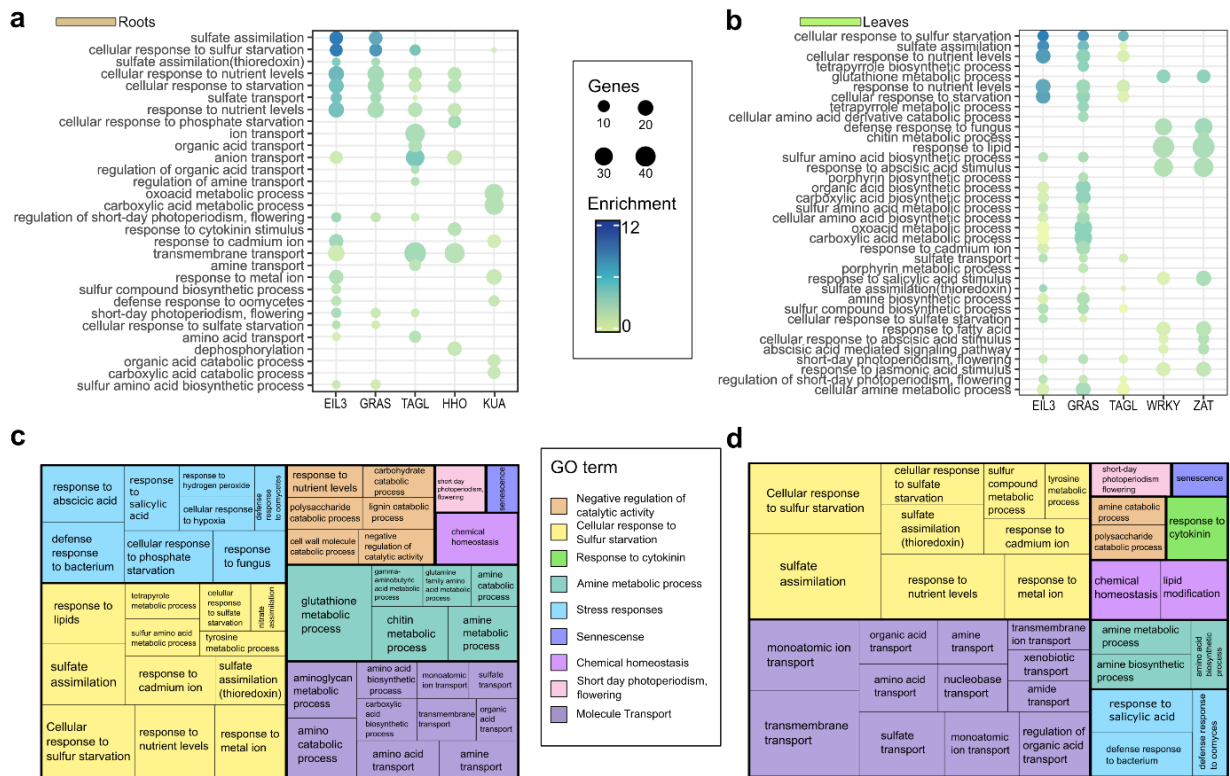


FIGURE N°14. Top five organ-specific TFs identified as key regulators of sulfate deficiency responses. (a) Dot plot showing GSEA results (FDR-adjusted p-value < 0.05) for individual root TF candidates. (b).Dot plot showing GSEA results for individual leaf TF candidates. (c) Treemap summarizing GSEA (FDR-adjusted p-value < 0.05) results for root candidate TF targets. (d) Treemap summarizing GSEA results for leaf candidate TF targets.

A treemap visualization of the genes regulated by these candidate TFs indicates that, as expected, the most enriched biological processes are related to sulfate transport and metabolism. Furthermore, the analysis grouped overrepresented biological processes in categories like the cellular response to sulfur starvation, molecule transport, stress responses, amine metabolism, and processes associated with growth reduction, such as negative regulation of catalytic activity and senescence-related genes (Figure 14c-d) —all of which are considered common biological processes influenced by sulfate deficiency (Henríquez-Valencia *et al.*, 2018; Canales *et al.*, 2020; Fernández *et al.*, 2024). These findings provide insights into how sulfate deficiency impacts tomato plant growth and highlight the potential regulatory role of the selected TFs in the control of gene expression during this nutrient deficiency.

To limit our candidate TFs group and identify the most promising key regulator of the sulfate deficiency regulatory cascades for further experimental validation, we focused on the TF Solyc01g006650, called ETHYLENE-INSENSITIVE3-LIKE 3 (*S/EIL3*), that emerged as a strong candidate in both roots and leaves GRNs. Additionally, the GSEA analysis of *S/EIL3* targets indicate significant enrichment for sulfate-related GO terms in both roots and leaves, as well as processes such as amine metabolism, photoperiodism, cell transport, and stress responses (FDR adj.p.val < 0.05) (Figure 14a-b). The *S/EIL3* is reported as a homolog of *AtEIL3* (also called *SLIM1*, SULFUR LIMITATION 1), a well-studied TF that controls sulfate deficiency-responsive genes in *Arabidopsis* (Maruyama-Nakashita *et al.*, 2006; Watanabe and Hoefgen, 2019, Preprint; Fernández *et al.*, 2024). Notably, we found that *S/EIL3* belongs to the same clade than *SLIMI* (Fernández *et al.*, 2024), a clade within the EIL/EIN3 family that includes other plant TFs suggested as controllers of the sulfate deficiency response such as the rice

Os09g0490200 and *Os08g0508700* TFs (Maruyama-Nakashita et al., 2006). Furthermore, the *S/EIL3* regulatory pairings from the roots and leaves GRNs, suggest that it regulates several well-known sulfate deficiency marker genes such as *Sulfur Deficiency Induced (SDIs)*, *Response to Low Sulfur (LSUs)*, *APR3*, *Gamma-Glutamyl Cyclotransferase 2;1 (GGCT2;1)* and *Sulfate affinity transporters (SULTRs)* (Hubberten et al., 2012, Preprint; Rakpenthai et al., 2022). In addition, previous network analysis performed by our team, suggested that *S/EIL3* might be an important regulator of genes involved in sulfate deficiency responses (Canales et al., 2020; Fernández et al., 2024), however no experimental validation of its role was determined.

2.3 TARGET analysis supports the EIL3 role as a regulator of sulfate important genes.

We optimized a tomato protoplast isolation protocol and performed the TARGET perturbation analysis (Bargmann et al., 2013, Preprint) in tomato protoplasts to induce the EIL3 expression in order to identify its direct genome-wide regulatory target genes. In detail, the EIL3 TF was transiently overexpressed in tomato protoplasts after a plasmid DNA transfection, then treated to induce controlled nuclear import, the resulting effect of the EIL3 on genome-wide expression was assayed using a RNA-Seq in three replicates and compared to a control of a transfected empty vector under the same treatments. After analyzing the counts, TARGET detected 2367 upregulated genes, and 1694 downregulated genes associated to EIL3 direct regulation (adjusted p-value < 0.05) (Supplementary table 15). Notably, we observed a substantial overlap between the gene lists of DEGs under sulfate deficiency, the EIL3 targets on the organ-level GRNs, and the regulatory targets identified by TARGET in both roots and leaves

(Figure 15a). Moreover, we conducted an enrichment analysis that confirmed these overlaps as statistically significant (Figure 15b), indicating that EIL3 directly regulates a considerable portion of genes involved in sulfate deficiency responses. Furthermore, the significant overlap between TARGET-validated and GRN-predicted targets further demonstrate the accuracy of our regulatory networks. Notably, the EIL3 targets in root and leaf GRNs revealed that over 60% of key sulfur-related genes were validated by TARGET as direct targets for both tomato roots and leaves (Figure 15c). These findings demonstrate the complementary nature of GENIE3-predicted GRNs and TARGET for the identification of regulatory interactions and establish EIL3 as a key regulator of sulfate deficiency responses in tomato. Based on these findings, the *S/EIL3* can be considered as the most promising candidate TF for transcriptional regulation of sulfate deficiency responses in *S. lycopersicum* and was chosen for functional validation tests covered in Aim 3.

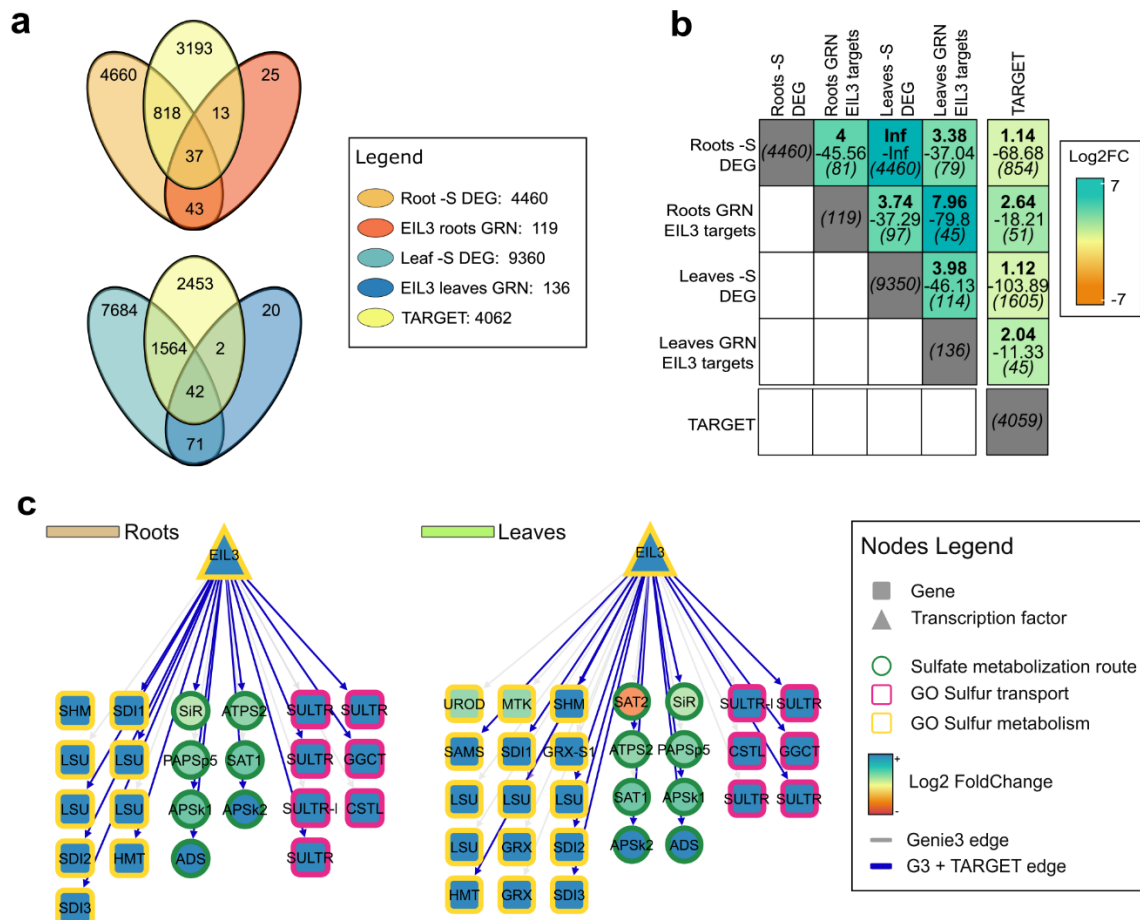


FIGURE N°15. TARGET analysis supports *S/EIL3* as a regulator of sulfate-responsive genes. (a) Venn diagrams showing overlap between sulfate deficiency DEGs (roots and leaves), *S/EIL3* GRN targets, and TARGET-validated regulatory targets. (b) Enrichment analysis of these gene sets. Box heatmaps display log₂ fold change, p-values, and intersection sizes. (c) Network visualization of *S/EIL3*-regulated sulfate-responsive genes (GO terms: sulfate metabolism route (green), sulfate metabolism (yellow), sulfate transport (pink)). Blue edges indicate TARGET-validated genes. G3: GENIE3 GRN.

3. To experimentally validate the function of a central TF candidate in the regulation of plant growth under sulfate deficiency.

Rationale: Sulfate deficiency negatively affects tomato plant growth and development, yet the molecular mechanisms involved in the regulation of this response are poorly understood. To investigate this, we generated a stable overexpression (OX) lines of *Arabidopsis thaliana* expressing a candidate *S/TF* discovered in Aim 2 as a key hub in the sulfate-responsive GRNs, with the purpose of validating its role as a key TF by assessing its regulatory impact on gene expression reprogramming and plant development effects in both control and sulfate-deficient conditions.

3.1 OX-*S/EIL3* plants reveal increased growth and enhanced S accumulation.

To analyze the role of *S/EIL3* in the regulation of plant growth and gene expression changes under sulfate deficiency, we generated *S/EIL3* overexpressor lines in *Arabidopsis thaliana*. Plants were transformed by the floral dip method, and two independent lines were chosen for all analyses. The OX-*S/EIL3* lines exhibit a significant accumulation of the *EIL3* transcript, with highest expression observed in the OX-1 line, confirming overexpression of *S/EIL3* (Figure 16a).

Visual inspection of OX-*S/EIL3* lines revealed significant differences in seedling growth relative to control (wild type, WT) plants under both control and sulfur-deficient (-S) treatments. Analysis of growth parameters showed that the OX lines presented an increased growth of root and shoot organs, with longer primary and secondary roots, and increased foliar area (Figure 16b).

A multifactorial analysis of primary root length and total foliar area (Figures 16c-d) revealed that OX-*S/EIL3* plants developed roots 1.3–1.8 times longer and a foliar area 1–3 times larger than WT plants, indicating that *S/EIL3* overexpression considerably increased plant growth ($p < 0.001$, two-way ANOVA, and Tukey test). This phenotype is consistent with the reported growth effect of SLIM1 overexpression in *Arabidopsis* plants (Apodiakou *et al.*, 2024). While S deficiency affected the growth of WT plants, it had a smaller effect on OX-*S/EIL3* plants. Under sulfur-deficient conditions, root length increased 1.5-2 times, and foliar area was 2.4-4.2 times larger than in WT plants ($p < 0.05$, two-way ANOVA, and Tukey test). Notably, there were no significant differences between OX-*S/EIL3* lines 1 and 2, indicating that the two transgenic lines are functionally consistent.

Plants that were deprived of sulfate accumulated less S in their tissues, as expected. Total S measurements (Figure 16e) showed a significant treatment effect on S accumulation ($p < 0.001$), the OX-*S/EIL3*-1 plants accumulated considerably more sulfur than WT plants, with a median of 0.4 μg per gram of tissue. However, the OX-*S/EIL3*-2 did not show significant differences when compared to WT. This demonstrates that OX-*S/EIL3*-1 may have a more efficient S uptake mechanism and/or metabolism potentially related to the observed higher expression of *S/EIL3* (Figure 16a-e). These findings show that *Arabidopsis* OX-*S/EIL3* lines exhibit improved growth and S accumulation than WT plants. The OX-*S/EIL3*-1 line's higher gene expression levels, together with its stronger phenotypic effects on plant growth and sulfur uptake, made it a suitable line for further transcriptomics analysis.

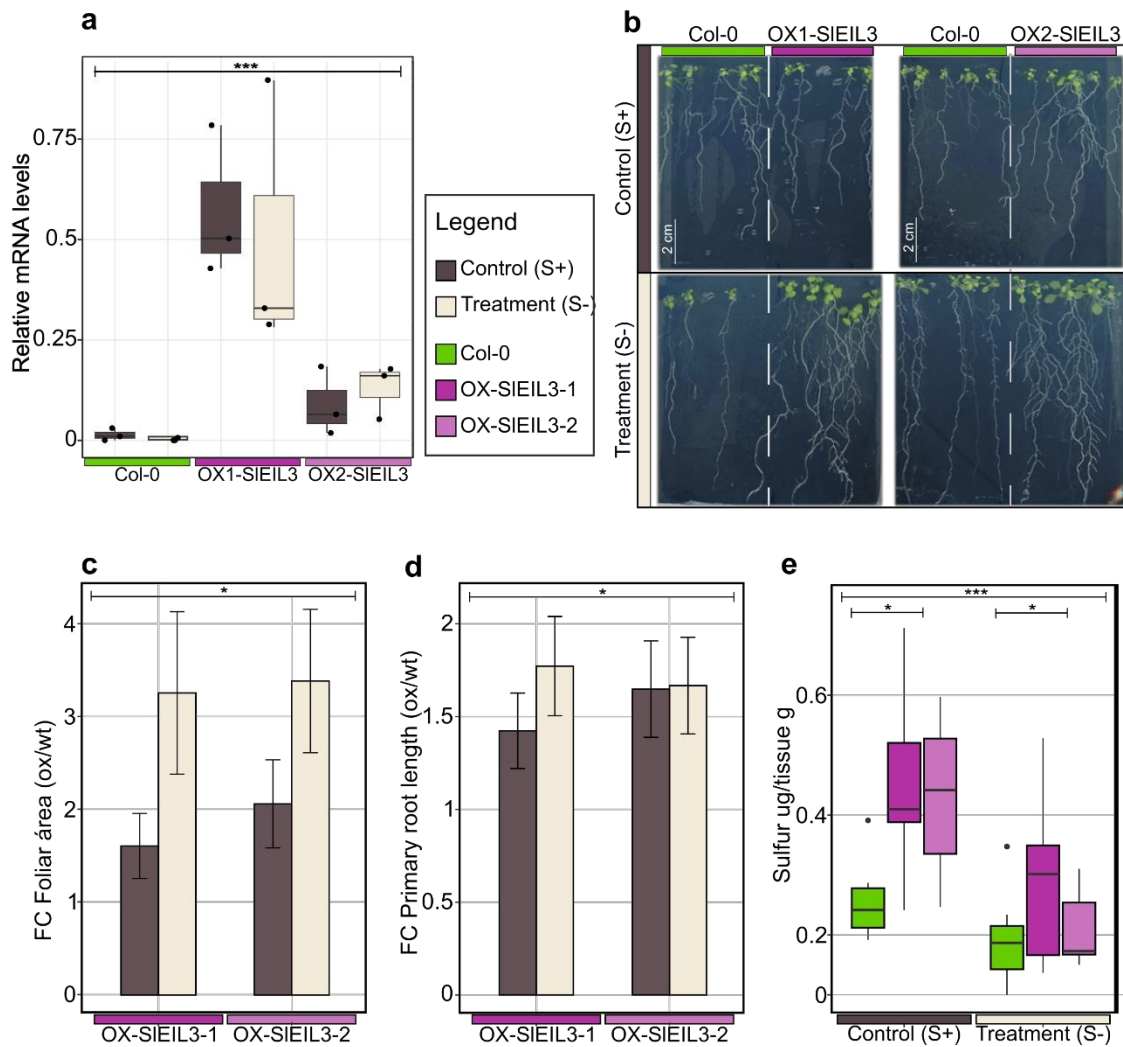


FIGURE N°16. Phenotypic analysis of Col-0 and OX-SIEIL3 Arabidopsis under contrasting sulfate treatments. (a) RT-qPCR analysis of *SIEIL3* (*Solyc01g006650*) in control and OX plants, normalized to *UBQ1* (*AT3G52590*). Mean \pm SD from three biological replicates (Student's t-test, $p < 0.05$). (b) Photographs of *A. thaliana* plants grown under full-nutrient or sulfate-deficient conditions for two weeks. (c) Root length measurements. (d) Aerial organ area. (e) Sulfur content ($\mu\text{mol}/\mu\text{g}$). For (c–e), values represent mean \pm SD from >15 biological replicates. Error bars = 3. Statistical significance was assessed using two-way ANOVA with Tukey and Dunnett's post hoc tests (* $p < 0.05$, ** $p < 0.01$).

3.2 Transcriptomic changes of the OX-*S/EIL3* plants are equivalent to responses to sulfate deficiency treatment.

In order to understand the regulatory effect of the overexpression of *S/EIL3* on the plant's transcriptome, we performed a mRNA-seq analysis comparing the effects of the different genotypes (WT and OX1) under sulfate deficiency conditions. Total mRNA was extracted and sequenced from two-week-old seedlings of both genotypes (WT and OX-*S/EIL3*) under control and sulfate-deficient conditions. Following standard RNA-seq procedures, a count table was generated, and differential expression analysis was performed using the DESeq2 package. A multifactorial analysis identified 3,266 DEGs associated with genotype, 1,317 DEGs associated with treatment, and 468 DEGs resulting from the interaction between genotype and treatment (adjusted p-value < 0.05), with the majority of genes found shared between the genotype and interaction gene lists (Figure 17a) (Supplementary Table 16). To contrast the enrichment of the DEG lists obtained in this study to other sulfate deficiency transcriptomes, we conducted enrichment analyses using a one-tailed Fisher's exact test to compare our RNA-seq DEG lists to gene sets reported in previous studies, to the analysis of controls vs sulfate deficiency treated plants from (Maruyama-Nakashita *et al.*, 2006; Dietzen *et al.*, 2020) and to the analysis of WT and SLIM1-overexpressing plants (Apodiakou *et al.*, 2024) (Figure 17b). Additionally, we included a list of S-related genes identified according to GO annotations (genes belonging to sulfur metabolism, transport, and sulfate signaling pathway). The analysis revealed a significant overlap between the DEGs identified in our genotype, treatment, and interaction G+T lists and those found in previous studies, confirming the consistency of our transcriptomic data to other *Arabidopsis* DEG profiles under similar conditions. Furthermore, the gene overlaps suggest the presence of a significant representation of S-related genes, emphasizing the potential of our

experiment to uncover regulatory networks related to the sulfate deficiency response. Given that our primary objective is to understand the impact of *S/EIL3* on the transcriptome of OX plants, we selected the DEGs identified from the genotype factor and the genotype-treatment interaction factor for further analysis.

To analyze the expression patterns of OX-*S/EIL3* DEGs and determine the regulatory effects of *S/EIL3* overexpression, we generated a heatmap and used k-means clustering using the DEGs z-scored normalized expression values to identify four distinct clusters based on their expression profiles (Figure 17c). The cluster 1 contains 215 genes that show a reduced expression under sulfate deficiency, with this reduction being more pronounced in OX-*S/EIL3* plants. Cluster 2 includes 321 genes that are upregulated during sulfate deficiency, with consistently higher expression levels in OX-*S/EIL3* plants. Cluster 3 includes 570 genes with relatively stable expression patterns across genotypes, and cluster 4 includes 1233 genes predominantly upregulated in OX-*S/EIL3* plants under sulfate-sufficient conditions.

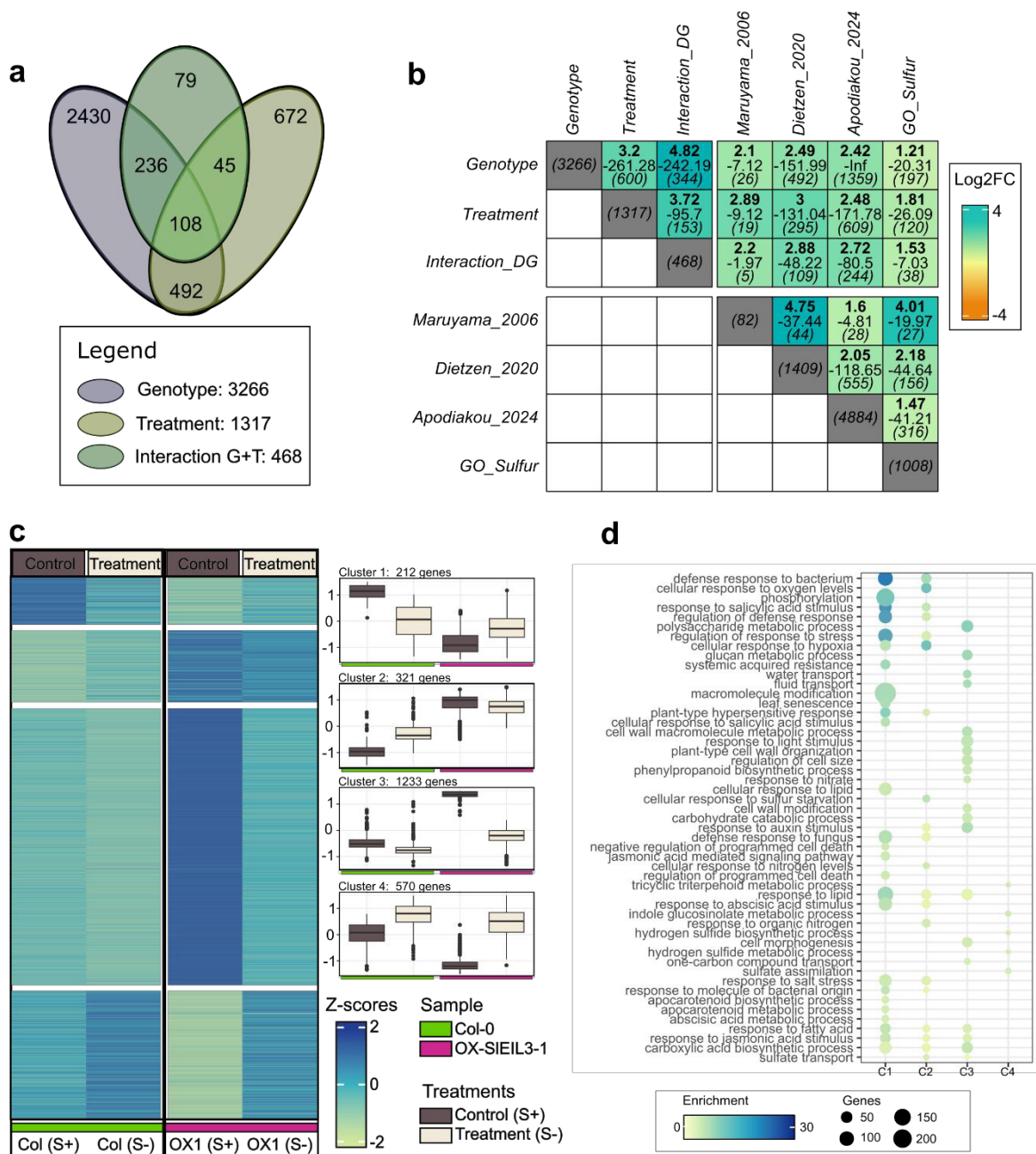


FIGURE N°17. Transcriptome analysis of Col-0 and OX-S/EIL3 Arabidopsis under sulfate deficiency treatments. (a). Venn diagram of genes significantly regulated by genotype, sulfate treatment, or their interaction (G + T). (b) Enrichment analysis comparing DEG enrichment across sulfate-related transcriptome datasets (Apodiakou et al., 2024; Dietzen et al., 2020; Maruyama-Nakashita et al., 2006) using Fisher's exact test (one-tailed). (c) Heatmap of z-scored expression levels of DEGs in OX-S/EIL3 plants, clustered via K-means. (d) Dot plot of GSEA results (FDR-adjusted p-value < 0.05) for DEGs in OX-S/EIL3 Arabidopsis, grouped by K-means clustering.

A GSEA of these clusters revealed details regarding their functional roles (FDR adj.p.val< 0.05) (Figure 17d). Cluster 2 showed an enrichment for defense responses and highlighted the presence of sulfur starvation responses and sulfate transport, indicating that *S/EIL3* may have a role in upregulating sulfate-responsive genes, like its homolog SLIM1. Cluster 1 was enriched for stress responses and defense mechanisms, indicating the activation of stress pathways associated with sulfate deficiency and growth inhibition. Cluster 3 contained genes involved in cell transport, cell wall metabolism, auxin signaling, and cell size regulation, which could explain the observed altered-growth phenotype of OX-*S/EIL3* plants. Cluster 4 consisted of genes involved in the metabolism of S-containing compounds such as glucosinolates, as well as few genes related to sulfate assimilation (Figure 17d). The gene lists and their associated biological process indicate that *S/EIL3* can regulate a variety of S-related and stress-responsive pathways in Arabidopsis.

3.3 The *S/EIL3* controls sulfate deficiency marker genes and recapitulates tomato predicted regulatory cascades.

As mentioned above *S/EIL3* is a homolog of *AtEIL3* also known as Sulfur Limitation 1 (SLIM1) a master regulator of sulfate deficiency responses in Arabidopsis, previously validated as a key regulator of multiple gene markers associated to sulfate deficiency transcriptomic responses (Maruyama-Nakashita *et al.*, 2006; Wawrzyńska and Sirko, 2014; Rakpenthai *et al.*, 2022). To investigate whether *S/EIL3* regulates genes predicted to be controlled by SLIM1, we generated a regulatory network that illustrates the connections of *S/EIL3* to the DEGs in OX-*S/EIL3* plants. Furthermore, we incorporated the results of a FIMO analysis to identify potential *S/EIL3* binding sites in the promoters of Arabidopsis genes, utilizing the *S/EIL3* PWM derived from the analysis of tomato GRNs (Figure 18a). From the 3,391 genes in the DEG list, 52% (1,763 genes) were identified as predicted binding targets of *S/EIL3* based on their promoter sequences, suggesting they could be direct targets of *S/EIL3* (Supplementary Table 17). The remaining 48% are likely indirect targets, regulated downstream of *S/EIL3*. Focusing on S-related genes (as defined by GO annotations), we identified important sulfate deficiency markers within the network that overlap with our predicted tomato *S/EIL3* GRNs for roots and leaves (Figure 18b). The network included a variety of indirect and direct targets of *S/EIL3*, including four *Response to Low Sulfur (LSU)* genes, a *Sulfur Deficiency Induced (SDI)*, three members of the sulfur signaling cascade (*APRS2*, *ATPS1*, and *APSk3*), and five genes encoding *SULTRs* and the *Gamma-Glutamyl Cyclotransferase (GGCT)*, all of which were also found to have predicted direct binding by the FIMO analysis. These results demonstrate that *S/EIL3* and SLIM1 share highly conserved regulatory pathways, with *S/EIL3* effectively regulating important S-related

genes in tomato and Arabidopsis. Furthermore, our results validate the accuracy of our tomato GRNs in the prediction of sulfate deficiency regulatory cascades, highlighting the conserved nature of *S/EIL3* and *SLIM1* regulatory mechanisms.

To observe the specific regulatory effect of the DEG list of OX-*S/EIL3* on biological processes in Arabidopsis, we performed a GSEA as a treemap visualization. This analysis showed that *S/EIL3* overexpression in Arabidopsis regulates a diverse set of biological processes, involving S-specific pathways as well as broader physiological functions (FDR adj.p.val < 0.05) (Figure 18c). As expected, sulfate-related processes, including sulfate transport and S compound metabolism are enriched, confirming the role of *S/EIL3* in maintaining S homeostasis and its functional parallel to *SLIM1* as a master regulator of sulfate deficiency responses (Maruyama-Nakashita, 2004, 2017, Preprint; Dietzen *et al.*, 2020). However, the results also highlight the regulation of additional processes, such as chemical homeostasis, transport mechanisms, and metabolic adjustments, reflecting the plant's broader adaptive responses to sulfate deficiency.

The results reported in this section support our research hypothesis, demonstrating that sulfate deficiency triggers a transcriptome reprogramming that is partially controlled by TFs like *S/EIL3*. This TF regulates a broad set of genes involved in sulfate deficiency responses influencing processes beyond S metabolism. We show that multiple other biological processes such a defense response, cell wall development and other stress responses were also regulated by this TF, results that could partially explain the growth repression phenotype observed in sulfate-starved plants and underscore the potential of this TF and support the complexity of the plant regulatory mechanisms under nutrient stress.

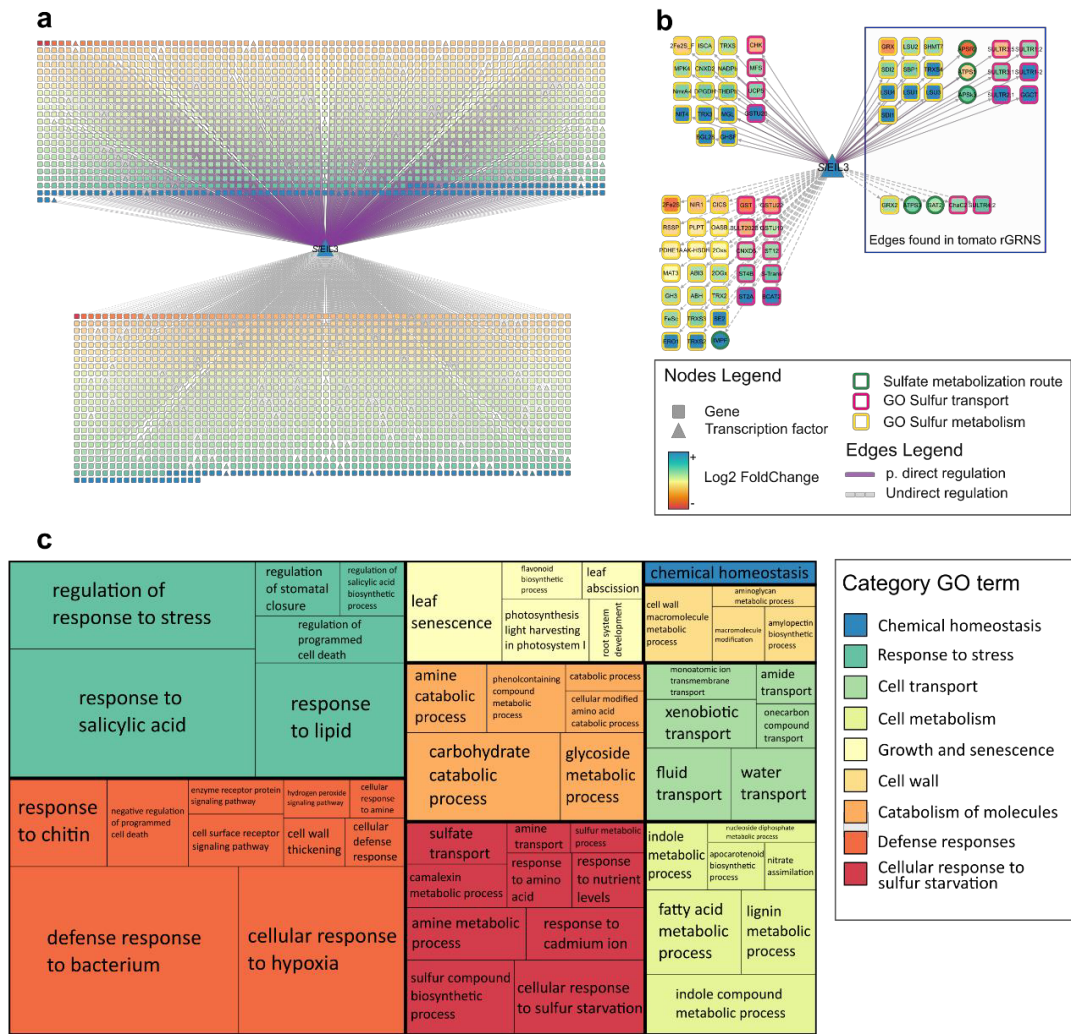


FIGURE N°18. Regulatory effects of *S/EIL3* on *Arabidopsis* sulfate-responsive genes. (a) Network visualization of *S/EIL3* regulation in *Arabidopsis* transcriptome. Colored edges represent predicted TF-binding, grey edges indicate indirect regulation. (b) Subnetwork of key sulfate-related genes (GO terms: sulfur metabolism, sulfur transport, sulfur utilization pathways). Genes within the blue rectangle were identified in tomato-predicted *S/EIL3* GRNs. (c) Treemap summarizing GSEA results (FDR-adjusted p-value < 0.05) for *S/EIL3* regulatory effects in the transcriptome. p.direct regulation: predicted direct regulation.

Regulatory model of TFs regulation of sulfate deficiency response in tomato

To illustrate the potential regulatory cascade underlying sulfate deficiency in tomato/Arabidopsis, we generated a regulation model based on our findings. This model demonstrates how the seven TF candidates identified in the organ-level GRNs may contribute to the sulfur deficiency transcriptomic regulation and how the target genes are linked to biological processes based on a GSEA (Figure 19a). By examining the complete set of targets for each TF, we determined what proportion of their total target genes are part of the DEG lists in response to sulfate deficiency. In roots, the TFs HHO and KUA1 have 35% and 24% of their total targets, respectively, belonging to the sulfate deficiency DEG list. The targets found for HHO in roots revealed that its potentially a regulatory control point between sulfate and phosphate regulation, since the most enriched biological process is cellular response to phosphate starvation, it includes more than 20 genes directly involved with phosphate transport and metabolism GO, with 57.2% (184/326) identified in a phosphate deficiency transcriptome analysis (Satheesh *et al.*, 2022) (Supplementary Table 18). Additionally, the HHO is connected to 23 genes involved in anion transport, including genes involved in sulfate, phosphate, molybdate and multiple carbohydrate transporters. The KUA1 TF demonstrated to be enriched to diverse biological processes, is particularly notable for its role in drought responses, as it targets 29 genes directly related to water deprivation, with 29.8% (193/656) of its targets identified in a drought transcriptome (Wang *et al.*, 2023b) (Supplementary Table 19).

In leaves, we found the candidates WRKY71 and ZAT11 to have 71% and 79% of their total targets, respectively, part of the sulfate deficiency DEGs. The most enriched biological processes among their target lists are glutathione metabolism and defense responses. For WRKY71 we found 69 genes involved in defense response, including 29 specifically associated with "response to fungus," with 18.49% (339/1834) of its targets were identified in a fungal infection transcriptome analysis (Coubier et al., 2021) (Supplementary Table 20). Similarly, the ZAT11 is implicated in glutathione metabolism and defense responses, with 24 genes linked to "response to fungus" and 21.9% (403/1834) of its targets overlapping with the same fungal infection dataset (Coubier *et al.*, 2021) (Supplementary Table 21). Notably, both TFs share nearly 50% (289 genes) of their targets, suggesting a strong correlation between sulfate deficiency and defense responses in leaves through changes in glutathione metabolism.

Among TFs shared between roots and leaves, the TAGL-1 was found to have 39% and 60% of its total targets as DEGs in roots and leaves, respectively; SCL14, 50% and 88%; and EIL3, 68% and 84% of the DEGs in roots and leaves, respectively. The most enriched biological processes for all three TFs are associated with sulfate metabolism, highlighting their potential crucial role in regulating sulfate-related pathways and metabolism. The TAGL-1 is linked to sulfate metabolism, and associated to molecule transport regulation in roots, targeting 41 ion transport-related genes, including aluminum, potassium, nitrate, sulfate, zinc, and phosphate transporters identified in the root GRN (Supplementary Table 22). The SCL14 is also strongly enriched in sulfate metabolism and associated to 25 genes encoding amino acid metabolism enzymes in the leaf GRN, suggesting a previously unrecognized regulatory role in amino acid metabolism in tomato (Supplementary Table 23). As mentioned above, the EIL3 exhibits the

highest percentage of total targets involved in sulfate deficiency response, and demonstrate the highest enrichment in sulfate-related metabolism (Supplementary Table 24), confirming its high involvement in tomato plants responses to sulfate deficiency.

In the model we also included a representation of OX-*SIEIL3* Arabidopsis plants observed phenotype (increased root growth and aerial organs area) and included potential genes involved in physiological responses that could explain the phenotype observed (Figure 19b). The DEGs with evidences for potentially contributing to this phenotype were categorized into three functional groups: TFs associated with accelerated growth and senescence responses (*MYB1*, *MYB60*, *NAC016*, *NAC046*, *WRKY75*, *PIF3*), genes involved in sulfate uptake (*ATPS1*, *APRI-3*, *SULTR1;1*, *SULTR1;2*, *SULTR2;1*, *SULTR4;2*), and sulfate deficiency markers (*LSUs*, *SDIs*, *GGCC*). These genes represent key components of the regulatory cascades potentially activated downstream of *SIEIL3* in tomato, providing insights into its role in sulfate deficiency response.

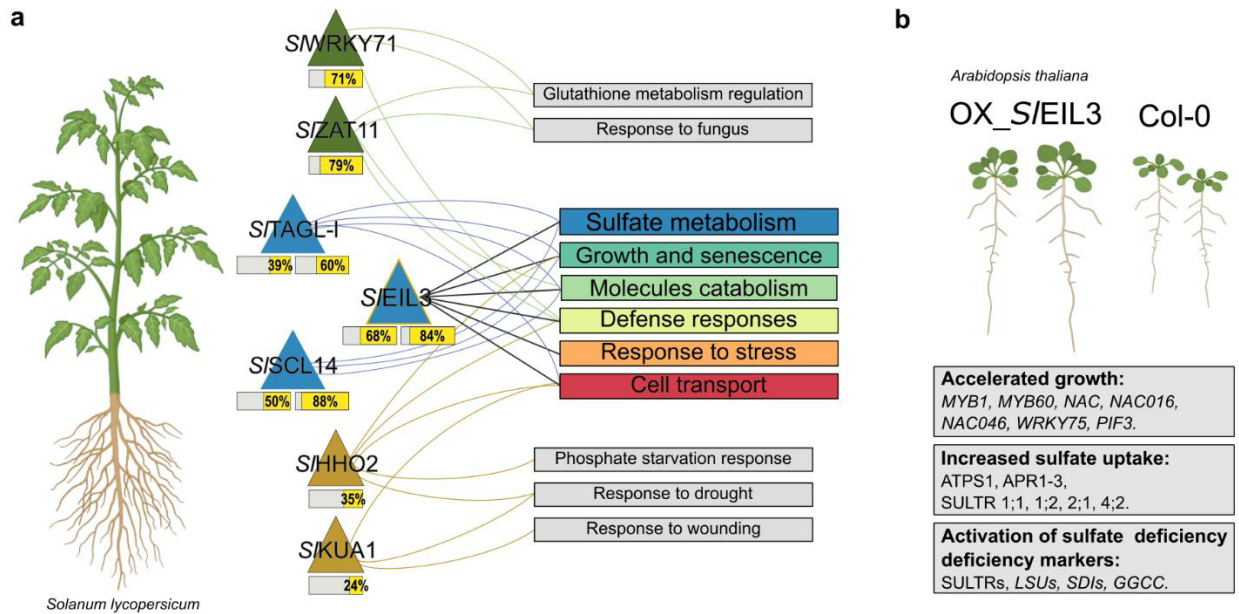


FIGURE N°19. Model of key TFs regulating sulfate deficiency responses in *Solanum lycopersicum*. (a) Candidate key TFs regulating sulfate deficiency in tomato. TFs are represented as triangles: brown (root-specific), green (leaf-specific), and blue (shared between both organs). Yellow bars indicate the percentage of DEGs among TF targets under sulfate deficiency. Colored rectangles denote top enriched GO biological processes (GSEA, FDR-adjusted p-value < 0.05), with lines linking TFs to associated processes. (b) Phenotypic summary of OX-S/EIL3 Arabidopsis plants. Genes linked to accelerated growth, increased sulfate uptake, and activation of sulfate deficiency markers are listed.

VII. DISCUSSION

1. To generate organ-specific reference Gene Regulatory Networks models for *Solanum lycopersicum*.

To generate tomato GRNs, our first step was to generate an updated resource of gene models, TFs and functional annotations, because it was necessary to compile and organize the gene annotations that were so diverse between different experiments, only then we can be capable of comprehensive detecting the regulatory cascades in tomato, and further using the networks to reveal key regulatory points for multiple biological processes. at the organ level. We compiled the gene annotations from the latest genome *Sl4.0* into ITAG4.1c. Using widely adopted annotation pipelines (Jones *et al.*, 2014; Cantalapiedra *et al.*, 2021), we ere able to assign functional annotations to 25,689 of the 37,468 genes of ITAG4.1c, considerably improving the gene coverage compared to iTAG4.1 in SolGenomics (13,142 genes with functional annotations) [(https://solgenomics.net/ftp/tomato_genome/annotation/ITAG4.1_release/ITAG4.1_goterms.txt)] or previous annotations for iTAG4.0 (25,285 genes) (Hosmani *et al.*, 2019; Rivera-Silva *et al.*, 2024).

TF prediction remains a challenging task, as automated approaches usually rely on protein sequence scanning for known DNA-binding domains, which may lead to the inclusion of proteins with DNA-binding capabilities unrelated to TF function (Itzkovitz *et al.*, 2006; Liebold *et al.*, 2024). To avoid such proteins and refine the tomato TF list, we integrated multiple levels of evidence to filter and extract a curated set of 1,840 TFs (representing around 5% of tomato genes). This number closely aligns with TF counts reported for tomato in PlantTFDB (1,845 TFs) (Jin *et al.*, 2017) and is slightly higher than those in CisBP (1,773 TFs) (Weirauch *et al.*,

2014) and other annotated TFs from previous studies (1,069 TFs in Kumar *et al.*, 2021). Overall, the percentage of TF coding genes we found is slightly lower than TFs reported for Arabidopsis (approximately 5-10%) (Riechmann and Ratcliffe, 2000) but consistent with estimates reported for other crops, including wheat (5.7%) and rice (6.1%) (Zheng *et al.*, 2016). It is also comparable to values reported for other Solanaceae species, such as eggplant (5.3%) (Wei *et al.*, 2020). Our efforts provide a comprehensive framework to start the development of genomic tools for studying tomato regulatory cascades.

A vast number of transcriptomic studies have been conducted in tomato, covering diverse experimental conditions, organs, and developmental stages. While several efforts have aimed to generate gene expression atlases for tomato gene expression (Ozaki *et al.*, 2010; Fukushima *et al.*, 2012; Gao *et al.*, 2013; Koenig *et al.*, 2013; Arhondakis *et al.*, 2016; Zouine *et al.*, 2017; Bae *et al.*, 2021; Bizouerne *et al.*, 2021; Kumar *et al.*, 2021; Kusano *et al.*, 2022; Li *et al.*, 2024) many studies are limited in scope, often focusing on specific experimental conditions, using outdated genome assemblies (SL2.4 or SL3.0 with iTAG2.5 or iTAG3.0 annotations), or relying on microarray data. To our knowledge, the gene expression dataset collected in this study represents the most comprehensive to date, compiling over 10,000 RNA-Seq libraries from five major organs and integrating hundreds of Bioprojects performed worldwide. Moreover, the transcriptomes were processed utilizing the latest genome version (SL4.0) and the updated ITAG4.1c annotation, resulting in greater gene coverage. This extensive dataset enabled us to characterize general gene expression patterns at the organ level, facilitating the identification of genes involved in organ-specific functions. Notably, organ identity has been shown to be the strongest determinant of differential gene expression, surpassing other experimental variables and highlighting the role of developmental processes in shaping transcriptome profiles (Aceituno

et al., 2008). Thus, consistent with previous studies (Li *et al.*, 2024), we found that most tomato genes meet the threshold for expression across all organs. Similar ubiquitous expression patterns have been reported in other plants, including *Linum usitatissimum* (Qi *et al.*, 2023) and *Zea mays* (Huang *et al.*, 2018), where over 50% of genes are expressed across multiple tissues.

Beyond broadly expressed genes, we identified a substantial subset of genes with organ-specific expression that were enriched in biological processes critical for organ function. Our analyses successfully captured known organ-specific genes (Siloto *et al.*, 2006; Martín-Trillo *et al.*, 2011; Ezura *et al.*, 2017; Bizouerne *et al.*, 2021; Bres *et al.*, 2022; Hawar *et al.*, 2022; Aviña-Padilla *et al.*, 2023). Moreover, genes such as *SULTRI;1* and *FER* in roots, *TPD1-l* genes in flowers, *LNG1* and *SIBRC1a* in leaves, stems, and hypocotyls, and ABI TF in seeds were also identified in a study focused on characterizing organ specific expression (Li *et al.*, 2024). The identification of these well-documented markers supports the robustness of our expression threshold standards. Furthermore, the TFs also displayed widespread expression across tomato organs, mirroring findings in *Arabidopsis* (Ranjan *et al.*, 2024). Prior studies in tomato indicate that fewer than 20% of expressed TFs are organ-specific (Rohrmann *et al.*, 2012). Nonetheless, despite their broad expression, variations in TF expression levels across organs highlight the dynamic and context-dependent regulation of transcriptional networks governing organ function.

Transcriptomic data has been extensively used to generate biological network models with the purpose of identifying key candidates for functional genomics analyses. Due to the limited availability of TF-target interaction data existing for tomato, the majority of studies have relied on GCNs to infer regulatory relationships and identify co-regulated gene groups (Fukushima *et al.*, 2012; Koenig *et al.*, 2013; Ichihashi *et al.*, 2014; Arhondakis *et al.*, 2016; Yue *et al.*, 2016; Kim *et al.*, 2017; Zouine *et al.*, 2017; Bizouerne *et al.*, 2021; Kusano *et al.*, 2022; Manosalva

and Vandepoele, 2023; Pirona *et al.*, 2023; Wang *et al.*, 2023a). Notably, the GCNs lack directionality, making it difficult to establish regulatory interactions. Additionally, many rely on correlations such as Pearson coefficients, which fail to capture non-linear relationships (Escorcia-Rodríguez *et al.*, 2023). To address these limitations, we employed GENIE3, a widely used algorithm for reconstructing directed GRNs in plants (Chen *et al.*, 2023; De Clercq *et al.*, 2021; Harrington *et al.*, 2020; Huang *et al.*, 2018; Ranjan *et al.*, 2024; Tu *et al.*, 2020) and other organisms (Huynh-Thu *et al.*, 2010; Huynh-Thu and Geurts, 2019; Cuesta-Astroz *et al.*, 2021; Olivares-Yañez *et al.*, 2021). GENIE3 requires only gene expression data as input, making it particularly suitable for tomato, where TF gene targets remain poorly characterized.

To validate our GRNs, we benchmarked them against available ChIP-Seq data standard networks, employing the AUPR and AUROC curves. This strategy, previously used to assess GRN performance in plants (Brooks *et al.*, 2019; Contreras-López *et al.*, 2022), provides a more centered evaluation of TF-target interactions than alternative methods that utilize gene co-association to biological processes or metabolic pathways (Kim *et al.*, 2017; Orduña *et al.*, 2023). Our analysis determined that a 2% GENIE3 scores threshold—comprising 660,000–800,000 edges—was ideal, aligning with previous GENIE3-based GRN studies in crops, which typically consider networks containing around 1 million edges (Harrington *et al.*, 2020; Huang *et al.*, 2018; Ramírez-González *et al.*, 2018). Notably, the GENIE3-derived GRNs outperformed other tomato networks from public resources such as PlantRegMap (Tian *et al.*, 2020) and other genome-scale biological network models (Kim *et al.*, 2017). Additionally, more than 50% of GENIE3-predicted edges were supported by one or more independent evidence, including cis-regulatory motif binding predictions, further reinforcing the biological relevance of these regulatory connections, as was proven in other networks (De Clercq *et al.*, 2021; Chen *et al.*,

2023). This integration of multiple validation strategies enhances the accuracy and functional significance of inferred GRNs, providing a robust framework for studying transcriptional regulation in tomato. Our analysis revealed that while most genes are broadly expressed across organs, the vast majority of TF-target interactions remain organ-specific. This pattern has been observed in GRNs from other crops (Huang *et al.*, 2018; Ranjan *et al.*, 2024), suggesting that gene expression levels play a relevant role in establishing regulatory interactions underlying organ-specific functions. Notably, we identified a positive correlation between TF connectivity and target conservation across organs. Highly connected TFs (hubs) tend to regulate a similar set of targets in all organs, whereas TFs with fewer connections are more likely to control organ-specific processes. An evolutionary constraint may underlie this phenomenon, as TF-target interactions involving hub genes are more conserved. Disruptions in these interactions are more likely to be deleterious, leading to reduced genetic diversity and slower evolutionary rates among hub TFs. In contrast, tissue-specific TFs, which are less connected, have been described to evolve faster (Mack *et al.*, 2019).

Understanding how TFs initiate gene expression changes in response to various cues and stimuli is crucial for developing new strategies to mitigate stress responses and overcome climate change. By utilizing tomato organ-specific reference GRNs, we can identify biologically relevant interactions and potential regulatory candidates that control gene responses to stimuli. We utilized the fruit-specific GRNs to identify important TF regulators of fruit ripening, including RIN and TAGL1 (Karlova *et al.*, 2014). These TFs were tested against validated target lists, which included genes confirmed by binding studies (Fujisawa *et al.*, 2013; Zhong *et al.*, 2013; Gao *et al.*, 2019) and regulatory studies of RIN-deficient plants (Gao *et al.*, 2019; Ito *et al.*, 2020; Li *et al.*, 2018; Zhao *et al.*, 2018). Our analysis showed significant enrichment between

our GRNs and the experimentally validated targets, supporting the networks' ability to capture in vivo regulatory events. Notably, our networks identified RIN targets such as *FUL1*, which were validated using yeast one-hybrid assays (Fujisawa *et al.*, 2014), as well as essential ripening genes such as *ACS2*, *ACS4*, *E8*, *EXPI*, *PSY*, *NOR*, *PSY* and *CNR*, which were validated using ChIP-PCR (Martel *et al.*, 2011). Similarly, qPCR validation supported TAGL1 targets, including TF *FUL2* (Fujisawa *et al.*, 2014), as well as genes such as *ACS2*, *ETR1*, *ERF2* and *PL* (Itkin *et al.*, 2009). These findings demonstrate our GRNs strong prediction capacity for identifying important regulatory relationships.

Interestingly, RIN and TAGL1 regulatory target genes are extensively connected due to their effect on fruit ripening, but a direct regulation link between both TFs does not exist in the fruit GRN. Our findings indicate that these transcription factors may influence the ripening process via indirect regulation possibly by epistatic synergistic control of ripening-responsive genes as suggested in previous studies (Fujisawa *et al.*, 2014; Jeon *et al.*, 2024). In our fruit ripening GRN, we identified ARF2A and ERF2.E2 as central hubs, which may serve as key regulatory nodes influencing fruit ripening cascades. ARF2A had previously been proposed as a potential control point in the hormonal regulation of ripening (Breitel *et al.*, 2016). The direct gene targets identified in our network are consistent with an analysis of OX-ARF2A plants where the *ETR*, *ACS4*, *AP2A*, *ETR3*, *ETR4*, *NOR*, and *RIN* genes were found as DEGs (Breitel *et al.*, 2016). We recommend testing the binding targets of both ERF2.E2 and ARF2A TFs, by TF-binding analysis such as ChIP-seq to validate the potential key hub effect we found for ripening responsive genes.

On the other hand, as additional evidence, we evaluated the cellular response to ABA since it was one of the ubiquitously enriched biological processes found in our organ specific gene

lists. We detected an important correlation between the *SlABF3* and *SlABF5* TFs with drought responsive genes in addition to classical important genes for ABA signaling such as *PYL/RCAR* transporters, *PP2Cs* phosphatases and protein kinases *SnRK2s* (Fujii *et al.*, 2009). *SlABF3* was found to be able to regulate *SlABF5* and two *PP2C* phosphatases. The direct regulation between these genes was previously found in a Yeast two-hybrid experiment (Chen *et al.*, 2016). A strong relationship of *SlABF5* with drought was observed in the enrichment analysis between the drought responsive transcriptome and the leaf GRN targets and its own expression changes during drought, as reported earlier (Orellana *et al.*, 2010; Wang *et al.*, 2023). The analysis of *ABF3/ABF5* further confirmed their regulatory potential over drought-responsive and ABA-related genes identified in the leaf GRN. These findings highlight the integral role of *SlABF5* in coordinating ABA signaling and drought responses, reinforcing the potential of the GRNs to recapitulate the effect of key TFs on tomato stress responsive regulatory cascades.

Through network analysis, we were able to identify *SlGBF3* TF as a new key hub in the ABA signaling responsive genes network. This TFs was found as a part of a coexpression module of drought responsive genes in tomato (Bortolami *et al.*, 2024), and we found that it is an homolog to *AtGBF3*, reported in Arabidopsis as key regulator of drought sensitivity/tolerance and to genes involved in ABA signaling cascade (Ramegowda *et al.*, 2017). Moreover, in kiwifruit, an homolog of *GBF3* was found to be important in vitamin C metabolism, a regulatory cascade also modulated by ABA (Liu *et al.*, 2022). The GRNs of *SlGBF3* revealed a potential to regulate multiple *PP2C* genes, and three ABFs TFs consistently and ubiquitously on tomato, thus revealing a strong potential to control ABA regulatory cascades (Fujii *et al.*, 2009; Korwin Krukowski *et al.*, 2023; Park *et al.*, 2009). We hypothesize that *SlGBF3* functions as a key regulator of ABA-related genes and may be closely linked to drought-responsive pathways in

leaves and potentially other tomato organs. This suggests a broader role for *S/GBF3* in integrating ABA signaling with environmental stress responses. Further analysis, including functional validation is required to confirm its regulatory function and elucidate its contribution to drought adaptation mechanisms.

The *Solanum lycopersicum* organ-specific GRNs, which are accessible via the TomViz platform in the tomato GRNs app in PlantaeViz platform(Santiago *et al.*, 2024), provide comprehensive insights into TF-target relationships and organ-specific regulatory pathways in tomato. This resource outperforms other web-based tools by excelling in gene coverage, dataset integration, and specificity of regulatory cascades. In contrast, existing tools primarily rely on GCNs and are limited to a narrow set of genes, often focusing predominantly on fruit tissue. The organ-specific reference GRNs web app in TomViz can be considered a relevant tool for tomato research community, since it integrates accessibility and depth analysis, offering a platform that expands the understanding of tomato gene regulation across various developmental stages, conditions, and varieties, thereby paving the way for novel discoveries in tomato biology.

In this section, our integrated omic analysis produced a valuable resource for the investigation of tomato regulatory cascades. We examined known regulatory cascades of relevant biological processes to demonstrate the potential of organ-specific GRNs to predict TF-target interactions validated *in vivo*, since prior networks, were limited by deficient gene coverage and a lack of enrichment for regulatory relationships, as shown in this study. By using the organ-specific GRNs as a baseline for tomato regulatory cascades, we can now concentrate on understanding the regulatory mechanisms that govern sulfate deficiency responses in tomato.

2. To identify candidate TFs that are central regulators of the sulfate deficiency response in *S. lycopersicum*.

Most of the existing knowledge on sulfate deficiency gene expression response in plants has been derived from studies in *Arabidopsis thaliana*, with relatively few investigations focusing on crop species (Watanabe and Hoefgen, 2019, Preprint; Fernández *et al.*, 2024). In tomato, the gene expression changes under sulfate deficiency were explored by Canales *et al.* (Canales *et al.*, 2020) who identified a group of TFs that could be potential key regulators, based on regulatory evidence from *Arabidopsis* pathways. Using the reanalyzed transcriptomes, we generated context-specific GRNs for sulfate deficiency in tomato roots and leaves. The GRNs for roots are smaller due to a reduced number of DEGs lists; in contrast, the GRNs for leaves encompass a broader set of nodes, indicating a more complex regulatory cascade triggered by sulfate deficiency, as demonstrated by Canales *et al.* (2020). Our findings suggest that the 3–4-week transcriptome gap has no effect on the main regulatory pathways or the primary TFs influencing each organ's response to sulfate deficiency. This result demonstrates that, despite most genes are not shared between different time points, the key TFs controlling the regulatory cascades upstream remain conserved.

We used our context-specific sulfate deficiency GRNs for tomato roots and leaves to identify a new group of key regulatory TFs that could be controlling the sulfate deficiency transcriptome. The analysis was based on network properties, influentiality analysis, quantified expression, and the direct regulation of putative targets analysis in conjunction with approximations to detect masters regulatory TFs in other nutrient deficiency studies (Alvarez *et al.*, 2014). The final candidate selection prioritized TFs with homologs with verified roles in sulfur metabolism, transport, amino acid catabolism, and/or growth regulation pathways. Notably, the functions of

many tomato TFs remain uncharacterized. To address this, we conducted enrichment analysis of biological processes associated with their target genes and include information about their homologs in Arabidopsis to provide further insights into their potential functions.

In the leaves GRN, we identified the TF *SlZAT11* (Soly05g054650), an ortholog of *AtZAT11* and *AtZAT18* (AT3G53600 and AT2G37430). *AtZAT18* has been implicated in drought stress and ROS metabolism (Yin *et al.*, 2017), and it is also reported as a positive regulator of defense responses and a negative regulator of auxin and cytokinin signaling, thereby influencing plant growth (Li *et al.*, 2022). Similarly, *AtZAT11* is associated with growth regulation and nickel responses (Liu *et al.*, 2014) and is activated during salt stress and pathogen infections (Mittler *et al.*, 2006). These findings suggest that *SlZAT11* may influence immune responses and growth repression under sulfate deficiency. The TF *SlWRKY71* (Soly02g071130), was found linked to auxin-dependent axillary bud development and lateral branch growth (Yang *et al.*, 2024) and shares significant similarity with *AtWRKY71* (Kumar *et al.*, 2023), which is involved in reproductive development and early senescence in Arabidopsis (Yu *et al.*, 2016, 2021). Possibly, the *SlWRKY71* may partially explain the early senescence expected in tomato plants under sulfate deficiency. We may consider that the two leaf candidate TFs may have a strong

In the root GRN, we identified *SlHHO* (Soly05g009720), found to be involved in the regulatory cascades of phosphate and nitrate starvation responses (Marro *et al.*, 2022). Its homolog, *AtNIGT1.2* (AT1G68670), modulates phosphate and nitrate uptake and regulates nitrate-responsive genes (Wang *et al.*, 2020). These findings indicate that *SlHHO* may serve as a connection between sulfate deficiency and phosphate deficiency response pathways. The transcription factor *SlKUA1* (Soly08g078340), was classified as a master transcriptional

regulator during virus infection (Aviña-Padilla *et al.*, 2022), and is an homolog of *AtKUA1* indicated as a regulator of cell development in leaves, a repressor of peroxidase transcription, thus involved in ROS balance, and an activator of other stress-responsive TFs (Kwon *et al.*, 2013; Liu *et al.*, 2018). Furthermore, this TF was suggested as a possible regulator of sulfate deficiency response in tomato (Canales *et al.*, 2020), pointing out to have a significant role in the regulation of this response.

The TFs shared between root and leaf GRNs emerge as potential plant-wide master regulators of the sulfate deficiency response in tomato. These TFs were chosen as the top-scoring regulators in both networks, highlighting their key significance in regulatory cascades associated with sulfate deficiency. The *S/TGA-1* (Solyc04g072460), an ortholog of multiple *AtTGA* TFs, has been reported to be upregulated in tomato plants during drought, salt, and heat stress (Li *et al.*, 2015). The TGA family is well known for its role in nutrient starvation regulatory cascades and in systemic acquired resistance pathways (Alvarez *et al.*, 2014; Sun *et al.*, 2018; Yildiz *et al.*, 2023). The *S/SCL14* (Solyc10g086530) is a homolog of *AtSCL14*, a member of the GRAS/SCARECROW TF family in Arabidopsis (AT1G07530 and AT3G46600). GRAS TFs are involved in key cellular pathways, including gibberellin signaling, shoot meristem maintenance, and growth responses (Stuurman *et al.*, 2002; Tian *et al.*, 2004). The *AtSCL14* is involved in xenobiotic detoxification regulatory cascades and is known to interact with TGA TFs (Fode *et al.*, 2008; D'alessandro *et al.*, 2018). Due to their interaction in Arabidopsis, the roles of *S/SCL14* and *S/TGA-1* TFs may be correlated, and both may be able to affect stress response pathways that intersect with sulfate deficiency responses, potentially contributing to the activation of stress pathways observed under sulfur-limited conditions.

The Solyc01g006650, or ETHYLENE LIMITATION LIKE 3 (*SIEIL3*), is a TF homolog to *AtEIL3*, also called SLIM1 (SULFUR LIMITATION 1). This TF is known to function as an activator of sulfate deficiency responsive genes (Maruyama-Nakashita *et al.*, 2006). The *AtEIL3* function was discovered in mutant *A. thaliana* plants that showed a 60% reduction of high-affinity sulfate uptake transporters (*SULTR1;1*, *SULTR1;2*, and *SULTR4;2*) under low sulfate conditions; moreover, this TF can regulate more than 70 genes during sulfate deficiency (Maruyama-Nakashita *et al.*, 2006; Kawashima *et al.*, 2011). The *SIEIL3* has been proposed as a master regulator of sulfate deficiency by Canales *et al.* (Canales *et al.*, 2020) and is further supported by our systems biology analysis of shared regulatory cascades in sulfate-deficient plants (Fernández *et al.*, 2024).

The TARGET protocol enables rapid identification of TF targets by transiently expressing TFs in protoplasts and analyzing gene expression changes (Bargmann *et al.*, 2013, Preprint). Originally developed for *Arabidopsis thaliana*, where it has been proven as a valuable tool for generating GRNs (Brooks *et al.*, 2019; Alvarez *et al.*, 2020; Li *et al.*, 2020; Safi *et al.*, 2021). Nonetheless, the TARGET protocol has only been applied to *Oryza sativa* and *Catharanthus roseus* (Guedes *et al.*, 2022; Shanks *et al.*, 2022). In this study, we adapted TARGET protocol for the first time to study tomato regulatory cascades and identify the direct regulatory targets of *SIEIL3*. Our findings revealed a strong overlap between genes responsive to sulfate deficiency, the GRN-predicted targets, and TARGET-validated interactions, confirming *SIEIL3* as a central regulator of sulfate deficiency responses. These results demonstrate the feasibility of TARGET in tomato and highlights its potential for guiding crop improvement strategies under nutrient stress.

We found that *S/EIL3* ranked highest in root and leaf GRN analyses and showed functional similarities with its *Arabidopsis* homolog, *AtSLIM1*. Ontology analysis further linked its targets to sulfur deficiency markers, reinforcing its regulatory role. The integration of GRN predictions with TARGET validation provided robust evidence that *S/EIL3* directly regulates key genes involved in sulfate deficiency responses. Based on this comprehensive support, *S/EIL3* was selected as the most promising master regulator of sulfate deficiency in tomato and prioritized for functional validation.

3. To experimentally validate the function of a central TF candidate in the regulation of plant growth under sulfate deficiency.

Sulfate deficiency in plants has been shown to cause delayed development, chlorosis, and reduced yields (Hawkesford, 2000; Maruyama-Nakashita, 2017, Preprint; Nakai and Maruyama-Nakashita, 2020, Preprint). We analyzed the phenotype of *Arabidopsis* seedlings overexpressing *S/EIL3*; Notably, the OX-*S/EIL3* plants outgrew wild-type (WT) plants under both control and sulfate-deficient conditions during the observation period (two weeks after sowing). As discussed earlier, the *S/EIL3* is homologous to *Arabidopsis* SLIM1 TF, previous studies have shown that *slim1* mutants exhibit significantly reduced root growth, whereas overexpression of SLIM1 rescues this phenotype in *Arabidopsis* and rice plants (Maruyama-Nakashita *et al.*, 2006). Possibly the OX-*S/EIL3* plants develop the inverse phenotype of *slim1* mutants, accelerating plant growth. Similarly, the SLIM1 overexpression lines reported by Apodiakou *et al.* (Apodiakou *et al.*, 2024) demonstrated accelerated growth accounted for larger foliar area, also revealed premature senescence, as indicated by chlorotic leaf tips and altered chlorophyll and

anthocyanin levels. Many of these symptoms were not observed in our OX plants, probably since our observations were made only during two weeks after sowing; Nevertheless, we consider that overexpressed *S/EIL3* triggers a similar accelerated growth effect that was also present in OX-SLIM1 plants. We hypothesize that overexpressed *S/EIL3* prevents growth retardation phenotypes in these plants by suppressing the sense of sulfate deficiency, at least in the early stages.

The OX-*S/EIL3* lines also exhibited enhanced sulfate uptake compared to WT plants, as indicated by higher sulfur content under normal sulfate conditions. WT plants typically induce *SULTRs* transporters expression during sulfate deficiency (Maruyama-Nakashita *et al.*, 2004); conversely, the *slim1* mutants exhibit impaired transporter induction, leading to a 30% reduction in sulfur content (Maruyama-Nakashita *et al.*, 2006; Kawashima *et al.*, 2011). Contrary to the expected, Apodiakou *et al.* (Apodiakou *et al.*, 2024) found that SLIM1 overexpression under sulfate-sufficient media did not significantly affect total sulfur content; an explanation of this effect probably because the control of SULTR transporters and other molecules activated during sulfate deficiency is influenced by additional TFs such as *AtEIL1*, which also responds to sulfate deficiency and acts concomitantly with SLIM1 (Dietzen *et al.*, 2020). Our findings suggest that the OX-*S/EIL3* plants could mimic a sulfate deficiency treatment by activating regulatory pathways associated with sulfate uptake, thereby explaining the increase in sulfur levels. However, further studies are necessary to confirm this hypothesis and elucidate the underlying mechanisms.

To confirm our hypothesis and validate the function of *S/EIL3* as a master regulator of sulfate deficiency gene expression responses we performed an RNA-seq analysis of OX-*S/EIL3* plants. We observed a higher accumulation of DEG genes due to genotype much higher than the DEG

due to sulfate deficiency treatment, in addition to the high enrichment of our study gene lists in comparison to other sulfate deficiency treatments in *Arabidopsis* (Maruyama-Nakashita *et al.*, 2006; Dietzen *et al.*, 2020) and the OX-SLIM1 plants (Apodiakou *et al.*, 2024) which led us to assume that the overexpression of *S/EIL3* manage to imitate a sulfur deficiency treatment and its able to exacerbate this response, the same trend that we observed in the OX-*S/EIL3* plants phenotype.

The TFs SLIM1 and *S/EIL3* were identified in a phylogenetic analysis of 1,051 EIN3/EIL genes from 120 species, which revealed *S/EIL3* as a closely related homolog of SLIM1 (Fernández *et al.*, 2024). However, *S/EIL3* exhibits distinct regulatory behavior, as its expression is upregulated by sulfate deficiency (Canales *et al.*, 2020), in contrast to SLIM1, whose transcript levels and subcellular localization remain unaffected by sulfate availability (Maruyama-Nakashita *et al.*, 2006). Our network analysis of *S/EIL3* binding predictions demonstrated that *S/EIL3* and SLIM1 share highly conserved regulatory pathways, since *S/EIL3* is predicted to bind multiple of its regulatory targets found by overexpression, many of which were also identified as SLIM1 targets (Maruyama-Nakashita *et al.*, 2006; Piotrowska *et al.*, 2022; Rakpenthai *et al.*, 2022). These findings demonstrate the accuracy of our tomato GRNs in the prediction of sulfate deficiency regulatory cascades and highlight the conserved nature of the regulatory mechanisms under the control of the *S/EIL3* and the SLIM1 TFs. While our analysis was conducted in *Arabidopsis* plants instead of tomato, the use of this model system is justified, as we demonstrated in Fernandez et al. (2024) that *S/EIL3* and its *Arabidopsis* homolog share over 88% sequence similarity in their DNA-binding domains. Nevertheless, to conclusively confirm *S/EIL3*'s function in tomato, further validation to demonstrate the regulatory control of TF *S/EIL3* in tomato, we recommend studying knockout experiments in tomato plants or by

directly assessing S/EIL3's regulatory interactions with its target genes via TF-binding assays such as ChIP-seq or TARGET (Bargmann *et al.*, 2013, Preprint).

The GO analysis of DEGs on OX-S/EIL3 plants revealed significant enrichment in diverse biological processes, revealing that this TF regulatory effect is not limited to sulfate metabolism control, regulatory cascades involving stress response pathways, including plant immune responses mediated by salicylic acid and ABA may indicate an active survival strategy during sulfate deficiency, potentially linked to the observed growth inhibition phenotype. The processes of growth regulation, cell wall metabolism, and senescence all highlight the complicated limitations that plants face during nutrient starvation stress (Zhang *et al.*, 2020). The integration of sulfate-specific responses with broader metabolic and stress pathways may be responsible for the altered growth rates and eventual repression observed during sulfate deprivation observed in sulfate starved plants (Canales *et al.*, 2020; Dietzen *et al.*, 2020; Fernández *et al.*, 2024).

Model of regulatory effect of TFs during sulfate deficiency in tomato

We developed a model to elucidate the role of key TF regulators in the sulfate deficiency response of *Solanum lycopersicum*. Our findings show that most of the TFs exhibit sulfate-specific regulatory potential, with a high percentage of their target genes found as differentially expressed during sulfate deficiency. Notably, the S/EIL3 emerged as the most prominent and specific regulator in this response.

In order to further explore its function, we generated OX-S/EIL3 Arabidopsis plants, which demonstrated a phenotype of accelerated growth and increased sulfate accumulation, accompanied by activation of sulfate deficiency marker genes. Analysis of the genes in these

plants identified key regulators potentially driving the observed phenotype. The TFs MYB1, MYB60, and NAC1, known to mediate auxin signaling and promote plant growth (Yang *et al.*, 2020), were significantly upregulated. Additionally, NAC016 and NAC046, associated with senescence regulation in *Arabidopsis* (Kim *et al.*, 2016), as well as WRKY70–75, known regulators of root development in tomato (Rosado *et al.*, 2022), were also induced. Furthermore, AIR12 and SHY2, which play essential roles in auxin response and root development (Gibson and Todd, 2015), support SIEIL3's involvement in growth regulation. The induction of PIF3, a TF involved in photosynthesis and reproductive development (Liu *et al.*, 2013; Rosado *et al.*, 2016), further supports its role in developmental regulation. Additionally, genes involved in sulfate metabolism—ATPSs, APRs, APSKs, and sulfate-responsive genes such as SDIs, LSUs, GGCC, and Chac—were found as DEG in the OX-SIEIL3 plants, consistent with their established roles as sulfate deficiency markers in *Arabidopsis* and other crops (Fernández *et al.*, 2024).

These findings support our hypothesis that TFs such as SIEIL3 regulate sulfur metabolism while also influencing broader biological processes, which are likely to contribute to the phenotypic growth changes observed in our overexpressing plants. However, further analysis will be necessary to determine whether these important physiological changes are caused directly by the SIEIL3 effect in the control of plant growth and stress responses. Additionally, we do not rule out the possibility that the other important TFs found in this research could also play a role in coordinating sulfate deficiency gene expression and associated phenotypic responses.

VIII. CONCLUSION

This investigation illustrates the substantial potential of utilizing the extensive omics data stored in online repositories to enhance our comprehension of non-model organisms. By meticulously evaluating and interpreting data generated in a wide set of conditions, bioinformatics can detect crucial insights about the internal regulation of cells and find resources to enrich the scientific knowledge for these species. Specifically, the generation of GRNs is a valuable tool for deciphering regulatory cascades, giving light on the intricate signaling cascades that govern critical biological processes. Our findings demonstrate that GRNs can be positively enhanced by the integration of multiple omic datasets and demonstrated the power of GRNs to find molecular regulators in charge of responses to biologically relevant problems such as sulfate deficiency and identifying important regulators with potential implications in crop development. Notably, TFs such as *S/EIL3* function as crucial control points in signaling cascades, because the validated role of EIL3 in Arabidopsis and the potential effects discovered in this investigation for tomato plants *S/EIL3* is predicted to perform equivalent regulatory functions for other major crop species. Additionally, given its impact on plant growth and sulfate uptake, we believe that *S/EIL3* plays an important role in improving crop resilience and nutritional quality. As future directions, its necessary improve and validate the answers provided by GRNs, with experimental verification of the key TFs and the target genes identified in this study, possibly by employing loss-of-function mutants or determining the TFS binding sites in vivo, The knowledge generated by the analysis of non-model plant GRNs could be used to develop techniques to improve crop performance in a variety of environments, paving the way for more robust and productive agricultural systems.

IX. REFERENCES

- Aarabi F, Kusajima M, Tohge T, et al.** 2016. *Sulfur deficiency-induced repressor proteins optimize glucosinolate biosynthesis in plants.*
- Abramoff MD, Magalhães PJ, Ram SJ.** 2004. ImageJ. *Biophotonics International* **7**, 36–41.
- Abuqamar S, Luo H, Laluk K, Mickelbart M V., Mengiste T.** 2009. Crosstalk between biotic and abiotic stress responses in tomato is mediated by the AIM1 transcription factor. *The Plant Journal* **58**, 347–360.
- Aceituno FF, Moseyko N, Rhee SY, Gutiérrez RA.** 2008. The rules of gene expression in plants: Organ identity and gene body methylation are key factors for regulation of gene expression in *Arabidopsis thaliana*. *BMC Genomics* **9**, 1–14.
- Albert R.** 2005. Scale-free networks in cell biology. *Journal of Cell Science* **118**, 4947–4957.
- Alhendawi RA, Kirkby EA, Pilbeam DJ.** 2005. Evidence That Sulfur Deficiency Enhances Molybdenum Transport in Xylem Sap of Tomato Plants. *Journal of Plant Nutrition* **28**, 1347–1353.
- Alvarez JM, Riveras E, Vidal EA, et al.** 2014. Systems approach identifies TGA1 and TGA4 transcription factors as important regulatory components of the nitrate response of *Arabidopsis thaliana* roots. *Plant Journal* **80**, 1–13.
- Alvarez JM, Schinke AL, Brooks MD, Pasquino A, Leonelli L, Varala K, Safi A, Krouk G, Krapp A, Coruzzi GM.** 2020. Transient genome-wide interactions of the master transcription factor NLP7 initiate a rapid nitrogen-response cascade. *Nature Communications* **11**.
- Apodiakou A, Alseekh S, Hoefgen R, Whitcomb SJ.** 2024. Overexpression of SLIM1 transcription factor accelerates vegetative development in *Arabidopsis thaliana*. *Frontiers in Plant Science* **15**, 1327152.
- Arhondakis S, Bitá CE, Perrakis A, Manioudaki ME, Krokida A, Kaloudas D, Kalaitzis P, Pezzotti M.** 2016. In silico transcriptional regulatory networks involved in tomato fruit ripening. *Frontiers in Plant Science* **7**, 195142.
- Aviña-Padilla K, Zambada-Moreno O, Herrera-Oropeza GE, Jimenez-Limas MA, Abrahamian P, Hammond RW, Hernández-Rosales M.** 2022. Insights into the Transcriptional Reprogramming in Tomato Response to PSTVd Variants Using Network Approaches. *International Journal of Molecular Sciences* **23**, 5983.

Aviña-Padilla K, Zambada-Moreno O, Jimenez-Limas MA, Hammond RW, Hernández-Rosales M. 2023. Dynamic co-expression modular network analysis of bHLH transcription factors regulation in the potato spindle tuber viroid-tomato pathosystem. *bioRxiv*, 2023.11.10.566618.

Bae SH, Park J, Park SJ, Han J, Oh JH. 2021. Transcriptome data for tissue-specific genes in four reproductive organs at three developmental stages of micro-tom tomato. *Data in Brief* **34**, 106715.

Bargmann BOR, Marshall-Colon A, Efroni I, Ruffel S, Birnbaum KD, Coruzzi GM, Krouk G. 2013. *TARGET: A transient transformation system for genome-wide transcription factor target discovery.* Oxford University Press.

Van Bel M, Silvestri F, Weitz EM, Kreft L, Botzki A, Coppens F, Vandepoele K. 2022. PLAZA 5.0: extending the scope and power of comparative and functional genomics in plants. *Nucleic Acids Research* **50**, D1468–D1474.

Berardini TZ, Reiser L, Li D, Mezheritsky Y, Muller R, Strait E, Huala E. 2015. The arabidopsis information resource: Making and mining the “gold standard” annotated reference plant genome. *genesis* **53**, 474–485.

Bielecka M, Watanabe M, Morcuende R, Scheible W-R, Hawkesford MJ, Hesse H, Hoefgen R. 2015. Transcriptome and metabolome analysis of plant sulfate starvation and resupply provides novel information on transcriptional regulation of metabolism associated with sulfur, nitrogen and phosphorus nutritional responses in *Arabidopsis*. *Frontiers in Plant Science* **5**.

Bizouerne E, Buitink J, Vu BL, Vu JL, Esteban E, Pasha A, Provart N, Verdier J, Leprince O. 2021. Gene co-expression analysis of tomato seed maturation reveals tissue-specific regulatory networks and hubs associated with the acquisition of desiccation tolerance and seed vigour. *BMC Plant Biology* **21**, 1–23.

Bonnot T, Martre P, Hatte V, *et al.* 2020. Omics Data Reveal Putative Regulators of Einkorn Grain Protein Composition under Sulfur Deficiency. *Plant Physiology* **183**, 501–516.

Bortolami G, de Werk TA, Larter M, Thonglim A, Mueller-Roeber B, Balazadeh S, Lens F. 2024. Integrating gene expression analysis and ecophysiological responses to water deficit in leaves of tomato plants. *Scientific Reports* 2024 14:1 **14**, 1–18.

Bray NL, Pimentel H, Melsted P, Pachter L. 2016. Near-optimal probabilistic RNA-seq quantification. *Nature Biotechnology* **34**, 525–527.

- Breitel DA, Chappell-Maor L, Meir S, et al.** 2016. AUXIN RESPONSE FACTOR 2 Intersects Hormonal Signals in the Regulation of Tomato Fruit Ripening. *PLOS Genetics* **12**, e1005903.
- Bres C, Petit J, Reynoud N, Brocard L, Marion D, Lahaye M, Bakan B, Rothan C.** 2022. The SISHN2 transcription factor contributes to cuticle formation and epidermal patterning in tomato fruit. *Molecular Horticulture* **2**, 1–20.
- Brooks MD, Cirrone J, Pasquino A V., et al.** 2019. Network Walking charts transcriptional dynamics of nitrogen signaling by integrating validated and predicted genome-wide interactions. *Nature Communications* **10**.
- Canales J, Uribe F, Henríquez-Valencia C, Lovazzano C, Medina J, Vidal EA.** 2020. Transcriptomic analysis at organ and time scale reveals gene regulatory networks controlling the sulfate starvation response of *Solanum lycopersicum*. *BMC Plant Biology* **20**.
- Canene-Adams K, Campbell JK, Zaripheh S, Jeffery EH, Erdman JW.** 2005. *Symposium: Relative Bioactivity of Functional Foods and Related Dietary Supplements The Tomato As a Functional Food 1,2*.
- Cantalapiedra CP, Hernández-Plaza A, Letunic I, Bork P, Huerta-Cepas J.** 2021. eggNOG-mapper v2: Functional Annotation, Orthology Assignments, and Domain Prediction at the Metagenomic Scale. *Molecular Biology and Evolution* **38**, 5825–5829.
- Cao Y, Ma C, Yu H, Tan Q, Dhankher OP, White JC, Xing B.** 2023. The role of sulfur nutrition in plant response to metal(loid) stress: Facilitating biofortification and phytoremediation. *Journal of Hazardous Materials* **443**, 130283.
- Castro-Mondragon JA, Riudavets-Puig R, Rauluseviciute I, et al.** 2022. JASPAR 2022: the 9th release of the open-access database of transcription factor binding profiles. *Nucleic Acids Research* **50**, D165–D173.
- Chai LE, Loh SK, Low ST, Mohamad MS, Deris S, Zakaria Z.** 2014. A review on the computational approaches for gene regulatory network construction. *Computers in Biology and Medicine* **48**, 55–65.
- Chen Y, Guo Y, Guan P, et al.** 2023. A wheat integrative regulatory network from large-scale complementary functional datasets enables trait-associated gene discovery for crop improvement. *Molecular Plant* **16**, 393–414.
- Chen P, Sun YF, Kai W Bin, Liang B, Zhang YS, Zhai XW, Jiang L, Du YW, Leng P.** 2016. Interactions of ABA signaling core components (SIPYLs, SIPP2Cs, and SISnRK2s) in tomato (*Solanum lycopersicon*). *Journal of Plant Physiology* **205**, 67–74.

Chen S, Zhou Y, Chen Y, Gu J. 2018. fastp: an ultra-fast all-in-one FASTQ preprocessor. *Bioinformatics* **34**, i884–i890.

Chong L, Xu R, Huang P, Guo P, Zhu M, Du H, Sun X, Ku L, Zhu JK, Zhu Y. 2022. The tomato OST1–VOZ1 module regulates drought-mediated flowering. *The Plant Cell* **34**, 2001–2018.

De Clercq I, Van de Velde J, Luo X, Liu L, Storme V, Van Bel M, Pottier R, Vaneechoutte D, Van Breusegem F, Vandepoele K. 2021. Integrative inference of transcriptional networks in *Arabidopsis* yields novel ROS signalling regulators. *Nature Plants* 2021 7:4 7, 500–513.

Clough SJ, Bent AF. 1998. Floral dip: a simplified method for *Agrobacterium*-mediated transformation of *Arabidopsis thaliana*. *The Plant Journal* **16**, 735–743.

Contreras-López O, Vidal EA, Riveras E, et al. 2022. Spatiotemporal analysis identifies ABF2 and ABF3 as key hubs of endodermal response to nitrate. *Proceedings of the National Academy of Sciences of the United States of America* **119**, e2107879119.

Coppa E, Vigani G, Aref R, Savatin D, Bigini V, Hell R, Astolfi S. 2023. Differential modulation of Target of Rapamycin activity under single and combined iron and sulfur deficiency in tomato plants. *The Plant Journal* **115**, 127–138.

Courbet G, D’oria A, Maillard A, et al. 2021. Comparative omics analysis of brassica napus roots subjected to six individual macronutrient deprivations reveals deficiency-specific genes and metabolomic profiles. *International Journal of Molecular Sciences* **22**, 11679.

Courbet G, Gallardo K, Vigani G, Brunel-Muguet S, Trouverie J, Salon C, Ourry A. 2019. Disentangling the complexity and diversity of crosstalk between sulfur and other mineral nutrients in cultivated plants. *Journal of Experimental Botany* **70**, 4183–4196.

Courbier S, Snoek BL, Kajala K, Li L, Van Wees SCM, Pierik R. 2021. Mechanisms of far-red light-mediated dampening of defense against *Botrytis cinerea* in tomato leaves. *Plant Physiology* **187**, 1250–1266.

Cuesta-Astroz Y, Gischkow Rucatti G, Murgas L, SanMartín CD, Sanhueza M, Martín AJM. 2021. Filtering of Data-Driven Gene Regulatory Networks Using *Drosophila melanogaster* as a Case Study. *Frontiers in Genetics* **12**.

D’alessandro S, Ksas B, Havaux M. 2018. Decoding β -Cyclocitral-Mediated Retrograde Signaling Reveals the Role of a Detoxification Response in Plant Tolerance to Photooxidative Stress. *The Plant Cell* **30**, 2495–2511.

Dietzen C, Koprivova A, Whitcomb SJ, Langen G, Jobe TO, Hoefgen R, Kopriva S. 2020. The transcription factor EIL1 participates in the regulation of sulfur-deficiency response. *Plant Physiology* **184**, 2120–2136.

- Ding X, Zhang D, Gu D, Li Z, Liang H, Zhu H, Jiang Y, Duan X.** 2022. The histone H3K27 demethylase SIJMJ4 promotes dark- and ABA-induced leaf senescence in tomato. *Horticulture Research* **9**.
- Dixit SK, Gupta A, Fatima U, Senthil-Kumar M.** 2019. AtGBF3 confers tolerance to *Arabidopsis thaliana* against combined drought and *Pseudomonas syringae* stress. *Environmental and Experimental Botany* **168**, 103881.
- Dobin A, Davis CA, Schlesinger F, Drenkow J, Zaleski C, Jha S, Batut P, Chaisson M, Gingeras TR.** 2013. STAR: ultrafast universal RNA-seq aligner. *Bioinformatics* **29**, 15–21.
- Doidy J, Li Y, Neymotin B, Edwards MB, Varala K, Gresham D, Coruzzi GM.** 2016. ‘Hit-and-Run’ transcription: De novo transcription initiated by a transient bZIP1 ‘hit’ persists after the ‘run’. *BMC Genomics* **17**.
- Dolgikh VA, Pukhovaya EM, Zemlyanskaya E V.** 2019. Shaping Ethylene Response: The Role of EIN3/EIL1 Transcription Factors. *Frontiers in Plant Science* **10**.
- Du M, Zhao J, Tzeng DTW, et al.** 2017. MYC2 orchestrates a hierarchical transcriptional cascade that regulates jasmonate-mediated plant immunity in tomato. *Plant Cell* **29**, 1883–1906.
- Earley KW, Haag JR, Pontes O, Opper K, Juehne T, Song K, Pikaard CS.** 2006. Gateway-compatible vectors for plant functional genomics and proteomics. *The Plant Journal* **45**, 616–629.
- Emms DM, Kelly S.** 2019. OrthoFinder: Phylogenetic orthology inference for comparative genomics. *Genome Biology* **20**, 1–14.
- Escorcia-Rodríguez JM, Gaytan-Nuñez E, Hernandez-Benitez EM, Zorro-Aranda A, Tello-Palencia MA, Freyre-González JA.** 2023. Improving gene regulatory network inference and assessment: The importance of using network structure. *Frontiers in Genetics* **14**, 1143382.
- Ezura K, Ji-Seong K, Mori K, Suzuki Y, Kuhara S, Ariizumi T, Ezura H.** 2017. Genome-wide identification of pistil-specific genes expressed during fruit set initiation in tomato (*Solanum lycopersicum*). *PLoS ONE* **12**.
- Fernández JD, Miño I, Canales J, Vidal EA.** 2024. Current understanding of gene regulatory networks underlying the sulfate deficiency response in plants. *Journal of Experimental Botany* doi: 10.1093/JXB/ERA051.
- Fernandez-Pozo N, Menda N, Edwards JD, et al.** 2015. The Sol Genomics Network (SGN)—from genotype to phenotype to breeding. *Nucleic Acids Research* **43**, D1036–D1041.

Fode B, Siemsen T, Thurow C, Weigel R, Gatz C. 2008. The Arabidopsis GRAS Protein SCL14 Interacts with Class II TGA Transcription Factors and Is Essential for the Activation of Stress-Inducible Promoters. *The Plant Cell* **20**, 3122–3135.

Forieri I, Sticht C, Reichelt M, Gretz N, Hawkesford MJ, Malagoli M, Wirtz M, Hell R. 2017. System analysis of metabolism and the transcriptome in *Arabidopsis thaliana* roots reveals differential co-regulation upon iron, sulfur and potassium deficiency. *Plant, Cell & Environment* **40**, 95–107.

Frerigmann H. 2016. Glucosinolate Regulation in a Complex Relationship – MYC and MYB – No One Can Act Without Each Other. *Advances in Botanical Research* **80**, 57–97.

Fujii H, Chinnusamy V, Rodrigues A, Rubio S, Antoni R, Park SY, Cutler SR, Sheen J, Rodriguez PL, Zhu JK. 2009. In vitro reconstitution of an abscisic acid signalling pathway. *Nature* 2009 462:7273 **462**, 660–664.

Fujisawa M, Nakano T, Ito Y. 2011. Identification of potential target genes for the tomato fruit-ripening regulator RIN by chromatin immunoprecipitation. *BMC Plant Biology* **11**.

Fujisawa M, Nakano T, Shima Y, Ito Y. 2013. A Large-Scale Identification of Direct Targets of the Tomato MADS Box Transcription Factor RIPENING INHIBITOR Reveals the Regulation of Fruit Ripening. *The Plant Cell* **25**, 371–386.

Fujisawa M, Shima Y, Nakagawa H, Kitagawa M, Kimbara J, Nakano T, Kasumi T, Ito Y. 2014. Transcriptional Regulation of Fruit Ripening by Tomato FRUITFULL Homologs and Associated MADS Box Proteins. *The Plant Cell* **26**, 89–101.

Fukushima A, Nishizawa T, Hayakumo M, Hikosaka S, Saito K, Goto E, Kusano M. 2012. Exploring Tomato Gene Functions Based on Coexpression Modules Using Graph Clustering and Differential Coexpression Approaches . *Plant Physiology* **158**, 1487–1502.

Gao C, Ju Z, Li S, Zuo J, Fu D, Tian H, Luo Y, Zhu B. 2013. Deciphering Ascorbic Acid Regulatory Pathways in Ripening Tomato Fruit Using a Weighted Gene Correlation Network Analysis Approach. *Journal of Integrative Plant Biology* **55**, 1080–1091.

Gao Y, Zhu N, Zhu X, et al. 2019. Diversity and redundancy of the ripening regulatory networks revealed by the fruitENCODE and the new CRISPR/Cas9 CNR and NOR mutants. *Horticulture Research* **6**.

Gascuel Q, Diretto G, Monforte AJ, Fortes AM, Granell A. 2017. Use of natural diversity and biotechnology to increase the quality and nutritional content of tomato and grape. *Frontiers Media S.A.*

Gibson SW, Todd CD. 2015. Arabidopsis AIR12 influences root development. *Physiology and Molecular Biology of Plants* **21**, 479–489.

- Grant CE, Bailey TL, Noble WS.** 2011. FIMO: Scanning for occurrences of a given motif. *Bioinformatics* **27**, 1017–1018.
- Guedes JG, Leitão C, Meireles C, Duarte P, Sottomayor M.** 2022. TARGETing Transcriptional Regulation in the Medicinal Plant *Catharanthus roseus*. *Methods in Molecular Biology* **2505**, 191–202.
- Hao Y, Hu G, Breitel D, Liu M, Mila I, Frasse P, Fu Y, Aharoni A, Bouzayen M, Zouine M.** 2015. Auxin Response Factor SIARF2 Is an Essential Component of the Regulatory Mechanism Controlling Fruit Ripening in Tomato. *PLOS Genetics* **11**, e1005649.
- Haque S, Ahmad JS, Clark NM, Williams CM, Sozzani R.** 2019. Computational prediction of gene regulatory networks in plant growth and development. *Current Opinion in Plant Biology* **47**, 96–105.
- Harrington SA, Backhaus AE, Singh A, Hassani-Pak K, Uauy C.** 2020. The Wheat GENIE3 Network Provides Biologically-Relevant Information in Polyploid Wheat. *G3 Genes|Genomes|Genetics* **10**, 3675–3686.
- Hasan MK, Liu CX, Pan YT, Ahammed GJ, Qi ZY, Zhou J.** 2018. Melatonin alleviates low-sulfur stress by promoting sulfur homeostasis in tomato plants. *Scientific Reports* **8**.
- Hawar A, Xiong S, Yang Z, Sun B.** 2022. Histone Acetyltransferase SIGCN5 Regulates Shoot Meristem and Flower Development in *Solanum lycopersicum*. *Frontiers in Plant Science* **12**, 805879.
- Hawkesford MJ.** 2000. Plant responses to sulphur deficiency and the genetic manipulation of sulphate transporters to improve S-utilization efficiency. **51**, 131–138.
- Heinz S, Benner C, Spann N, Bertolino E, Lin YC, Laslo P, Cheng JX, Murre C, Singh H, Glass CK.** 2010. Simple Combinations of Lineage-Determining Transcription Factors Prime cis-Regulatory Elements Required for Macrophage and B Cell Identities. *Molecular Cell* **38**, 576–589.
- Hendelman A, Zebell S, Rodriguez-Leal D, et al.** 2021. Conserved pleiotropy of an ancient plant homeobox gene uncovered by cis-regulatory dissection. *Cell* **184**, 1724-1739.e16.
- Henríquez-Valencia C, Arenas-M A, Medina J, Canales J.** 2018. Integrative transcriptomic analysis uncovers novel gene modules that underlie the sulfate response in *Arabidopsis thaliana*. *Frontiers in Plant Science* **9**.
- Hirai MY, Sugiyama K, Sawada Y, et al.** 2007. Omics-based identification of *Arabidopsis* Myb transcription factors regulating aliphatic glucosinolate biosynthesis. *Proceedings of the National Academy of Sciences* **104**, 6478–6483.

- Hitz BC, Lee J-W, Jolanki O, et al.** 2023. The ENCODE Uniform Analysis Pipelines. *bioRxiv*, 2023.04.04.535623.
- Hosmani PS, Flores-Gonzalez M, Van De Geest H, et al.** 2019. An improved de novo assembly and annotation of the tomato reference genome using single-molecule sequencing, Hi-C proximity ligation and optical maps. *bioRxiv*, 767764.
- Hsieh TH, Li CW, Su RC, Cheng CP, Sanjaya, Tsai YC, Chan MT.** 2010. A tomato bZIP transcription factor, SIAREB, is involved in water deficit and salt stress response. *Planta* **231**, 1459–1473.
- Huang Y, An J, Sircar S, et al.** 2023. HSFA1a modulates plant heat stress responses and alters the 3D chromatin organization of enhancer-promoter interactions. *Nature Communications* **14**, 469.
- Huang J, Zheng J, Yuan H, McGinnis K.** 2018. Distinct tissue-specific transcriptional regulation revealed by gene regulatory networks in maize. *BMC Plant Biology* **18**.
- Hubberten HM, Klie S, Caldana C, Degenkolbe T, Willmitzer L, Hoefgen R.** 2012. Additional role of O-acetylserine as a sulfur status-independent regulator during plant growth.
- Huynh-Thu VA, Geurts P.** 2019. Unsupervised Gene Network Inference with Decision Trees and Random Forests. 195–215.
- Huynh-Thu VA, Irrthum A, Wehenkel L, Geurts P.** 2010. Inferring Regulatory Networks from Expression Data Using Tree-Based Methods. *PLoS ONE* **5**, e12776.
- Ichihashi Y, Aguilar-Martínez JA, Farhi M, Chitwood DH, Kumar R, Millon L V., Peng J, Maloof JN, Sinha NR.** 2014. Evolutionary developmental transcriptomics reveals a gene network module regulating interspecific diversity in plant leaf shape. *Proceedings of the National Academy of Sciences of the United States of America* **111**.
- Itkin M, Seybold H, Breitel D, Rogachev I, Meir S, Aharoni A.** 2009. TOMATO AGAMOUS-LIKE 1 is a component of the fruit ripening regulatory network. *The Plant Journal* **60**, 1081–1095.
- Ito Y, Sekiyama Y, Nakayama H, et al.** 2020. Allelic Mutations in the Ripening -Inhibitor Locus Generate Extensive Variation in Tomato Ripening. *Plant Physiology* **183**, 80–95.
- Itzkovitz S, Tlusty T, Alon U.** 2006. Coding limits on the number of transcription factors. *BMC Genomics* **7**, 1–15.
- Iyer-Pascuzzi AS, Jackson T, Cui H, Petricka JJ, Busch W, Tsukagoshi H, Benfey PN.** 2011. Cell Identity Regulators Link Development and Stress Responses in the Arabidopsis Root. *Developmental Cell* **21**, 770–782.

- Jeon C, Chung MY, Lee JM.** 2024. Reassessing the contribution of TOMATO AGAMOUS-LIKE1 to fruit ripening by CRISPR/Cas9 mutagenesis. *Plant Cell Reports* **43**, 1–7.
- Jiang G, Li Z, Ding X, Zhou Y, Lai H, Jiang Y, Duan X.** 2023. WUSCHEL-related homeobox transcription factor SIWOX13 regulates tomato fruit ripening. *Plant Physiology* doi: 10.1093/PLPHYS/KIAD623.
- Jin J, Tian F, Yang D-C, Meng Y-Q, Kong L, Luo J, Gao G.** 2017. PlantTFDB 4.0: toward a central hub for transcription factors and regulatory interactions in plants. *Nucleic Acids Research* **45**, D1040–D1045.
- Jones P, Binns D, Chang HY, et al.** 2014. InterProScan 5: genome-scale protein function classification. *Bioinformatics (Oxford, England)* **30**, 1236–1240.
- Jones-Rhoades MW, Bartel DP.** 2004. Computational Identification of Plant MicroRNAs and Their Targets, Including a Stress-Induced miRNA. *Molecular Cell* **14**, 787–799.
- Kajala K, Gouran M, Shaar-Moshe L, et al.** 2021. Innovation, conservation, and repurposing of gene function in root cell type development. *Cell* **184**, 3333–3348.e19.
- Kang JY, Choi HI, Im MY, Soo YK.** 2002. Arabidopsis Basic Leucine Zipper Proteins That Mediate Stress-Responsive Abscisic Acid Signaling. *The Plant Cell* **14**, 343–357.
- Kans J.** 2010. Entrez Direct: E-utilities on the Unix Command Line.
- Karlova R, Chapman N, David K, Angenent GC, Seymour GB, De Maagd RA.** 2014. Transcriptional control of fleshy fruit development and ripening. *Journal of Experimental Botany* **65**, 4527–4541.
- Kawashima CG, Matthewman CA, Huang S, et al.** 2011. Interplay of SLIM1 and miR395 in the regulation of sulfate assimilation in Arabidopsis. *Plant Journal* **66**, 863–876.
- Khanin R, Wit E.** 2006. How Scale-Free Are Biological Networks. <https://home.liebertpub.com/cmb> **13**, 810–818.
- Kim H, Kim BS, Shim JE, Hwang S, Yang S, Kim E, Iyer-Pascuzzi AS, Lee I.** 2017. TomatoNet: A Genome-wide Co-functional Network for Unveiling Complex Traits of Tomato, a Model Crop for Fleshy Fruits. *Molecular Plant* **10**, 652–655.
- Kim HJ, Nam HG, Lim PO.** 2016. Regulatory network of NAC transcription factors in leaf senescence. *Current Opinion in Plant Biology* **33**, 48–56.
- Kimura S, Sinha N.** 2008. Tomato (*Solanum lycopersicum*): A model fruit-bearing crop. *Cold Spring Harbor Protocols* **3**.

- Koenig D, Jiménez-Gómez JM, Kimura S, et al.** 2013. Comparative transcriptomics reveals patterns of selection in domesticated and wild tomato. *Proceedings of the National Academy of Sciences of the United States of America* **110**, E2655–E2662.
- Kopriva S, Malagoli M, Takahashi H.** 2019. Sulfur nutrition: Impacts on plant development, metabolism, and stress responses. *Journal of Experimental Botany* **70**, 4069–4073.
- Kou XH, Zhou JQ, Wu CE, Yang S, Liu YF, Chai LP, Xue ZH.** 2021. The interplay between ABA/ethylene and NAC TFs in tomato fruit ripening: a review. *Plant Molecular Biology* **106**, 223–238.
- Krukowski P, Colanero S, Sutti A, Martignago D, Conti L.** 2023. How Changes in ABA Accumulation and Signaling Influence Tomato Drought Responses and Reproductive Development. *International Journal of Plant Biology* **14**, 162–176.
- Kumar A, Sichov N, Bucki P, Miyara SB.** 2023. SIWRKY16 and SIWRKY31 of tomato, negative regulators of plant defense, involved in susceptibility activation following root-knot nematode *Meloidogyne javanica* infection. *Scientific Reports* 2023 13:1 **13**, 1–17.
- Kumar V, Singh D, Majee A, Singh S, Roohi, Asif MH, Sane AP, Sane VA.** 2021. Identification of tomato root growth regulatory genes and transcription factors through comparative transcriptomic profiling of different tissues. *Physiology and Molecular Biology of Plants* **27**, 1173.
- Kusano M, Worarad K, Fukushima A, et al.** 2022. Transcriptomic, Hormonomic and Metabolomic Analyses Highlighted the Common Modules Related to Photosynthesis, Sugar Metabolism and Cell Division in Parthenocarpic Tomato Fruits during Early Fruit Set. *Cells* **11**, 1420.
- Kwon Y, Kim JH, Nguyen HN, Jikumaru Y, Kamiya Y, Hong S-W, Lee H.** 2013. A novel Arabidopsis MYB-like transcription factor, MYBH, regulates hypocotyl elongation by enhancing auxin accumulation. *Journal of Experimental Botany* **64**, 3911–3922.
- Langmead B, Salzberg SL.** 2012. Fast gapped-read alignment with Bowtie 2. *Nature Methods* **9**, 357–359.
- Lee YK, Kim GT, Kim IJ, Park J, Kwak SS, Choi G, Chung W II.** 2006. LONGIFOLIA1 and LONGIFOLIA2, two homologous genes, regulate longitudinal cell elongation in Arabidopsis. *Development* **133**, 4305–4314.
- Leinonen R, Sugawara H, Shumway M.** 2011. The Sequence Read Archive. *Nucleic Acids Research* **39**, D19–D21.
- Li Y, Brooks M, Yeoh-Wang J, et al.** 2020. SDG8-mediated histone methylation and RNA processing function in the response to nitrate signaling. *Plant Physiology* **182**, 215–227.

- Li B, Carey M, Workman JL.** 2007. The Role of Chromatin during Transcription. *Cell* **128**, 707–719.
- Li S, Chen K, Grierson D.** 2021a. Molecular and Hormonal Mechanisms Regulating Fleshy Fruit Ripening. *Cells* 2021, Vol. 10, Page 1136 **10**, 1136.
- Li D, Fu F, Zhang H, Song F.** 2015. Genome-wide systematic characterization of the bZIP transcriptional factor family in tomato (*Solanum lycopersicum* L.). *BMC Genomics* **16**.
- Li H, Handsaker B, Wysoker A, Fennell T, Ruan J, Homer N, Marth G, Abecasis G, Durbin R.** 2009. The Sequence Alignment/Map format and SAMtools. *Bioinformatics* **25**, 2078–2079.
- Li C, Hou X, Qi N, Liu H, Li Y, Huang D, Wang C, Liao W.** 2021b. Insight into ripening-associated transcription factors in tomato: A review. *Scientia Horticulturae* **288**, 110363.
- Li J, Sun B, Xu Q, Jiang L, Wang N.** 2024. Transcriptome-level analysis of gene expressions in different tissues of tomato and key gene identifications during seed germination. *Scientia Horticulturae* **337**, 113565.
- Li S, Xu H, Ju Z, Cao D, Zhu H, Fu D, Grierson D, Qin G, Luo Y, Zhu B.** 2018. The RIN-MC Fusion of MADS-Box Transcription Factors Has Transcriptional Activity and Modulates Expression of Many Ripening Genes. *Plant Physiology* **176**, 891–909.
- Li W, Zhang M, Zhang T, Liu Y, Liu L.** 2022. Arabidopsis Cys2/His2 Zinc Finger Transcription Factor ZAT18 Modulates the Plant Growth-Defense Tradeoff. *International Journal of Molecular Sciences* **23**, 15436.
- Liao Y, Smyth GK, Shi W.** 2014. featureCounts: an efficient general purpose program for assigning sequence reads to genomic features. *Bioinformatics* **30**, 923–930.
- Liebold J, Neuhaus F, Geiser J, Kurtz S, Baumbach J, Newaz K.** 2024. Transcription factor prediction using protein 3D secondary structures. (PL Martelli, Ed.). *Bioinformatics* **41**.
- Lira BS, Oliveira MJ, Shiose L, Wu RTA, Rosado D, Lupi ACD, Freschi L, Rossi M.** 2020. Light and ripening-regulated BBX protein-encoding genes in *Solanum lycopersicum*. *Scientific Reports* **10**, 19235.
- Liu X, An J, Han H, Kim S, Lim C, Yun D, Chung W.** 2014. ZAT11, a zinc finger transcription factor, is a negative regulator of nickel ion tolerance in Arabidopsis. *Plant Cell Reports* **33**, 2015–2021.
- Liu X, Chen CY, Wang KC, et al.** 2013. PHYTOCHROME INTERACTING FACTOR3 Associates with the Histone Deacetylase HDA15 in Repression of Chlorophyll Biosynthesis and Photosynthesis in Etiolated Arabidopsis Seedlings. *The Plant Cell* **25**, 1258.

- Liu M, Gomes BL, Mila I, et al.** 2016. Comprehensive Profiling of Ethylene Response Factor Expression Identifies Ripening-Associated ERF Genes and Their Link to Key Regulators of Fruit Ripening in Tomato. *Plant Physiology* **170**, 1732–1744.
- Liu Y, Shi Y, Zhu N, Zhong S, Bouzayen M, Li Z.** 2020. SGRAS4 mediates a novel regulatory pathway promoting chilling tolerance in tomato. *Plant Biotechnology Journal* **18**, 1620–1633.
- Liu C, Sun Q, Zhao L, Li Z, Peng Z, Zhang J.** 2018. Heterologous Expression of the Transcription Factor EsNAC1 in Arabidopsis Enhances Abiotic Stress Resistance and Retards Growth by Regulating the Expression of Different Target Genes. *Frontiers in Plant Science* **9**.
- Liu X, Wu R, Bulley SM, Zhong C, Li D.** 2022. Kiwifruit MYBS1-like and GBF3 transcription factors influence l-ascorbic acid biosynthesis by activating transcription of GDP-L-galactose phosphorylase 3. *New Phytologist* **234**, 1782–1800.
- Livak KJ, Schmittgen TD.** 2001. Analysis of Relative Gene Expression Data Using Real-Time Quantitative PCR and the $2^{-\Delta\Delta CT}$ Method. *Methods* **25**, 402–408.
- Lopez J, Tremblay N, Voogt W, Dubé S, Gosselin A.** 1996. Effects of varying sulphate concentrations on growth, physiology and yield of the greenhouse tomato. *Scientia Horticulturae* **67**, 207–217.
- López-Vidriero I, Godoy M, Grau J, Peñuelas M, Solano R, Franco-Zorrilla JM.** 2021. DNA features beyond the transcription factor binding site specify target recognition by plant MYC2-related bHLH proteins. *Plant Communications* **2**, 100232.
- Love MI, Huber W, Anders S.** 2014. Moderated estimation of fold change and dispersion for RNA-seq data with DESeq2. *Genome Biology* **15**, 550.
- Lü P, Yu S, Zhu N, et al.** 2018. Genome encode analyses reveal the basis of convergent evolution of fleshy fruit ripening. *Nature Plants* **4**, 784–791.
- Lyčka M, Barták M, Helia O, Kopriva S, Moravcová D, Hájek J, Fojt L, Čmelík R, Fajkus J, Fojtová M.** 2023. Sulfate supplementation affects nutrient and photosynthetic status of *Arabidopsis thaliana* and *Nicotiana tabacum* differently under prolonged exposure to cadmium. *Journal of Hazardous Materials* **445**, 130527.
- Mack KL, Phifer-Rixey M, Harr B, Nachman MW.** 2019. Gene Expression Networks Across Multiple Tissues Are Associated with Rates of Molecular Evolution in Wild House Mice. *Genes* 2019, Vol. 10, Page 225 **10**, 225.
- Maere S, Heymans K, Kuiper M.** 2005. BiNGO: a Cytoscape plugin to assess overrepresentation of Gene Ontology categories in Biological Networks. *Bioinformatics* **21**, 3448–3449.

Maher KA, Bajic M, Kajala K, et al. 2018. Profiling of accessible chromatin regions across multiple plant species and cell types reveals common gene regulatory principles and new control modules. *Plant Cell* **30**, 15–36.

Manosalva N, Vandepoele K. 2023. Prediction of Transcription Factor Regulators and Gene Regulatory Networks in Tomato Using Binding Site Information. *Methods in Molecular Biology* **2698**, 323–349.

Marro N, Lidoy J, Chico MÁ, Rial C, García J, Varela RM, Macías FA, Pozo MJ, Janoušková M, López-Ráez JA. 2022. Strigolactones: New players in the nitrogen–phosphorus signalling interplay. *Plant, Cell & Environment* **45**, 512–527.

Martel C, Vrebalov J, Tafelmeyer P, Giovannoni JJ. 2011. The Tomato MADS-Box Transcription Factor RIPENING INHIBITOR Interacts with Promoters Involved in Numerous Ripening Processes in a COLORLESS NONRIPENING-Dependent Manner. *Plant Physiology* **157**, 1568–1579.

Martin M. 2011. Cutadapt removes adapter sequences from high-throughput sequencing reads. *EMBnet.journal* **17**, 10.

Martín-Trillo M, Grandío EG, Serra F, Marcel F, Rodríguez-Buey ML, Schmitz G, Theres K, Bendahmane A, Dopazo H, Cubas P. 2011. Role of tomato BRANCHED1-like genes in the control of shoot branching. *The Plant Journal* **67**, 701–714.

Maruyama-Nakashita A. 2004. Regulation of high-affinity sulphate transporters in plants: towards systematic analysis of sulphur signalling and regulation. *Journal of Experimental Botany* **55**, 1843–1849.

Maruyama-Nakashita A. 2017. Metabolic changes sustain the plant life in low-sulfur environments. Elsevier Ltd.

Maruyama-Nakashita A, Nakamura Y, Tohge T, Saito K, Takahashi H. 2006. Arabidopsis SLIM1 is a central transcriptional regulator of plant sulfur response and metabolism. *Plant Cell* **18**, 3235–3251.

Maruyama-Nakashita A, Nakamura Y, Yamaya T, Takahashi H. 2004. A novel regulatory pathway of sulfate uptake in Arabidopsis roots: implication of CRE1/WOL/AHK4-mediated cytokinin-dependent regulation. *The Plant Journal* **38**, 779–789.

Maruyama-Nakashita A, Ohkama-Ohtsu N. 2017. Sulfur Assimilation and Glutathione Metabolism in Plants. *Glutathione in Plant Growth, Development, and Stress Tolerance*. Cham: Springer International Publishing, 287–308.

- McNeill AM, Eriksen J, Bergström L, Smith KA, Marstorp H, Kirchmann H, Nilsson I.** 2005. Nitrogen and sulphur management: challenges for organic sources in temperate agricultural systems. *Soil Use and Management* **21**, 82–93.
- Mercatelli D, Scalambra L, Triboli L, Ray F, Giorgi FM.** 2020. Gene regulatory network inference resources: A practical overview. *Biochimica et Biophysica Acta (BBA) - Gene Regulatory Mechanisms* **1863**, 194430.
- Meuleman W, Muratov A, Rynes E, et al.** 2020. Index and biological spectrum of human DNase I hypersensitive sites. *Nature* **584**, 244–251.
- Mitreiter S, Gigolashvili T.** 2021. Regulation of glucosinolate biosynthesis. *Journal of Experimental Botany* **72**, 70–91.
- Moyano TC, Gutiérrez RA, Alvarez JM.** 2021. Genomic Footprinting Analyses from DNase-seq Data to Construct Gene Regulatory Networks. 25–46.
- Murashige T, Skoog F.** 1962. A Revised Medium for Rapid Growth and Bio Assays with Tobacco Tissue Cultures. *Physiologia Plantarum* **15**, 473–497.
- Nakai Y, Maruyama-Nakashita A.** 2020. Biosynthesis of sulfur-containing small biomolecules in plants. MDPI AG.
- Narayan OP, Kumar P, Yadav B, Dua M, Johri AK.** 2022. Sulfur nutrition and its role in plant growth and development. *Plant Signaling & Behavior* **18**, 2030082.
- Olivares-Yañez C, Sánchez E, Pérez-Lara G, Seguel A, Camejo PY, Larrondo LF, Vidal EA, Canessa P.** 2021. A comprehensive transcription factor and DNA-binding motif resource for the construction of gene regulatory networks in *Botrytis cinerea* and *Trichoderma atroviride*. *Computational and Structural Biotechnology Journal* **19**, 6212–6228.
- Orduña L, Santiago A, Navarro-Payá D, Zhang C, Wong DCJ, Matus JT.** 2023. Aggregated gene co-expression networks predict transcription factor regulatory landscapes in grapevine. *Journal of Experimental Botany* **74**, 6522–6540.
- Orellana S, Yañez M, Espinoza A, Verdugo I, González E, Ruiz-Lara S, Casaretto JA.** 2010. The transcription factor SlAREB1 confers drought, salt stress tolerance and regulates biotic and abiotic stress-related genes in tomato. *Plant, Cell & Environment* **33**, 2191–2208.
- Ozaki S, Ogata Y, Suda K, et al.** 2010. Coexpression Analysis of Tomato Genes and Experimental Verification of Coordinated Expression of Genes Found in a Functionally Enriched Coexpression Module. *DNA Research* **17**, 105–116.

- Pan X, Wang C, Liu Z, Gao R, Feng L, Li A, Yao K, Liao W.** 2023. Identification of ABF/AREB gene family in tomato (*Solanum lycopersicum* L.) and functional analysis of ABF/AREB in response to ABA and abiotic stresses. *PeerJ* **11**, e15310.
- Park P.** 2009. ChIP-seq: advantages and challenges of a maturing technology. *Nature Reviews Genetics* 2009 10:10 **10**, 669–680.
- Park SY, Fung P, Nishimura N, et al.** 2009. Abscisic acid inhibits type 2C protein phosphatases via the PYR/PYL family of START proteins. *Science* **324**, 1068–1071.
- Piotrowska J, Jodoi Y, Trang NH, Wawrzynska A, Takahashi H, Sirko A, Maruyama-Nakashita A.** 2022. The C-Terminal Region of SLIM1 Transcription Factor Is Required for Sulfur Deficiency Response. *Plants* 2022, Vol. 11, Page 2595 **11**, 2595.
- Pirona R, Frugis G, Locatelli F, Mattana M, Genga A, Baldoni E.** 2023. Transcriptomic analysis reveals the gene regulatory networks involved in leaf and root response to osmotic stress in tomato. *Frontiers in Plant Science* **14**, 1155797.
- Qi F, Wang F, Xiaoyang C, Wang Z, Lin Y, Peng Z, Zhang J, Wang N, Zhang J.** 2023. Gene Expression Analysis of Different Organs and Identification of AP2 Transcription Factors in Flax (*Linum usitatissimum* L.). *Plants* **12**, 3260.
- Qiu Z, Li R, Zhang S, Wang K, Xu M, Li J, Du Y, Yu H, Cui X.** 2016. Identification of Regulatory DNA Elements Using Genome-wide Mapping of DNase I Hypersensitive Sites during Tomato Fruit Development. *Molecular Plant* **9**, 1168–1182.
- Quinlan AR, Hall IM.** 2010. BEDTools: a flexible suite of utilities for comparing genomic features. *Bioinformatics* **26**, 841–842.
- Rakpenthai A, Apodiakou A, Whitcomb SJ, Hoefgen R.** 2022. In silico analysis of cis-elements and identification of transcription factors putatively involved in the regulation of the OAS cluster genes SDI1 and SDI2. *The Plant Journal* **110**, 1286–1304.
- Ramegowda V, Gill US, Sivalingam PN, et al.** 2017. GBF3 transcription factor imparts drought tolerance in *Arabidopsis thaliana*. *Scientific Reports* 2017 7:1 **7**, 1–13.
- Ramírez-González RH, Borrill P, Lang D, et al.** 2018. The transcriptional landscape of polyploid wheat. *Science* **361**.
- Ranjan R, Srijan S, Balekuttira S, et al.** 2024. Organ-delimited gene regulatory networks provide high accuracy in candidate transcription factor selection across diverse processes. *Proceedings of the National Academy of Sciences of the United States of America* **121**, e2322751121.

- Ravasi T, Suzuki H, Cannistraci C V., et al.** 2010. An Atlas of Combinatorial Transcriptional Regulation in Mouse and Man. *Cell* **140**, 744–752.
- Reynoso MA, Kajala K, Bajic M, et al.** 2019. Evolutionary flexibility in flooding response circuitry in angiosperms. *Science* **365**, 1291–1295.
- Rhee SY, Beavis W, Berardini TZ, et al.** 2003. The Arabidopsis Information Resource (TAIR): a model organism database providing a centralized, curated gateway to Arabidopsis biology, research materials and community. *Nucleic Acids Research* **31**, 224–228.
- Ricardi MM, González RM, Zhong S, et al.** 2014. *Genome-wide data (ChIP-seq) enabled identification of cell wall-related and aquaporin genes as targets of tomato ASR1, a drought stress-responsive transcription factor.*
- Riechmann JL, Ratcliffe OJ.** 2000. A genomic perspective on plant transcription factors. *Current Opinion in Plant Biology* **3**, 423–434.
- Ristova D, Kopriva S.** 2022. Sulfur signaling and starvation response in Arabidopsis. *iScience* **25**, 104242.
- Rivera-Silva R, Chávez Montes RA, Jaimes-Miranda F.** 2024. Gene ontology functional annotation datasets for the ITAG3.2 and ITAG4.0 tomato (*Solanum lycopersicum*) genome annotations. *Data in Brief* **54**, 110401.
- Rosado D, Ackermann A, Spassibojko O, Rossi M, Pedmale U V.** 2022. WRKY transcription factors and ethylene signaling modify root growth during the shade-avoidance response. *Plant Physiology* **188**, 1294–1311.
- Rosado D, Gramegna G, Cruz A, Lira BS, Freschi L, De Setta N, Rossi M.** 2016. Phytochrome Interacting Factors (PIFs) in *Solanum lycopersicum*: Diversity, Evolutionary History and Expression Profiling during Different Developmental Processes. *PLOS ONE* **11**, e0165929.
- Safi A, Medici A, Szponarski W, et al.** 2021. GARP transcription factors repress Arabidopsis nitrogen starvation response via ROS-dependent and -independent pathways. *Journal of Experimental Botany* **72**, 3881–3901.
- Saito T, Rehmsmeier M.** 2017. Precrec: fast and accurate precision–recall and ROC curve calculations in R. *Bioinformatics* **33**, 145–147.
- Salavaty A, Ramialison M, Currie PD.** 2020. Integrated Value of Influence: An Integrative Method for the Identification of the Most Influential Nodes within Networks. *Patterns* **1**, 100052.

- Santiago A, Orduña L, David Fernández J, Vidal Á, de Martín-Agirre I, Lisón P, Vidal EA, Navarro-Payá D, Tomás Matus J.** 2024. The Plantae Visualization Platform: a comprehensive web-based tool for the integration, visualization, and analysis of omic data across plant and related species. *bioRxiv*, 2024.12.19.629382.
- Satheesh V, Zhang J, Li J, You Q, Zhao P, Wang P, Lei M.** 2022. High transcriptome plasticity drives phosphate starvation responses in tomato. *Stress Biology* **2**, 1–23.
- Shanks CM, Huang J, Cheng CY, Shih HJS, Brooks MD, Alvarez JM, Araus V, Swift J, Henry A, Coruzzi GM.** 2022. Validation of a high-confidence regulatory network for gene-to-NUE phenotype in field-grown rice. *Frontiers in Plant Science* **13**, 1006044.
- Shannon P, Markiel A, Ozier O, Baliga NS, Wang JT, Ramage D, Amin N, Schwikowski B, Ideker T.** 2003. Cytoscape: A Software Environment for Integrated Models of Biomolecular Interaction Networks. *Genome Research* **13**, 2498–2504.
- Shi J, Le Maguer M.** 2000. Lycopene in tomatoes: Chemical and physical properties affected by food processing. *Critical Reviews in Food Science and Nutrition* **40**, 1–42.
- Siddiqui MH, Alamri S, Alsubaie QD, Ali HM, Khan MN, Al-Ghamdi A, Ibrahim AA, Alsadon A.** 2020. Exogenous nitric oxide alleviates sulfur deficiency-induced oxidative damage in tomato seedlings. *Nitric Oxide - Biology and Chemistry* **94**, 95–107.
- Siloto RMP, Findlay K, Lopez-Villalobos A, Yeung EC, Nykiforuk CL, Moloney MM.** 2006. The Accumulation of Oleosins Determines the Size of Seed Oilbodies in Arabidopsis. *The Plant Cell* **18**, 1961–1974.
- Stuurman J, Jäggi F, Kuhlemeier C.** 2002. Shoot meristem maintenance is controlled by a GRAS-gene mediated signal from differentiating cells. *Genes & Development* **16**, 2213–2218.
- Sun T, Busta L, Zhang Q, Ding P, Jetter R, Zhang Y.** 2018. TGACG-BINDING FACTOR 1 (TGA1) and TGA4 regulate salicylic acid and pipelicolic acid biosynthesis by modulating the expression of SYSTEMIC ACQUIRED RESISTANCE DEFICIENT 1 (SARD1) and CALMODULIN-BINDING PROTEIN 60g (CBP60g). *New Phytologist* **217**, 344–354.
- Supek F, Bošnjak M, Škunca N, Šmuc T.** 2011. REVIGO Summarizes and Visualizes Long Lists of Gene Ontology Terms. *PLOS ONE* **6**, e21800.
- Swift J, Alvarez JM, Araus V, Gutiérrez C □ RA, Coruzzi GM.** 2020. Nutrient dose-responsive transcriptome changes driven by Michaelis-Menten kinetics underlie plant growth rates. *PNAS* **117**.
- Swift J, Coruzzi GM.** 2017. A matter of time — How transient transcription factor interactions create dynamic gene regulatory networks. *Biochimica et Biophysica Acta - Gene Regulatory Mechanisms* **1860**, 75–83.

- Tabatabai MA, Bremner JM.** 1970. A Simple Turbidimetric Method of Determining Total Sulfur in Plant Materials ¹. *Agronomy Journal* **62**, 805–806.
- Taiz L, Zeiger E.** 2010. *Plant Physiology. 5th Edition.* Sunderland.
- Takahashi H, Kopriva S, Giordano M, Saito K, Hell R.** 2011. Sulfur assimilation in photosynthetic organisms: Molecular functions and regulations of transporters and assimilatory enzymes. *Annual Review of Plant Biology* **62**, 157–184.
- Takahashi H, Watanabe-Takahashi A, Smith FW, Blake-Kalff M, Hawkesford MJ, Saito K.** 2000. The roles of three functional sulphate transporters involved in uptake and translocation of sulphate in *Arabidopsis thaliana*. *The Plant Journal* **23**, 171–182.
- The Tomato Genome Consortium.** 2012. The tomato genome sequence provides insights into fleshy fruit evolution. *Nature* **485**, 635–641.
- Tian C, Wan P, Sun S, Li J, Chen M.** 2004. Genome-wide analysis of the GRAS gene family in rice and *Arabidopsis*. *Plant Molecular Biology* **54**, 519–532.
- Tian F, Yang DC, Meng YQ, Jin J, Gao G.** 2020. PlantRegMap: charting functional regulatory maps in plants. *Nucleic Acids Research* **48**, D1104–D1113.
- Tu X, Mejía-Guerra MK, Valdes Franco JA, et al.** 2020. Reconstructing the maize leaf regulatory network using ChIP-seq data of 104 transcription factors. *Nature Communications* **11**, 5089.
- Tu X, Ren S, Shen W, et al.** 2022. Limited conservation in cross-species comparison of GLK transcription factor binding suggested wide-spread cistrome divergence. *Nature Communications* 2022 13:1 **13**, 1–12.
- Uno Y, Furihata T, Abe H, Yoshida R, Shinozaki K, Yamaguchi-Shinozaki K.** 2000. *Arabidopsis* basic leucine zipper transcription factors involved in an abscisic acid-dependent signal transduction pathway under drought and high-salinity conditions. *Proceedings of the National Academy of Sciences of the United States of America* **97**, 11632–11637.
- Vidal EA, Alvarez JM, Araus V, et al.** 2020. Nitrate in 2020: Thirty Years from Transport to Signaling Networks. *The Plant Cell* **32**, 2094–2119.
- Vishwakarma K, Upadhyay N, Kumar N, et al.** 2017. Abscisic acid signaling and abiotic stress tolerance in plants: A review on current knowledge and future prospects. *Frontiers in Plant Science* **8**, 228798.
- Wang X, Wang HF, Chen Y, Sun MM, Wang Y, Chen YF.** 2020. The Transcription Factor NIGT1.2 Modulates Both Phosphate Uptake and Nitrate Influx during Phosphate Starvation in *Arabidopsis* and Maize. *The Plant Cell* **32**, 3519–3534.

Wang B, Wang J, Yang T, Wang J, Dai Q, Zhang F, Xi R, Yu Q, Li N. 2023a. The transcriptional regulatory network of hormones and genes under salt stress in tomato plants (*Solanum lycopersicum* L.). *Frontiers in Plant Science* **14**, 1115593.

Wang L, Zhou Y, Ding Y, Chen C, Chen X, Su N, Zhang X, Pan Y, Li J. 2023b. Novel flavin-containing monooxygenase protein FMO1 interacts with CAT2 to negatively regulate drought tolerance through ROS homeostasis and ABA signaling pathway in tomato. *Horticulture Research* **10**.

Watanabe M, Hoefgen R. 2019. *Sulphur systems biology - Making sense of omics data.* Oxford University Press.

Wawrzyńska A, Sirko A. 2014. To control and to be controlled: understanding the Arabidopsis SLIM1 function in sulfur deficiency through comprehensive investigation of the EIL protein family. *Frontiers in Plant Science* **5**, 112399.

Wawrzyńska A, Sirko A. 2020. Proteasomal Degradation of Proteins Is Important for the Proper Transcriptional Response to Sulfur Deficiency Conditions in Plants. *Plant and Cell Physiology* **61**, 1548–1564.

Wei Q, Wang J, Wang W, Hu T, Hu H, Bao C. 2020. A high-quality chromosome-level genome assembly reveals genetics for important traits in eggplant. *Horticulture Research* 2020 7:1 7, 1–15.

Weirauch MT, Yang A, Albu M, et al. 2014. Determination and inference of eukaryotic transcription factor sequence specificity. *Cell* **158**, 1431–1443.

Wise AA, Liu Z, Binns AN. 2006. Three methods for the introduction of foreign DNA into *Agrobacterium*. *Methods in molecular biology (Clifton, N.J.)* **343**, 43–53.

Wolfe CJ, Kohane IS, Butte AJ. 2005. Systematic survey reveals general applicability of ‘guilt-by-association’ within gene coexpression networks. *BMC Bioinformatics* **6**, 227.

Xu T, Liu X, Wang R, Dong X, Guan X, Wang Y, Jiang Y, Shi Z, Qi M, Li T. 2016. SLARF2a plays a negative role in mediating axillary shoot formation. *Scientific Reports* 2016 6:1 6, 1–13.

Yang D, Liu Y, Ali M, Ye L, Pan C, Li M, Zhao X, Yu F, Zhao X, Lu G. 2022. Phytochrome interacting factor 3 regulates pollen mitotic division through auxin signalling and sugar metabolism pathways in tomato. *New Phytologist* **234**, 560–577.

Yang H, Zhou K, Wu Q, et al. 2024. The tomato WRKY-B transcription factor modulates lateral branching by targeting BLIND, PIN4, and IAA15. *Horticulture Research* **11**.

Yildiz I, Gross M, Moser D, Petzsch P, Köhrer K, Zeier J. 2023. N-hydroxypipicolinic acid induces systemic acquired resistance and transcriptional reprogramming via TGA transcription factors. *Plant, Cell & Environment* **46**, 1900–1920.

Yin W, Mendoza L, Monzon-Sandoval J, Urrutia AO, Gutierrez H. 2021. Emergence of co-expression in gene regulatory networks. *PLOS ONE* **16**, e0247671.

Yin M, Wang Y, Zhang L, Li J, Quan W, Yang L, Wang Q, Chan Z. 2017. The Arabidopsis Cys2/His2 zinc finger transcription factor ZAT18 is a positive regulator of plant tolerance to drought stress. *Journal of Experimental Botany* **68**, 2991–3005.

Yoo SD, Cho YH, Sheen J. 2007. Arabidopsis mesophyll protoplasts: a versatile cell system for transient gene expression analysis. *Nature Protocols* **2**:7 **2**, 1565–1572.

Yu Y, Liu Z, Wang L, et al. 2016. WRKY71 accelerates flowering via the direct activation of FLOWERING LOCUS T and LEAFY in Arabidopsis thaliana. *The Plant Journal* **85**, 96–106.

Yu Y, Qi Y, Xu J, Dai X, Chen J, Dong CH, Xiang F. 2021. Arabidopsis WRKY71 regulates ethylene-mediated leaf senescence by directly activating EIN2, ORE1 and ACS2 genes. *The Plant Journal* **107**, 1819–1836.

Yue J, Xu W, Ban R, Huang S, Miao M, Tang X, Liu G, Liu Y. 2016. PTIR: Predicted Tomato Interactome Resource. *Scientific Reports* **6**, 25047.

Zhang L, Kawaguchi R, Morikawa-Ichinose T, Allahham A, Kim SJ, Maruyama-Nakashita A. 2020a. Sulfur deficiency-induced glucosinolate catabolism attributed to two β -glucosidases, bglu28 and bglu30, is required for plant growth maintenance under sulfur deficiency. *Plant and Cell Physiology* **61**, 803–813.

Zhang Y, Liu T, Meyer CA, et al. 2008. Model-based analysis of ChIP-Seq (MACS). *Genome Biology* **9**, 1–9.

Zhang W, Zhang T, Wu Y, Jiang J. 2012. Genome-Wide Identification of Regulatory DNA Elements and Protein-Binding Footprints Using Signatures of Open Chromatin in *Arabidopsis*. *The Plant Cell* **24**, 2719–2731.

Zhang H, Zhao Y, Zhu JK. 2020b. Thriving under Stress: How Plants Balance Growth and the Stress Response. *Developmental Cell* **55**, 529–543.

Zhao S, Fernald RD. 2005. Comprehensive Algorithm for Quantitative Real-Time Polymerase Chain Reaction. <https://home.liebertpub.com/cmb> **12**, 1047–1064.

Zhao Q, Wu Y, Gao L, Ma J, Li C-Y, Xiang C-B. 2014. Sulfur nutrient availability regulates root elongation by affecting root indole-3-acetic acid levels and the stem cell niche. *Journal of Integrative Plant Biology* **56**, 1151–1163.

Zhao X, Yuan X, Chen S, Meng L, Fu D. 2018. Role of the tomato TAGL1 gene in regulating fruit metabolites elucidated using RNA sequence and metabolomics analyses. *PLOS ONE* **13**, e0199083.

Zheng Y, Jiao C, Sun H, et al. 2016. iTAK: A Program for Genome-wide Prediction and Classification of Plant Transcription Factors, Transcriptional Regulators, and Protein Kinases. *Molecular Plant* **9**, 1667–1670.

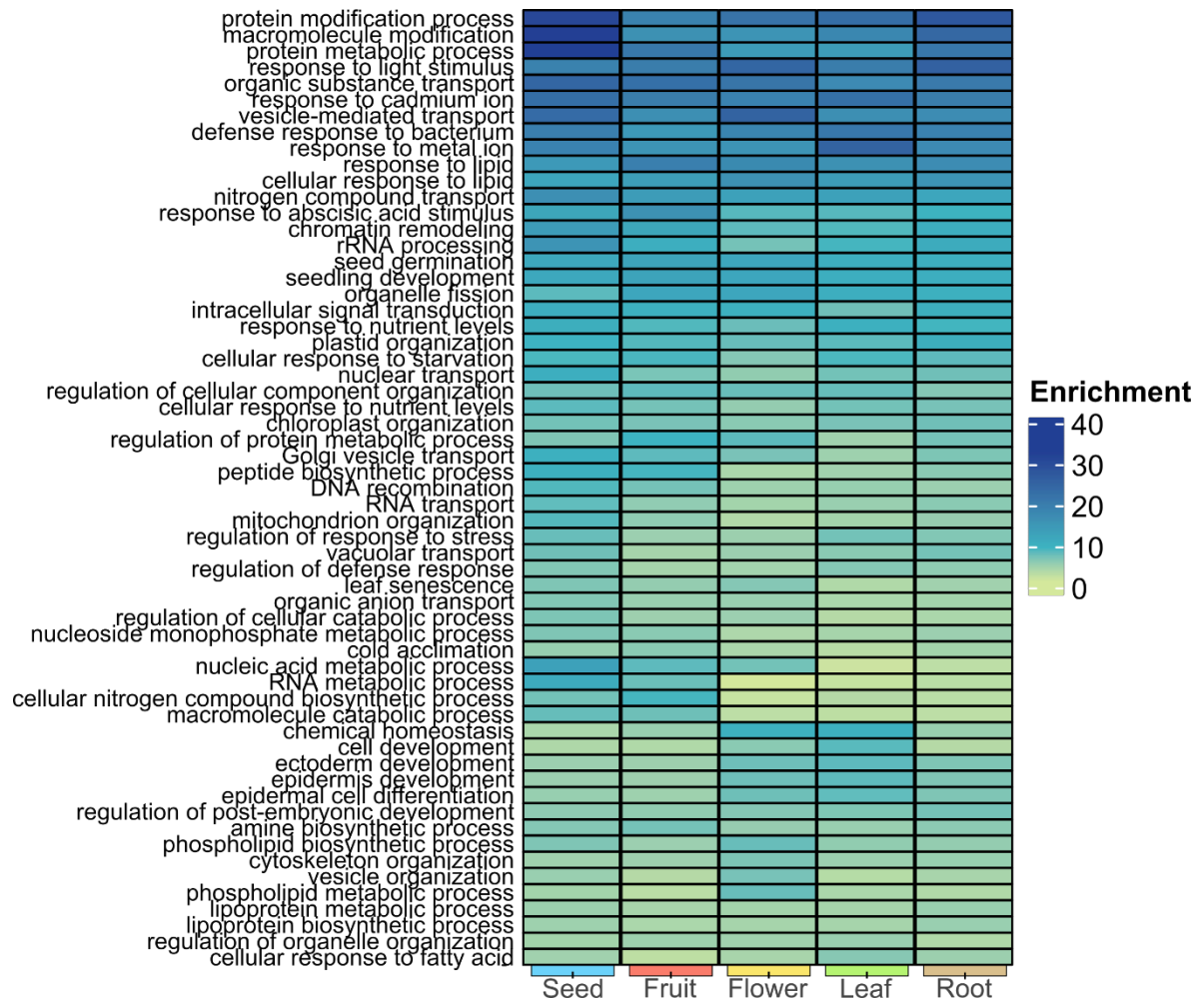
Zhong S, Fei Z, Chen YR, et al. 2013. Single-base resolution methylomes of tomato fruit development reveal epigenome modifications associated with ripening. *Nature Biotechnology* 2013 31:2 **31**, 154–159.

Zhu Y, Zhu G, Xu R, Jiao Z, Yang J, Lin T, Wang Z, Huang S, Chong L, Zhu JK. 2023. A natural promoter variation of SIBBX31 confers enhanced cold tolerance during tomato domestication. *Plant Biotechnology Journal* **21**, 1033–1043.

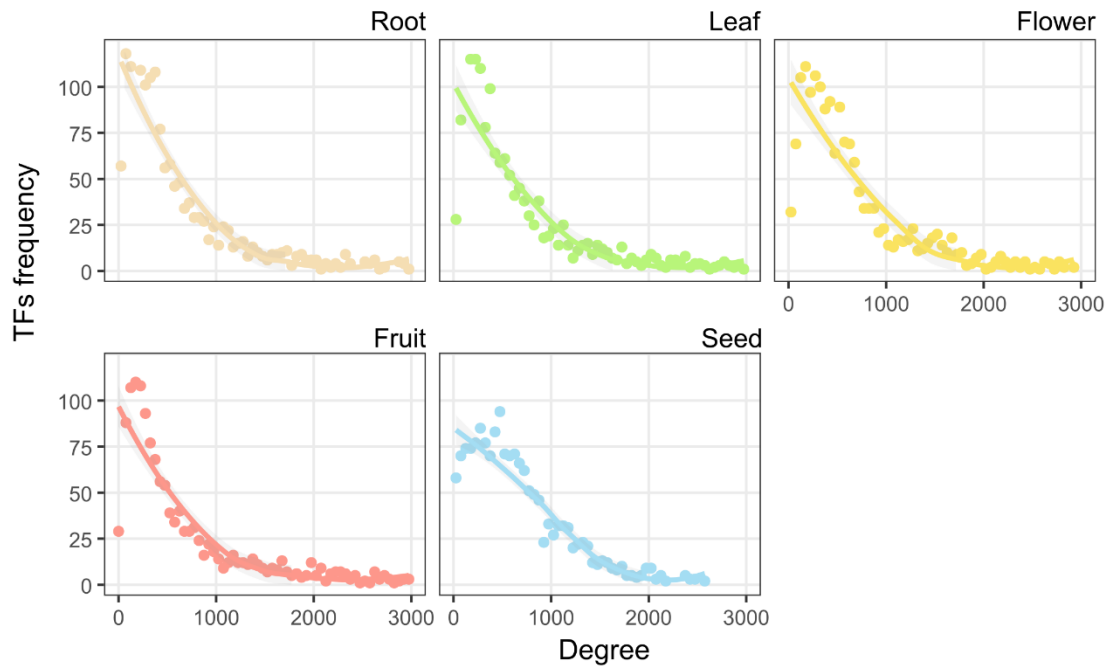
Zouine M, Maza E, Djari A, Lauvernier M, Frasse P, Smouni A, Pirrello J, Bouzayen M. 2017. TomExpress, a unified tomato RNA-Seq platform for visualization of expression data, clustering and correlation networks. *The Plant Journal* **92**, 727–735.

Zuchi S, Cesco S, Varanini Z, Pinton R, Astolfi S. 2009. Sulphur deprivation limits Fe-deficiency responses in tomato plants. *Planta* **230**, 85–94.

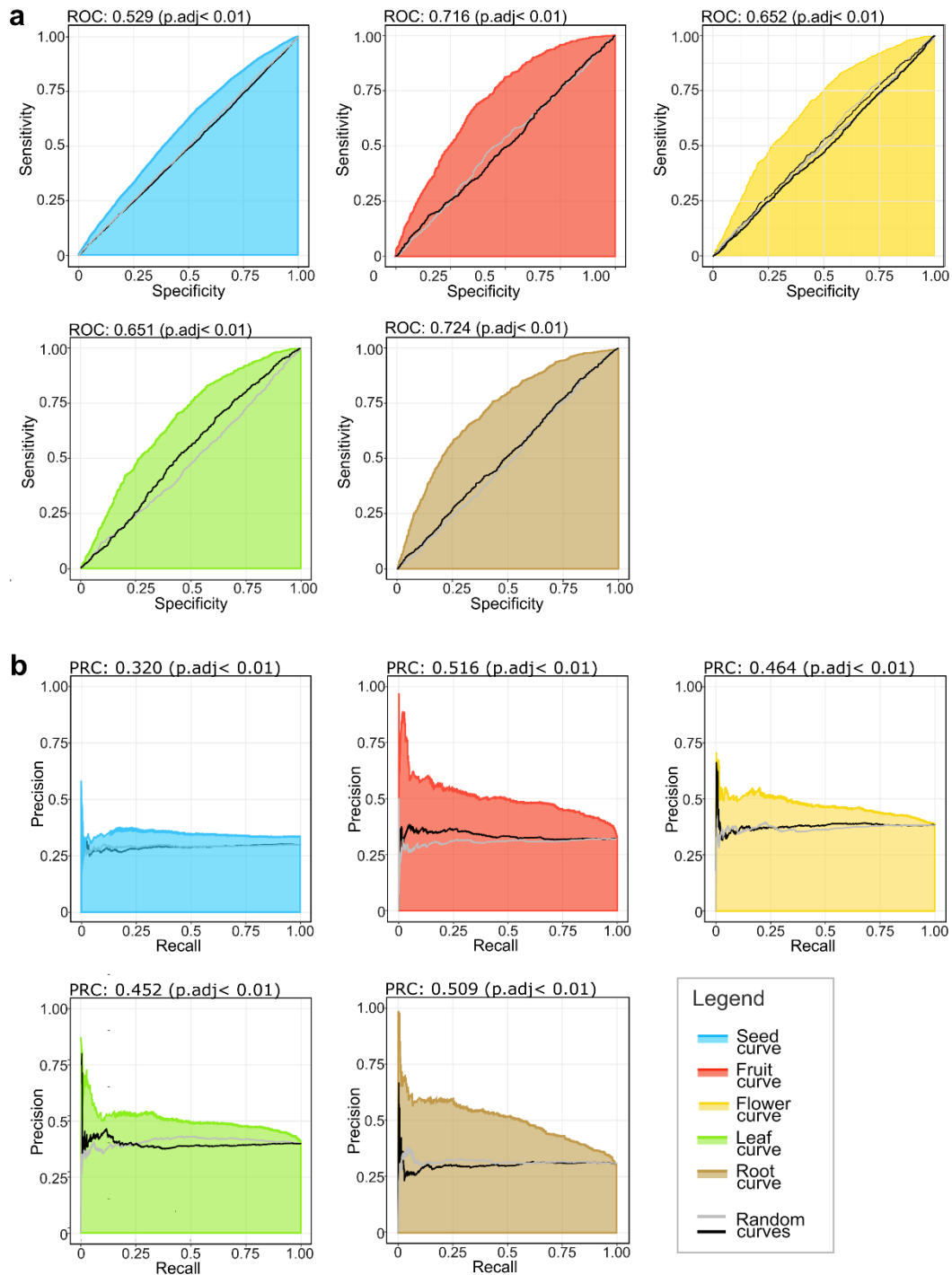
X. APPENDIX



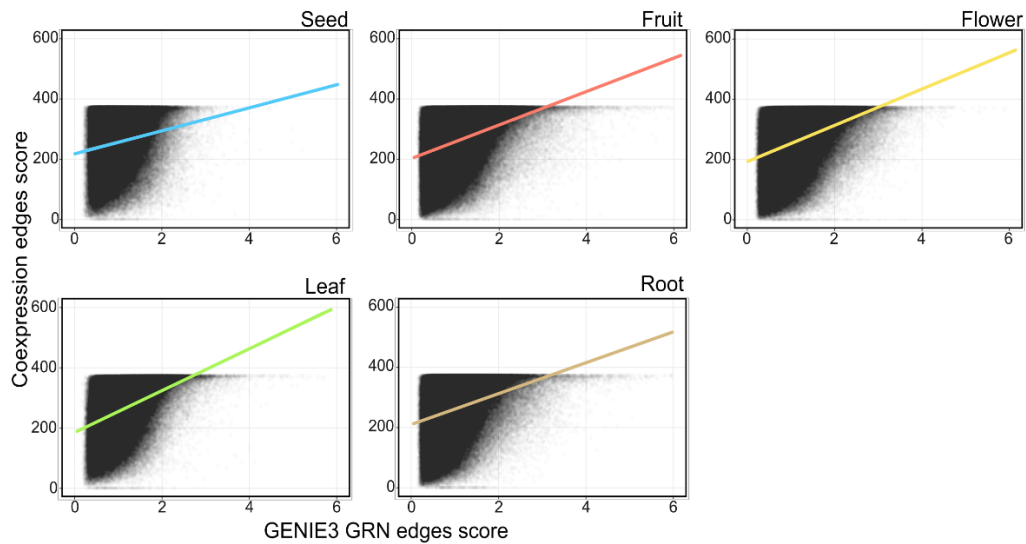
S. FIGURE N°1. Heatmap of enrichment levels (FDR adj.p.val< 0.05) representing GO terms calculated for organ-specific genes.



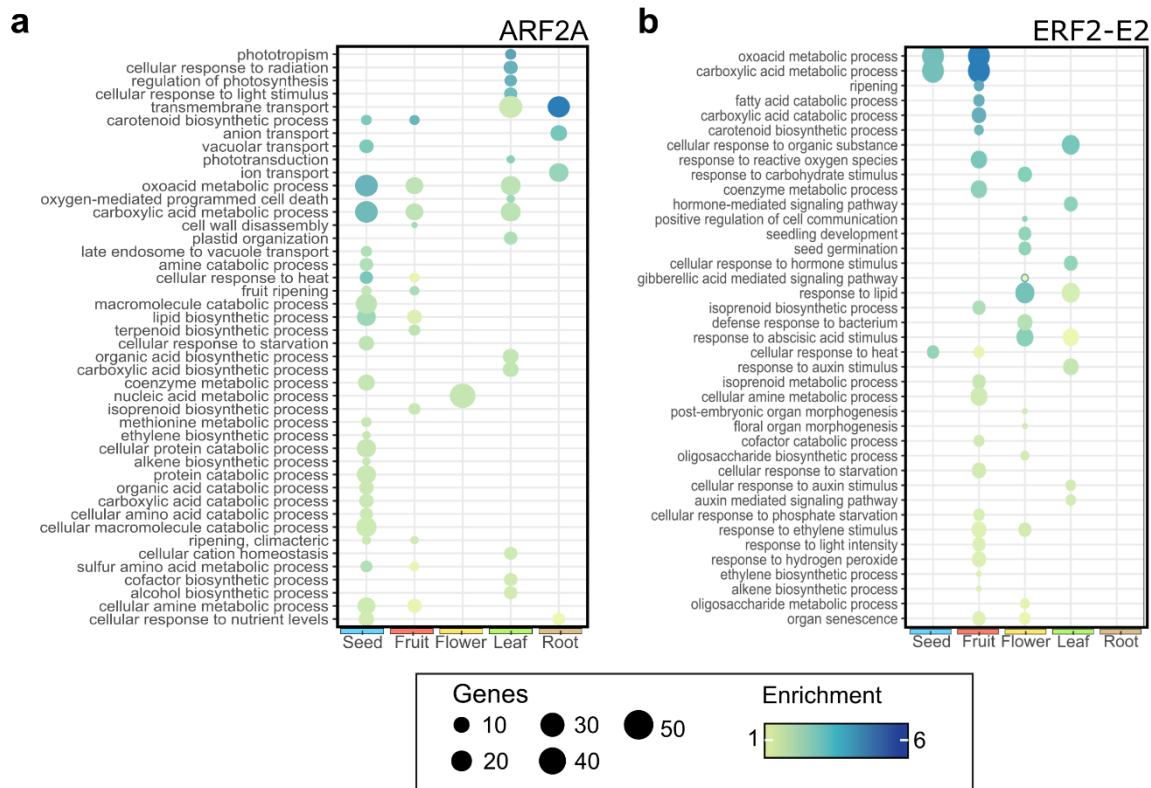
S. FIGURE N°2. Scale-free connectivity distribution of tomato organ-specific GENIE3 generated GRNs from tomato roots, leaves, flowers, fruits and seeds.



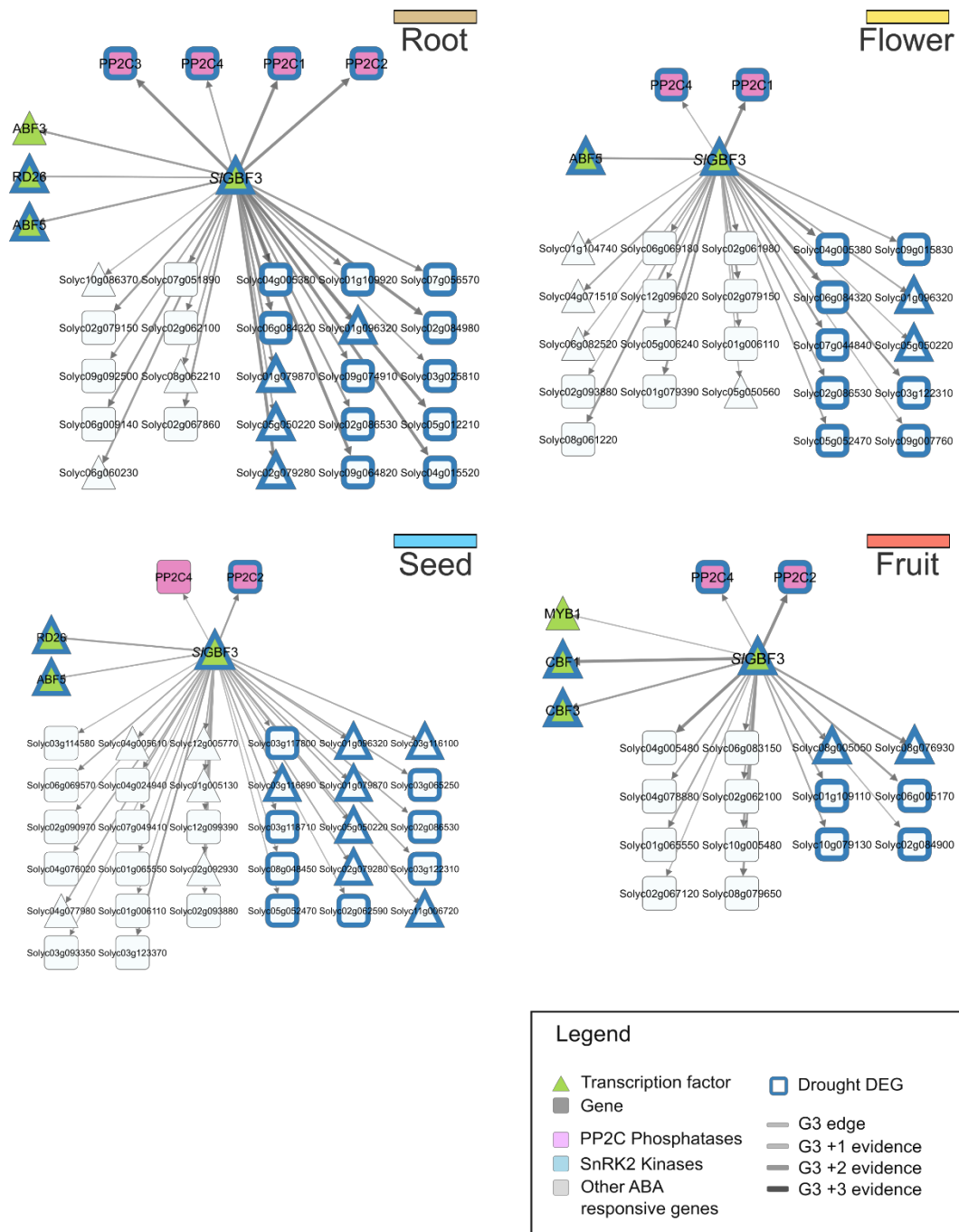
S. FIGURE N°3. Accuracy analysis of organ-specific GRNs. Receiver Operating Characteristic (ROC) curves (a) and Precision-Recall (PR) curves (b) comparing organ-specific GRNs to ChIP-seq validation networks. The shaded areas indicate variability across multiple iterations. Black and grey lines represent the maximum and minimum quartiles of randomly generated TF-target pairings, respectively.



S. FIGURE N°4. Scatterplots showing the correlation between GRN GENIE3 scores and GCN HRR scores. Colored lines represent the trend of data distribution, with colors indicating the organ of origin.



S. FIGURE N°5. GSEA of top 5 most connected TFs shared across organ-level GRNs. Dot plot of the results of a GSEA (FDR adj.p.val < 0.05) representing enriched GO terms for the top five most connected TFs shared across organ-specific GRNs. The size and color of the dots indicate the significance and enrichment levels, respectively.



S. FIGURE N°6. Organ-specific GRNs of *SIGBF3* on ABA-related target genes. Triangles represent TFs, rectangles represent target genes. Node colors indicate function. Blue-bordered nodes indicate DEGs from drought-stressed leaves (Gao et al., 2019). Edge darker shades indicate accumulated regulatory evidence.

